The PV-Battery Integrated Module: Energy Storage Sizing

Loic Barois

Technische Universiteit Delft

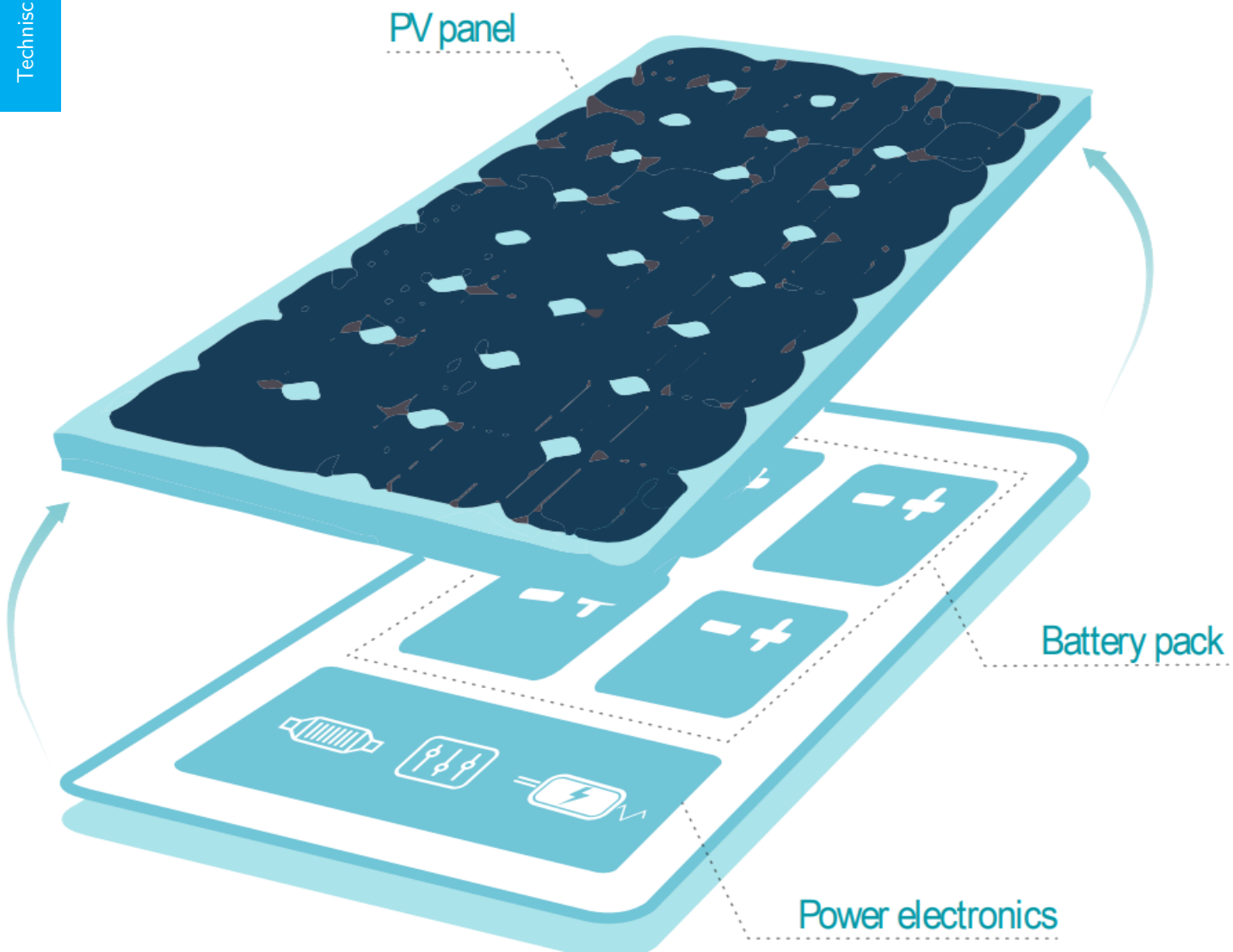

TU Delft Delft University of Technology

Challenge the future

THE PV-BATTERY INTEGRATED MODULE: ENERGY STORAGE SIZING

by

Loic Barois

in partial fulfillment of the requirements for the degree of

Master of Science
in Sustainable Energy Technology

at the Delft University of Technology,
to be defended publicly on Tuesday March 27, 2018 at 10:00 AM.

Supervisor:	Dr. ir. L. Ramirez Elizondo	TU Delft
Thesis committee:	Prof. dr. ir. P. Bauer,	TU Delft
	Dr. ir. Z. Qin,	TU Delft
	Dr. ir. M. Popov,	TU Delft

TU Delft Delft University of Technology

ABSTRACT

The physical integration of a battery system to the back of PV module provides solutions to the changing demands of the residential solar energy market. The PV-Battery Integrated Module (PBIM) concept is proposed and equips energy-users with a modular and user friendly solar system. With each PV panel equipped with its exclusive balance of system components, the PBIM aims to rival conventional solar home systems on an economic basis. With a potential to offer savings on the installation process and removing the need to customize every residential solar system the use of PBIM is a promising step towards the widespread implementation of solar systems.

This project contributes towards the PBIM design by exploring the effects of energy storage motivations and ambient conditions on the optimal PBIM energy storage capabilities and the subsequent impact on its performance as whole. To quantify these impacts realistic case studies are developed and test the PBIM's capabilities in Costa Rica and the Netherlands. The PBIM, for each location, was assessed for its application in a grid-tied system for peak shaving applications and its performance as a stand-alone solution.

As compared to conventional solar systems, the PBIM operates at higher temperatures, influencing the performance and lifetime of the incorporated components. This thesis commences by capturing the effects of elevated operating temperatures through the development of a PBIM model. The energy control strategy is devised to simulate the battery charging profiles for the identified applications. Location specific parameters are then implemented to asses the PBIM performance and the influence of different climates.

A sizing methodology is used to derive the appropriate battery capacity for each case study. A comparison is made between the dynamic characteristics of the optimally sized system for each of the locations, indicating the fulfillment of the respective system objectives, minimizing battery degradation and maximizing autarky. Furthermore, the technical and economic feasibility of the PBIM concept is assessed with respect to a conventional solar home system, leading to the conclusion that the PBIM, at this point in time, possesses technical characteristics comparable to that of a convectional PV system. The PBIM concept is still in the early stages of development and there are still many challenges that need to be overcome before its widespread usage.

CONTENTS

List of Figures

LIST OF TABLES

1

INTRODUCTION

1.1. GLOBAL ENERGY SCENARIO

Throughout the centuries, energy has played a key role in spurring industrialization, raising living standards and has aided the transformation of the global economy and society to that we see today. It is with no doubt that energy will continue to be a vital pillar of our civilization for years to come. With the Untied Nations predicting a drastic global population increase of 1.7 billion by the year 2035, the global energy demand is poised to follow a similar increasing trend. The rapid economic growth of developing nations has consistently lead to the dramatic increase of local electrification rates. As these emerging markets evolve, generally speaking, the standard of living of the local population rise: further accelerating the growing of energy demands. Essential for future progress and development of mankind is an uninterrupted and predictable source of energy. Nations which rely heavily on external stakeholders for energy resources become particularly vulnerable to factors such as limitations in energy supply, price and currency fluctuations, which are all influenced by numerous external factors. The key to develop a stable economy and society is energy security.

The global energy demand is estimated to double by 2060 [14]. Traditionally, a fossil fuel based approach has been adopted to meet growing energy demands; the flaws in this ideology has rapidly become indisputable for a number of reasons. Firstly, fossil fuel prices have consistently proven to be highly volatile and heavily influenced by political factors. Combined with its increasing scarcity the use of fossil-fuels as an energy source has archaic. To make matters worse the harmful carbon dioxide and greenhouse gas emissions directly associated with fossil fuel combustion has consistently been proven to be detrimental to the Earth's climate; negatively effecting the natural environment and humanity's living standards. To ensure energy security and the preservation of the natural environment an energy transition is needed.

The penetration rate of renewable energy has rapidly grown since the turn of the century currently accounting for 24.5% of electricity produced globally. Renewable energy technologies have proven to be an ideal replacement of fossil fuels. Harnessing energy from renewable abundant sources such as the sun, wind and waste allows for nations to become self-reliant in terms of meeting their energy needs. In this manner the issue of meeting rapidly growing energy demands and climate change mitigation are simultaneously addressed. With the field of renewable energy gathering increasing momentum and global attention, the development of the required technologies has lead to decreasing prices and their increasing effectiveness. These trends will allow renewable sources of energy to become a cost-effective and widespread solution in the energy market.

Unlike the traditional approach whereby a single technology and fuel has dominated the energy industry, the successful power system of the future will most likely employ a wide range of technologies to harness energy from a variety of sources. Due to its intermittent nature, energy harnessed from renewable sources such as the Sun and wind requires effective management ensuring a reliable delivery of energy. It is important nations do not rely on a single source of energy and that the energetic potential of each of the sources is fully understood.

1.2. SIGNIFICANCE OF SOLAR ENERGY

The immense magnitude of available solar energy makes it an appealing source of energy. The United Nations Development Programme (UNDP) has estimated that the available solar energy on Earth lies in the range 1,575-49,837 EJ. Compared to the world energy consumption,in 2012 of 559.8 EJ; the abundance of the energy source is apparent[15]. Photovolatic technology has developed rapidly over the last 30 years resulting in lower costs with increasing installed capacity, a trend that is expected to continue. Figure 1.1 shows the decreasing price trend for c-Si and CdTe solar cell technology as a function of cumulative production volume, a consistent trend spanning the last 40 years. According to the International Energy Agency (IEA) by 2050 solar energy is expected to account for 20% of the global energy production and by over 60% in 2100 [16]. However, as it currently stands a major barrier in limiting the penetration rate of PV technology is the high initial investment costs, resulting in lengthy, financially unattractive payback times.

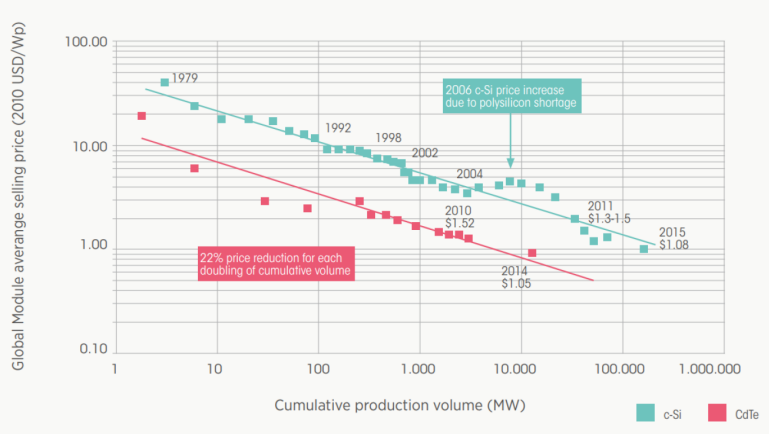

Figure 1.1: Historic trend of PV cost [1].

1.2.1. Role of PV-Battery Integrated Module

To combat the issue of high initial costs, the concept of a single PV-Battery Integrated (PBIM) module is proposed, Figure 1.3. Solar system costs can be reduced without improving component efficiencies. Instead to decrease overall costs, installation and Balance of System (BoS) costs are targeted. Figure 1.2 provides a cost breakdown for PV systems of various sizes for residential, commercial and utility applications. Residential systems are observed to be more expensive per watt-peak (W_p) since they do not benefit from economies of scale. Larger, more commercial systems have the benefit of acquiring large volumes of equipment at a time, driving down the price per unit. Commonly seen on the residential scale is the intricate customization of every PV system. Based on the available finances and the household energy requirements, the PV array, battery system and the compatible power electronics need to be identified and sized; a process which often requires the expertise of a hired professional. The installation of the PV system requires the connections between the various components to be completed and, as mentioned before requires the consultation of a technical expert to do so. These so called 'soft' costs that currently account for 40% of the total costs of a residential solar system. The proposed PBIM concept is aimed to reduce PV system 'soft' costs using existing and mature technology in an integrated modular fashion.

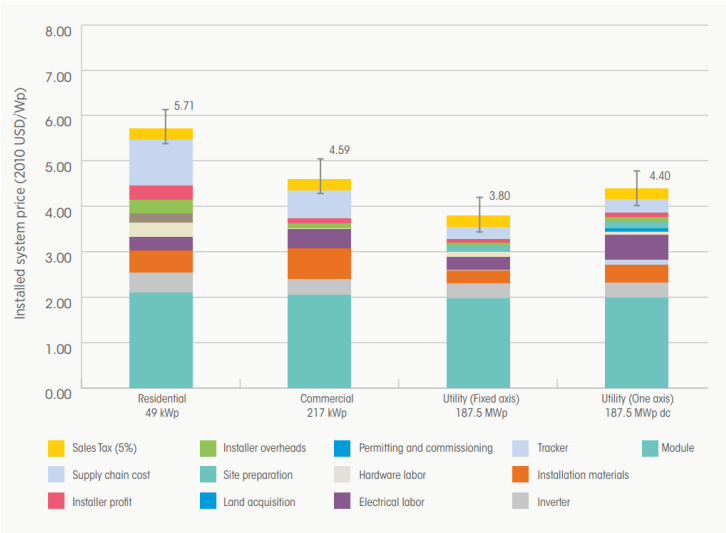

Figure 1.2: PV System cost breakdown [1].

Physically integrating the necessary BoS components at the rear of the actual PV module, creating a single modular and compact system, facilitates the installation process while making efficient use of the designated installation

space. With user-friendly characteristics the complexity of the installation process is reduced and thus requiring less technical expertise, influencing the installation costs. The development of a standardized solar system, such as the PBIM, removes the need for detailed system sizing customization. Such a system would then benefit from economies of scale and due to its modular nature be easily scalable. The capacity of the PBIM system can be altered by adding/ removing the desired number of PBIMs to match the current energy demands.

The potential role of the PBIM within the solar energy market is to address the high initial investment costs, commonly associated with conventional solar home systems. However, the physical integration of PV-battery systems is currently still in the early stages of development and does not come without any drawbacks. Due to its integrated nature the implemented design within the PBIM is expected to optimally perform in a wide range of applications and environments. The accurate sizing of the PBIM's energy storage capabilities has, to date, not been defined and will play a significant role in influencing the PBIM effectiveness. The energy storage sizing impacts the system's ability to store energy for use during times of low/no solar energy. Furthermore, the battery accounts for a significant amount of the total costs and thus over-sizing is to be avoided to ensure the PBIM is cost effective. This highlights the significance for the need for a robust system design. It would be essential to understand how the definition of an optimal PBIM system design varies with respect to its application and the surrounding environment.

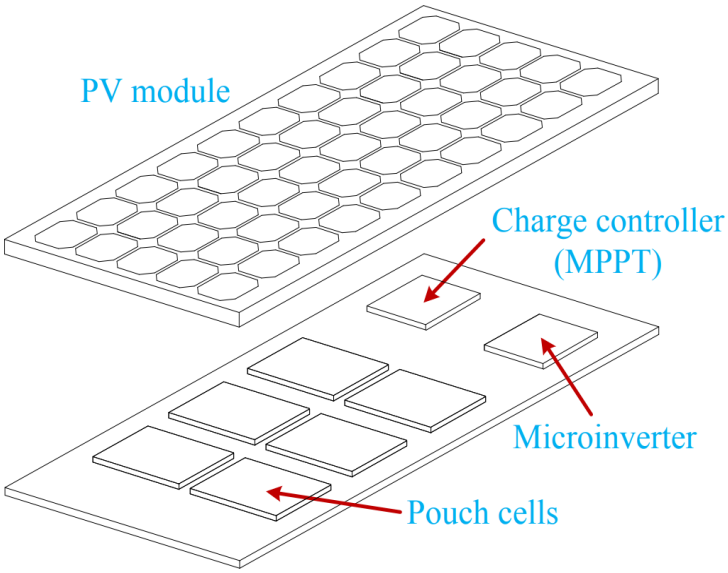

Figure 1.3: The PBIM concept; adapted from [2].

1.3. Thesis Objective

A core component essential for the effective application of the PBIM is its battery. This project is aimed at understanding the impact of external factors on the definition and sizing of the optimal battery capacity for enabling the competitive and optimal usage of the PBIM. The overall thesis objective is summarized in the following statement;

- *Propose and implement a sizing methodology to determine the optimal size of PBIM battery for its competitive application in selected scenarios.*

1.4. Research Questions

1. What is the impact of local weather conditions and energy storage motivations on the PV-Battery Integrated Module?
    - In which applications is the PBIM an effective solution?
2. What is the most appropriate battery size to install in a single PV-Battery Integrated Module for each energy storage scenario?
    - What are the system requirements for each energy storage scenario?
    - How can the appropriate battery size be identified?
3. How effective is an optimally sized PBIM for the identified scenarios?
4. How does an appropriately sized PV-Battery Integrated Module compare to a conventional solar system?

- How does the performance of the PV-Battery Integrated Module compare to a conventional system?
- Is the PV-Battery Integrated Module a financially viable solution?

1.5. Thesis Outline

Chapter 2 - Literature review
In this chapter, the evolution of the PBIM design is presented extending to include and justify the current design. Existing components are identified for their use in the PBIM concept, this selection is based on the compilation of identified components from previous studies. The potential applications of the PBIM are then discussed.

Chapter 3 - PBIM Modelling
The theory applied to model the dynamic characteristics of the incorporated components is presented. Included are simulation results capturing the dependence of the components on the operational conditions. The components are modeled taking into consideration the specific characteristics identified in chapter 1.

Chapter 4 - Grid-connected peak-shaving applications
The application of the PBIM for grid-connected peak shaving applications is modelled and assessed for different locations. The model of the individual components are grouped together and an energy control strategy is integrated to simulate a grid-connected system for peak shaving. This chapter includes an analysis of the system performance and implements a sizing methodology to identify the optimal storage capacity.

Chapter 5 - Off-grid applications
The effectiveness of the PBIM for off-grid applications in different locations is analyzed. Similarly to Chapter 4 the appropriate battery size to install in a single PBIM is identified. A comparison is made between the systems simulated for the different locations.

Chapter 6 - PV-Battery Integrated Module Feasibility
The feasibility of the PBIM concept with respect to technical and financial aspects are discussed in this Chapter and comparisons are made with a conventional system.

Chapter 7 - Conclusions & Recommendations
In this chapter the research questions are answered based on the findings of this project. Finally, in hindsight recommendations for future work and improvements are outlined.

2

Literature Review

The first step in investigating the dynamic behaviour of the PBIM is to explore previous research related to its design and application. This Chapter aims at explaining, in detail, the PV-Battery integrated Module concept and extends to include a literature study presenting the findings on the physical integration process of PV-Battery systems and identifying existing designs. Additionally, energy storage sizing methodologies for comparable projects are discussed.

2.1. PV-Battery Integration

The PBIM is a relatively recent concept sparking interest from both private firms and research institutes. The concept of integrating energy storage together with PV cells began on a small scale, with the integration of a capacitor into a solar cell and demonstrated a storage efficiency of 5.12% ; laying the foundations for future work [17]. This evolved into the integration of lithium-ion cells and solar cells; mainly low power systems for portable and wearable applications . However, these primitive solutions tended to be inefficient due to the lack of battery charging and discharging schemes[18]. This highlighted the need to also incorporate the appropriate power electronics. Early studies describe the integration of inverters to a PV module, an AC output PV module is presented in [19].

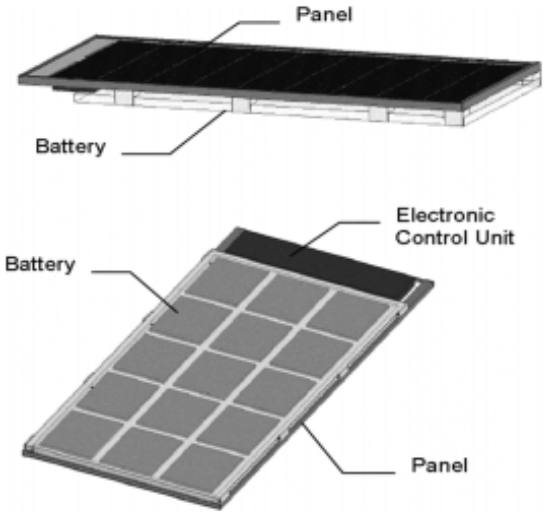

Figure 2.1: The 'Multifunctional lithium-ion module' [3]

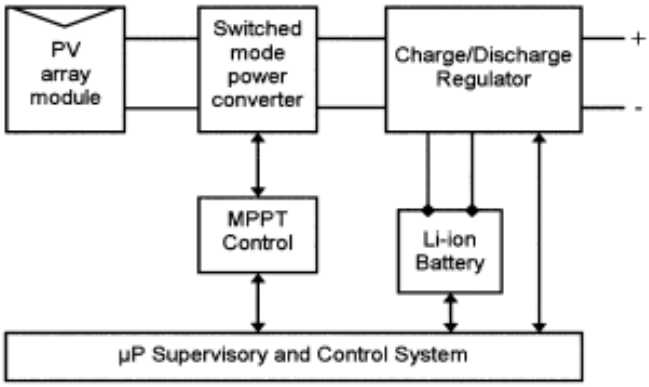

Figure 2.2: Architecture of the 'Multifunctional module' [3]

According to the literature study presented in [4], the integration of an energy storage unit, PV module and the electronic control was initially proposed by [3] (Figures 2.1 & 2.2). A prototype of this concept was built and tested; a pioneering design due to the inclusion of the supervisory and control system design to control both the Maximum Power Point Tracker (MPPT) and the charging cycles of the battery. This study demonstrates the dynamic manner in which the integrated concept can be used as well as outlining a few restrictions. However, it does not cover its key technical features. The evolutionary time-line of the PBIM concept extends further with additional studies directed towards the battery management system which is subsequently used to supply larger loads [18].

Additional Benefits

In addition to the benefits outlined in Chapter 1 additional advantages of PBIM usage have been identified.

1. **Reduced shading losses**
   Each PV module is connected to its exclusive MPPT, this implies better utilization per PV module. Shading effects across the entire PV array will have a smaller impact compared to a centralized conventional system [20].

2. **Modular approach**
   Appropriately scaling the system with respect to the energy demand is facilitated by adding/removing a PBIM in parallel. This eliminates having to initially oversize BoS components in a centralized solar system in anticipation of future system expansion.

3. **Portable**
   Due to its compact and modular nature the PBIM is portable, expanding its application spectrum to include back up solutions; increasing the system's reliability.

Expected Challenges

1. **Heat Management**
   High internal operation temperatures are expected in the PBIM, therefore in order to ensure component longevity and optimal performance the implementation of a cooling system is required.

2. **Optimal Sizing**
   The PBIM is expected to be used for a variety of applications, however to define the optimal storage size for such dynamic usage will result in a sub-optimal storage capacity as compared to the conventional solution whereby the optimal storage capacity is customized for each system.

3. **Component Selection**
   The appropriate underlying technology of the implemented components, especially the battery, is restricted. The desirable battery characteristics include high cycle lifetime, influencing the lifetime of the PBIM as a whole. Furthermore, the appropriate battery technology should be capable of nominal operation at a wide range of ambient temperatures. The maximum weight of the PBIM is limited. The PV panel and battery selection should reflect these restrictions. To make optimal use of the restricted space at the rear of the PV panel the battery energy density should be high, allowing for ample space thus facilitating heat removal.

2.2. PBIM Design

Incorporated into the PBIM design are decisions aimed towards tackling the previously mentioned challenges and system objectives. The design process takes a multitude of factors into account. The relation between the system variables are depicted in Figure 2.3 and highlights the dependence of the final component sizing on the external variables such as the applied technology. Previous studies have been conducted regarding the PBIM design and have been summarized in this section.

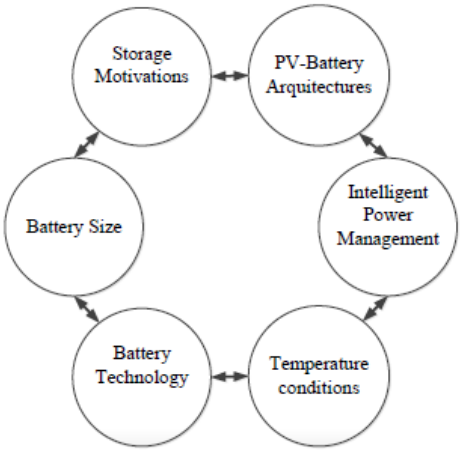

Figure 2.3: Interdependence of system variables. Image from [4].

2.2.1. Design Constraints

The modular and compact characteristics of the PBIM create design constraints that may have otherwise been inconsequential for conventional solar home systems. These constraints influence the overall design and component selection of the PBIM.

Parameter	Value
Efficiency (%)	16.19
Maximum power (W)	265
Nominal voltage (V)	31.4
Nominal current (A)	8.44
Open Circuit voltage (V)	38.6
Short Circuit current (A)	9.03
Module length (m)	1.65
Module width (m)	0.99
Module area (m^2)	1.63
Temp coeff Pmmp (%/°C)	-0.41
Temp coeff Voc (%/°C)	-0.31
Temp coeff Isc (%/°C)	-0.06

Table 2.1: PV Module Characteristics at Standard Testing Conditions (STC).

Parameter	Value
Dimensions (mm)	7.25 x 16
Capacity (Ah)	19.5
Nominal Voltage	3.3
Specific Energy (Wh/Kg)	131
Operating Temperature (°C)	-30 to 55

Table 2.2: Battery Characteristics

Heat Constraints

Incorporating the battery to the rear of the PV module will inevitably lead to higher operating temperatures of the PV module, battery and the power electronics. To minimize the negative effect of elevated temperatures the design takes into consideration the optimal distance between the PV module and the battery. Installing the battery bank too close to the module will severely limit the heat removal from the PBIM via natural convection. On the other hand, installing the battery at greater distance from the PV module will increase the size, weight and thus the ease of installation of the PBIM. An elaborate thermal analysis of the PBIM is presented in [4].

Component performance and lifetime are greatly dependent on temperature. The significance of temperature on the component partially depends on the component characteristics, therefore, by selecting components capable of efficiently operating in elevated temperatures, the negative influence of temperature can be minimized.

Physical constraints

The dimensions and weight of the PBIM play a role in ascertaining its effectiveness as a portable and modular solar system solution. For residential applications most of the PV modules are installed on rooftops, this implies that the weight of the PBIM is limited by the rooftop weight carrying capabilities. Furthermore the available area is also often limited thus requiring the PBIM to adhere to such constraints. Taken into consideration in the component selection process is the specific energy Wh/Kg of the components which ensures the PBIM to be energetically effective within the weight and dimension constraints.

2.2.2. Component Selection

The optimal battery capacity to incorporate into the PBIM is significantly impacted by the component characteristics and the implemented control strategy, it is therefore necessary to predefined these variables. In previous studies [18] & [21] the PV module, battery and power electronics have been separately defined. In this section the current PBIM design is outlined, and the component characteristics are used as data inputs in an effort to optimally size the battery.

PV Module

The performance of the solar module is heavily influenced by ambient irradiance and temperature. Optimally selecting a PV module based on the expected operational ambient conditions will enhance the PV module performance and thus result in a higher energy yield. In [21], a comparison was conducted between commercially available PV modules with the potential for PBIM usage. The module's weight, rated power, price and temperature coefficient properties were considered in this comparison, thereby ensuring the selected PV module had the necessary desirable characteristics and remain cost effective. As a conclusion of the comparison, the Jinko Solar 265Wp poly crystalline solar module was selected and its characteristics are presented in Table 2.1.

Energy Storage

The Prismatic Nanophosphate Lithium-ion pouch cell from A123 systems is implemented into the PBIM. Lithium-ion technology posses good power and energy density (Figure 2.4) as compared to other available battery technologies. Throughout the discharging process lithium-ion batteries maintain a constant voltage until the battery is almost discharged; allowing for greater discharging efficiency, unlike the previously popular lead-acid batteries. The implemented battery has an expected lifetime of 5000 cycles when operating at 25 °C, therefore ensuring the lifetime of the integrated module is maximized. In addition, the shape of the batteries are ideal. Their compact rectangular form allow for optimal space usage, Figure 2.5.

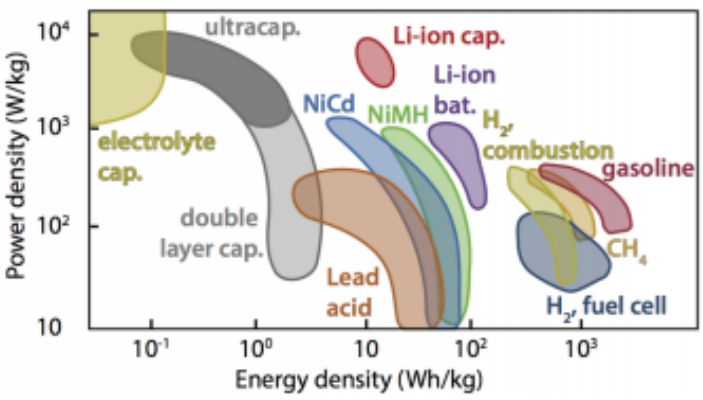

Figure 2.4: Ragone plot of various energy storage methods [5]

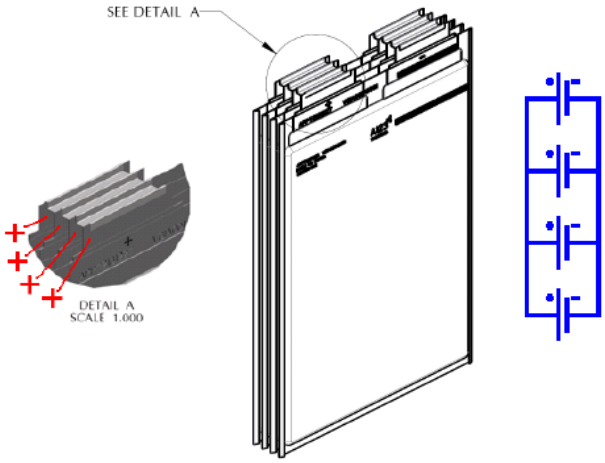

Figure 2.5: Assembly of multiple Prismatic cells connected in parallel [6]

2.2.3. System Architecture

Based on the work presented in [21] & [7], the AC coupled architecture has proven to be effective when considering the integrated PV-battery systems. An AC bus is utilized for the interconnection between the battery and PV module, Figure 2.6. This construction requires a unidirectional DC-AC inverter between the PV panel and AC bus. A bi-directional DC-AC inverter is also needed between the battery and the AC-bus and its function varies depending on the battery activity (charging/discharging). The AC loads or the grid is connected directly to the AC bus.

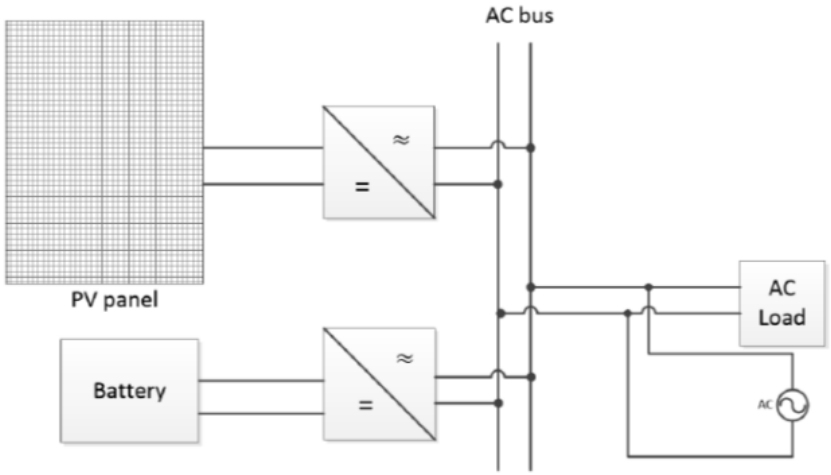

Figure 2.6: The AC-coupled system architecture [7].

2.2.4. Power Electronics

For the selected topology two power converters are needed. The uni-directional inverter connected to PV module is incorporated with MPPT capabilities to alter the operating voltage of the module in response to the weather conditions; ensuring its efficient operation. To optimize battery lifetime charging and discharging needs to occur in accordance with the nominal battery characteristics, a charge controller is used to serve this purpose. Based on the battery characteristics the charge controller can be programmed to dictate battery charging. In this setup the charge controller and the bi-directional inverter consist of a single device, converting between the DC battery requirements and the AC bus.

2.3. Applications

To reap the full benefits the PBIM has to offer, it application in the residential sector is deemed the most suitable. The PBIM is equipped with a battery, the motivation for its use varies depending on the required level of autonomy. In this section the residential applications in which the PBIM could potentially become a competitive technical solution in the solar energy market are defined. The energy storage motivations for residential applications depend on the whether the system is connected to the grid.

The use of batteries in grid connected systems is becoming increasingly common and are used for a variety of reasons. For instance, batteries are used for smoothing solar power generation and preventing sudden spikes in delivered energy. In terms of microgrid stabilization, the grid connected batteries provide frequency and voltage regulation or simply as a backup during islanding mode. Additional applications such as diminishing congestion and peak shaving may also be considered. However, solely from a single household point of view, few of the mentioned applications are relevant. On the other hand, solar systems that lack grid connectivity require a higher level of autonomy which intuitively requires a solar system with greater energy storage capabilities than grid-connected systems. Such off-grid applications are especially relevant for the PBIM, particularly for its application in rural regions of developing countries. Taking this into consideration the PBIM is potentially an effect solution for both grid-connected and off-grid scenarios.

The PBIM concept has, to date, been analyzed for a variety of energy storage motivations and locations. A case study presented in [21] analyses the effectiveness of the PBIM for grid-connected applications in Costa- Rica and the Netherlands. The considered energy storage scenarios are for peak-shaving and reducing the dependence of a household on the grid and extends to provide a comparison between conventional and PBIM systems. The off-grid application of the PBIM in Cambodia is presented in [22], whereby the system requirements and performance is assessed. This project aims to extend upon this previous work.

2.3.1. GRID-CONNECTED APPLICATIONS

From a residential energy consumer point of view, motivations for shifting to renewable energy technologies is predominately due lower overall cost. Since 71% of consumers would adopt renewable energy technologies for lower overall cost and only 48% for sustainability reasons [23], the implementation of the PBIM in a grid connected scenario would predominately be to reduce the household energy cost, and this objective can be accomplished in a number of ways. For a PV system without any energy storage, the generated energy from the PV array can be used directly by the loads. In the case excess energy is generated, this can be exported to the grid. Depending on the energy provider different compensation schemes are offered to the electricity consumer, who now becomes an electricity producer i.e a prosumer [5]. These concepts are net-metering and feed-in tariffs and in this manner the prosumer is able to reduce their energy costs. On the other hand, incorporating energy storage into the grid connected PV system, as is the case with the PBIM, the energy generated by the PV array can be stored and either be used or sold to the grid during a time period when the energy prices are high. Energy demands on a national scale vary throughout the day, based on the demand and supply energy providers set the energy selling price which therefore also varies throughout the day. A household's peak load often coincides with the peak demand hours of the grid, resulting in higher energy costs during this time period [8]. During weekdays the household peak load typically occurs during the morning or evening when people are at home [24]. Therefore, there is a mismatch between periods of high energy demands/costs and the PV generation. The implementation of the energy storage bridges the temporal gap between the PV array energy generation and the hours of high energy prices (peak hours) allowing for the prosumer to incur additional financial savings. The peak shaving concept is depicted in Figure 2.7, which illustrates the redistribution of power throughout the considered time period. The recharge period occurs during off-peak times, whereby energy is used to charge the battery; resulting in an increased apparent load. The battery is then discharged during the peak period, decreasing the apparent power during this time period. The peak of the load profile is shaved by meeting the peak load requirements with the energy stored from the battery.

As a worldwide trend, the design of energy distribution grids deviates from a centralized design and approaches a decentralized configuration. Traditional centralized bulk power systems are characterized by a uni-directional power flow from the generating units to the consumer. However as the penetration rate of renewable energy sources increases and with the introduction of new technologies such as electric vehicles a high variability of energy demand and supply is expected. This also results in the bi-directional power flow in power systems, whereby energy can be both imported and exported from the grid by private consumers. This deviation from the traditional centralized power system introduces increased dynamic energy pricing and therefore makes peak shaving a very interesting application for the PBIM.

2.3.2. OFF-GRID APPLICATIONS

The demand for autonomous energy systems is rapidly growing particularly in many unelectrifed regions across the globe. These regions tend to predominately be rural areas of developing countries, who either have access to an unreliable grid or no electricity access [25]. The introduction of off-grid solar systems in such circumstances face many barriers, with high upfront costs proving to be the biggest hurdle. Offering the advantages of lower upfront costs, scalability and ease of use that typical solar solutions did not offer, the PBIM possess characteristics to be a competitive solution in this field of application,and is therefore considered in this thesis.

2.4. ENERGY STORAGE SIZING

Appropriately sizing the energy storage capacity for PV systems has been widely researched and its typically dependent on the energy scenario for which it is applied. Energy storage costs account for a significant fraction of the overall system costs and thus for economic reasons, should be refrained from being oversized. On the other hand,

Figure 2.7: The peak-shaving concept [8].

undersized batteries potentially lead to a reduction in system functionality, this highlights the need of optimally sized energy storage capacities, ensuring low investment costs and full use of the system component. The system battery size is dependent on the application of the PV system (grid-connected or off-grid) and its location. Most the sizing methodologies found in literature are categorized into 4 groups and presented in Figure 2.8. With each sizing technique possessing their own benefits and challenges. Sizing parameters (decision variables) are selected to provide insight on the functionality of the system with respect to the task it has been designed for. Assessing the manner in which the sizing parameters and the system functionality are affected by different battery capacities, an optimum can be selected. In this section various decision variables are explored.

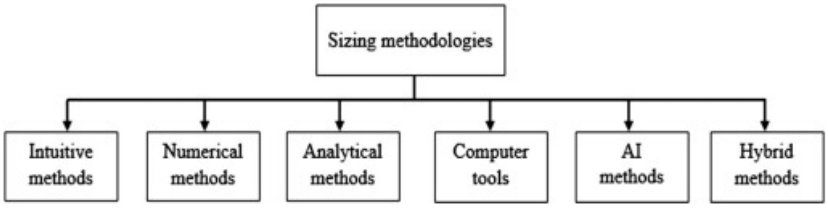

Figure 2.8: Potential sizing methodologies.

2.4.1. Performance Index

To obtain the optimum design a set of decision variables (evaluation parameters) need to be defined. These variables describe the system in terms of its technical, economic, social and political parameters; and are elaborated on in this section.

Technical Parameters

As a consequence of the intermittent nature of solar radiation, it is important to quantify the dynamic technical characteristics of the system. These parameters could relate to specific components or to the system as a whole. Characteristics such as the Loss of Load Probability (LLP), battery degradation or component operating efficiency.

Economic Parameters

A common parameter system designers strive for is a fully functional system operating at the lowest possible cost. These costs can describe either the initial capital investment, levelised cost of electricity or total life cycle cost. Economic parameters provide insight on the cost effectiveness of system and aims to distinguish between systems that are technically sound but with high costs and those that posses comparable technical capabilities and cost considerably less.

Social and political Parameters

Social and political parameters are often considered before installing renewable energy systems as it may affect the proposed design. Social acceptance is often considered, and can be described in terms of the use of land or any potential visual effects the system may impose. This category can also be expanded to include the incentives provided by governmental bodies for the development of renewable energy systems.

2.4.2. Sizing methodologies

A literature study has revealed an extensive range of sizing methodologies. A summary of which is presented in this section.

Intuitive Methods

The intuitive methodology is the simplest of sizing methods and disregards the the quantitative relation between the components of the PV system. Typically the system is sized based on simplified calculations using averaged out data inputs across a design period. The formulation of sizing coefficients are required and are chosen based on the designer's intuition and experience; increasing the chances of subjective results. Due to its simplistic nature, the implementation of intuitive methodologies has the disadvantage of resulting in sub-optimal configuration of the system; potentially causing low system reliability and/or higher capital costs than necessary [26].

Numerical Methods

In this case a system simulation is used for each time period (hour/day). This method is significantly more accurate than intuitive methods as the energy balance of the system is determined allowing for the performance assessments to be applied in quantitative manner. This method yields simulation results representing the dynamic behaviour of the system to allow optimization of the energy and financial costs of the system. The majority of optimal sizing methodologies researched were found to implement this technique [27].

Analytical Methods

The analytical approach is based on the characterization of the PV system components through mathematical models as a function of the system's performance indexes (LLP, economic benefit), to provide an insight on the system feasibility. The performance of the complete system is analyzed based on a feasible set of component sizes. The performance indexes for each of the feasible configurations are evaluation against one another. The computation effort needed for the implementation of analytical methods is minimal, however its major disadvantage is the need to estimate location dependent system performance coefficients [28].

Artificial intelligence.

This methods requires high computation effort for the implementation of algorithms such as Particle Swarm optimization (PSO), genetic algorithm (GA), artificial neural networks (ANN) and fuzzy logic (FL). Reported use of such algorithms for optimal storage sizing of PV systems is minimal. Typical usage in comparable projects has been reported for meteorological data prediction. However, the use Artificial intelligence methods are predominately used for hybrid PV systems whereby multiple sources of energy are considered.

2.4.3. Comparable Studies

In this section, the optimization methodology and decision variables used in comparable optimization problems are presented.

Off-grid

Batteries incorporated into off-grid systems are optimized to cover the load demand at a specified reliability [27]. For regions with greater solar irradiance variation throughout the year typically require larger batteries than in regions that experience minimal variations in annual solar irradiance. Such systems are undersized during the summer period and oversized in the winter; factors which are taken into consideration to ensure the optimal usage of the system. The implemented batteries are expected to posses discharge rates capable of meeting peak load demand and be large enough to ensure energy delivery for nighttime energy use and during periods of unfavorable ambient conditions [29]. In [30], optimally sized batteries for off-grid applications were obtained based on minimizing Loss of Power Supply Probability (LPSP) [30] using numerical methods. In [31], an analytical approach was adopted based, in the case the desired LLP is selected prior to any optimization, the system is then optimized based on the levelised energy cost of the possible system configurations. Another analytical approach is presented in [32] whereby general equations relating the LLP, PV capacity, battery capacity and load are derived. Similarly the desired LLP of the system is predefined. In [33], a numerical approach was adopted and the relation between the LLP unit cost of PV electricity was used as optimization parameters. Likewise, in [34], via numerical methods the system is optimized based on the LLP and the overall system cost. In [35] the LLP is described in economic terms namely as the Value of Lost Load (VLLP). This estimates the economic value incurred by the user when the energy demand is not met. The system is then sized based on the relation between the LLP and the life-cycle costs.The work presented in [36] uses a predefined LLP and system cost; using a generalized artificial neural network (GRNN) the PV sizing curves are predicted for a defined location.

GRID CONNECTED

On the other hand are grid-connected PV systems, whereby autonomy is typically a secondary goal. Instead the batteries of such systems are used for economic benefit via peak shaving or arbitrage in addition to reducing the fluctuating PV power generation or reducing strain on the grid. This highlights the variety of variables on which to base the optimization objective function. A numerical approach outlined in [37] regarding peak shaving applications, describes an optimization methodology based on minimizing the systems costs (Energy brought form the grid and costs relating to battery capacity loss).Similarly, in [38] the battery is sized to based on a economic objective function, which in this case, is defined as the benefit (profit) for system user. In [39], the optimization of the generation and storage of hybrid microgrid is solved via genetic algorithms to minimize costs whilst maximizing system reliability. Ultimately, the optimal solution is dependent on inputs by the decision maker to defined the relative weights of each decision variable.

2.5. CONCLUSIONS

The sizing methodology adopted for this project is the numerical method approach whereby simulations are performed to quantify the system characteristics and provide data on which to base the sizing methodology. Despite available literature presenting the sizing approaches for conventional PV system, the method in this case is adopted for the sizing of the PBIM, forming a core contribution of this project. The performance indexes considered for the PBIM's application for off-grid applications are based on reliability and capital cost characteristics. On the other hand for peak shaving applications the system's dependency on the grid and the system's capital cost will be considered. This project will also extend to consider the impacts and the extent of battery aging.

3

PBIM MODELLING

To size the energy storage capacity of the PBIM, the dynamic behaviour of the system characteristics need to be understood. A model of the PBIM was constructed in Simulink/MATLAB environment to incorporate the component interaction and operational characteristics. Since the component performance is dependent on ambient conditions such as available solar energy and ambient temperature, it consistently varies. To accurately propose an appropriate energy storage capacity these factors must be taken into consideration. Furthermore, with the battery contributing to a significant portion of the overall cost, its estimated lifetime is essential, especially due to its operation in the elevated temperature environment at the rear of the PV module. Therefore, this model dynamically assesses the degradation of the battery. In this section, the theory used to model the different components in the PBIM is outlined.

3.1. PHOTOVOLTAIC MODULE

The energy generation is determined by the PV module operating characteristics as well as the ambient weather conditions. The theory required to model the effect of temperature and incident irradiance on the PV module's output power is presented in this section.

3.1.1. AVAILABLE SOLAR ENERGY

As the incoming solar radiation enters the Earth's atmosphere it decomposes into different components; direct (G_M^{direct}), diffused (G_M^{diffuse}) and reflected from the ground (G_M^{ground}). Each contributes to the total apparent solar energy incident on the PV module, defined as the global irradiation G_M.

$$G_{\text{M}} = G_{\text{M}}^{\text{direct}} + G_{\text{M}}^{\text{diffuse}} + G_{\text{M}}^{\text{ground}} \tag{3.1}$$

Since orientation of the PV module remains fixed throughout the day and the year, the position of the Sun affects the amount of direct irradiance the PV module is exposed to. By quantifying the angle of incidence (γ) the amount of direct irradiance the PV module is exposed to is determined, taking into account the solar altitude (a_S), azimuth (A_S) and the PV module tilt angle (θ_M) and azimuth (A_M) the angle of incidence is defined to be:

$$\gamma = \cos^{-1}[\sin(\theta_{\text{M}})\cos(a_{\text{S}})\cos(A_{\text{M}} - A_{\text{S}}) + \cos(\theta_{\text{M}})\sin(a_{\text{S}})] \tag{3.2}$$

The direct irradiance can then be derived from the Direct Normal Irradiance (DNI) via equation 3.3

$$G_{\text{M}}^{\text{direct}} = \text{DNI} \cdot \cos(\gamma) \tag{3.3}$$

The power output of the PV module is also dependent on the module temperature, which dictates its operating efficiency. Through the implementation of the Fluid-Dynamics (FD) thermal model the fluctuating module temperature T_M is estimated. Meteorological effects affect the thermal process associated with the module, the FD model offers a good approximation as ambient wind speeds are taken into account into the energy balance between the surroundings and the PV module. The modelling methodology is based on the research presented in [40]. The simulation results of the module temperature during the daylight hours of a single day is presented in Figure 3.1.

PV manufacturers provide temperature coefficients for the module output characteristics such as the open circuit voltage, short circuit current and maximum power output. In the case of the Jinko 265Wp module, this is found to be -0.41 %/°C regarding its maximum power output. Combining efficiency as a function of temperature and irradiance, the module area A_M and the global irradiance incident on the PV module, the DC power generation is determined using equation 3.4.

$$PV_{\text{DC}} = \eta(T_{\text{M}}, G_{\text{M}}).G_{\text{M}}.A_{\text{M}} \tag{3.4}$$

3.1.2. PV PERFORMANCE

The effect of meteorological effects on the temperature of the PV module depends on whether a PBIM or conventional system is considered. In the case of the PBIM proper ventilation is impeded by the BoS components, causing less heat to dissipate from the module as compared to a conventionally installed PV module. As a consequence of lower heat dissipation the PBIM PV module is expected to operate at higher average temperatures which negatively impact its operating efficiency, indicating higher losses. Elevated temperatures have the effect of increasing the module's current, however the resulting voltage drop renders the current increase negligible [22]. The poor ventilation properties of the PBIM are presented in Figure 3.1 in which the module temperature of the PBIM is seen to be consistently higher than the module temperature of a conventional solar system. The methodology to estimate the PBIM PV module temperature is obtained from [18]. The operating efficiency is also shown to vary throughout the day. with the PBIM experiencing lower efficiencies particularly during the middle of the day.

3.1.3. METEOROLOGICAL DATA

The meteorological data inputs required to model the PV module power generation is obtained from Meteonorm, a widely accepted and used source of solar irradiation data, wind speed, cloud cover and ambient temperature. The data is acquired for a total time period of a year at a resolution of 10 minutes.

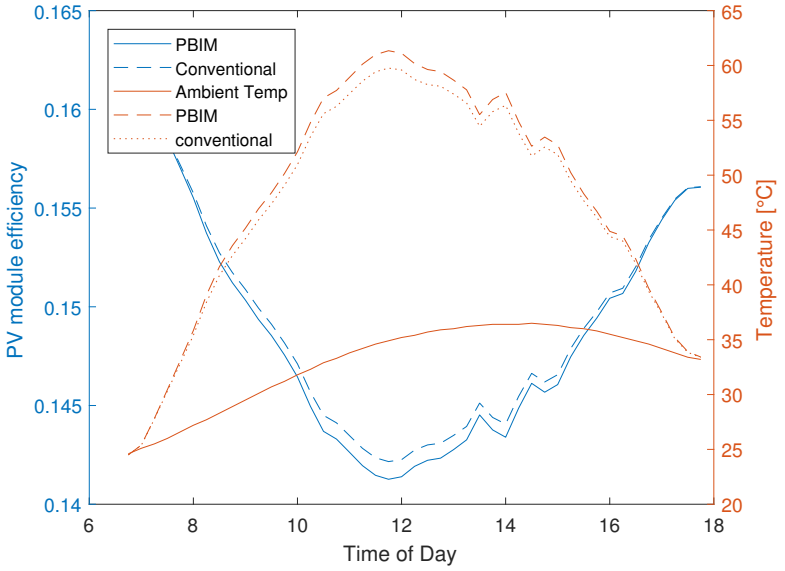

Figure 3.1: Change in PV efficiency as a function of module temperature for the 1st of January, Costa Rica.

3.2. BATTERY

To produce an accurate solution to the sizing problem the generated data takes into account dynamic battery characteristics under the influence of discharge rates, ambient temperatures and cycling to estimate battery degradation. This provides an insight on the decrease in the battery's usable capacity and determine a reliable indication on the expected battery lifetime under the defined conditions; influencing both the energetic and economical characteristics of the overall system. Once the capacity of the nano-phosphate battery in question reduces to 80% of its Beginning Of Life (BOL) capacity, battery replacement is required [6]. The incorporated battery modelling technique outlined in this section applies the battery characteristics provided by the battery manufacturer [6] to ensure realistic results.

3.2.1. AGING MECHANISMS

The aging mechanism in lithium-ion batteries are complex and aging effects such as capacity loss and power fade do not originate from a single cause. The aging mechanisms can be categorized into either mechanical or chemical degradation and vary depending on the applied cell chemistry. In this section the aging mechanisms of Lithium-ion batteries are considered.

- **Chemical Degradation**
  Chemical degradation can mostly be traced back to Solid electrolyte interface (SEI) formation, loss of lithium, electrolyte reduction and decomposition, active material dissolution, binder decomposition and gas evolution [41]. SEI formation occurs as a result of a side reaction from the chemical interaction between the electrolyte and the negative electrode. The build up of film on the electrode surface increases the electrode's impedance and thus contributing to the cell's capacity fade. Other side reactions occur and accelerate the cell's aging. Operation at elevated temperatures generally leads to acceleration of the unwanted side reaction and thus negatively impacts the cell's lifetime.

- **Mechanical Degradation**
  In addition to side reactions lithium extraction and insertion lead to volume shrinkage and expansion, which often occurs inhomogeneously. These volume changes in the electrodes lead to tensile stress which often results in the formation of cracks in the active material, reduced contact between neighbouring active particles and/or the current collector [42]. The extent of effects become more pronounced as a function of cycling. This has the negative effect of reducing the effective capacity of the battery.

A brief outline of the causes, effects and influences of battery aging are presented in Table 3.1. The aging effect of the battery was considered important in assessing the PBIM performance. Therefore these degradation effects are included in the PBIM model.

Cause	Effect	Leads to	Enhanced by
Electrolyte decomposition (SEI)	Loss of lithium	Capacity fade	High temperatures
Contact loss of active material due to structural changes	Loss of active material	Capacity fade	High Cycling rate
Continuous SEI growth causing decreasing accessible surface area	Impedance rise	Power fade	High temperatures

Table 3.1: Battery Aging; causes, effects, and influences. Adapted from [11]

3.2.2. Efficiency

Similarly to the other PV system components, the battery efficiency is not constant, instead it fluctuates over time and dependent on a number of characteristics. The two main types of battery efficiencies are coulombic and voltaic efficiency.

The coulombic (Faraday) efficiency is indicative of the effectiveness of electron transfer to and from the battery. Charge is lost due to chemical inefficiencies and directly influences the usable battery capacity. The coulombic efficiency (η_C) is defined by the ratio of the charge extracted from the battery ($Q_{\text{discharge}}$) and the total charge put in the battery (Q_{charge}), considering a complete charge cycle,

$$\eta_{\text{C}} = \frac{Q_{\text{discharge}}}{Q_{\text{charge}}} \tag{3.5}$$

The voltaic efficiency provides an indication of the non-ideality of the battery, and can be referred to as the internal resistance. The internal resistance of the battery can be modelled as a function of temperature and SoC. The voltaic efficiency (η_V) is described as the ratio between average charging (V_{charge}) and discharging ($V_{\text{discharge}}$) voltages,

$$\eta_V = \frac{V_{\text{discharge}}}{V_{\text{charge}}} \tag{3.6}$$

Taking both the voltaic and the coulombic efficiency into account the battery round trip efficiency is then defined as:

$$\eta_{\text{Batt}} = \eta_{\text{C}} \cdot \eta_{\text{V}} \tag{3.7}$$

Therefore the round trip efficiency of the battery is also expected to vary according to the operating temperature and the SoC.

3.2.3. State of Charge

An important aspect of the battery to model is the charging and discharging characteristics which allow for the determination of the energy stored in the battery. The battery charging and discharging is modelled using the equations adopted from [43],

$$SoC = 100\left(1 - \frac{1}{Q}\int_0^t i(t)\,dt\right) \tag{3.8}$$

where Q is the maximum battery capacity in [Ah] and i is the battery current in [A].

3.2.4. Battery Regulation

To optimize the battery lifetime and operation it is necessary to regulate its usage. In this system the charge controller is assigned the task of ensuring the battery continuously operates within its nominal range. The battery reaches its end of life (EOL) when its capacity is 80% of its beginning of life (BOL) capacity.

- **Charge Regulation**
  The battery lifetime is heavily influenced by the charging constraints imposed on the battery. Overcharging and

deep discharging of the Lithium-ion battery results in the breakdown of the cathode and should be avoided. The battery aging process is accelerated by operating the battery at a high depth of discharge.

- **Voltage Regulation**
  The charge of the battery is terminated once the measured voltage reaches the recommend cut-off voltage. If the cells are connected in strings then the charging of the entire string is to be terminated once any one cell reaches the cut-off voltage level.

- **C-rate**
  The C-rate refers to the rate of charge/discharge of the battery. According to [6] higher C-rates negatively influences the cycle life of the battery. Faster rates are commonly associated with increasing the degradation of the electrodes; negatively influencing the battery capacity. Furthermore, high C-rates increase the internal temperatures of the battery.

The properties of every battery differ, therefore to ensure the accurate modelling of the A123 pouch cell the battery characteristics as provide by the manufacturer were used [6]. After estimating the SoC (section 3.2.3) the dynamic battery characteristics can then be determined via a look-up table. Figure 3.2 depicts the change of voltage as a function of SoC, observable is the non-linear voltage region towards the SoC high and low extremes. To ensure the battery delivers a relatively constant voltage throughout each cycle SoC limits are imposed. The initial constraints used are presented in section 4.2.2, this has the dual effect of ensuring constant voltage and ensuring the battery is not over-charged and over-discharged.

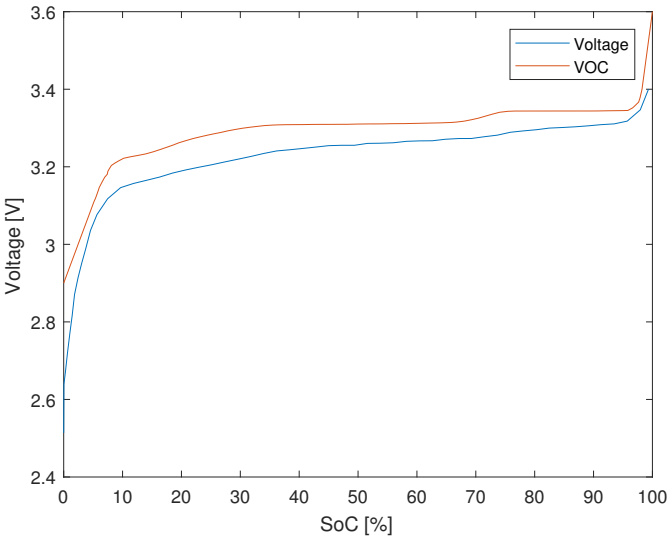

Figure 3.2: Cell voltage (1 C-rate)and VoC as a function of SoC.

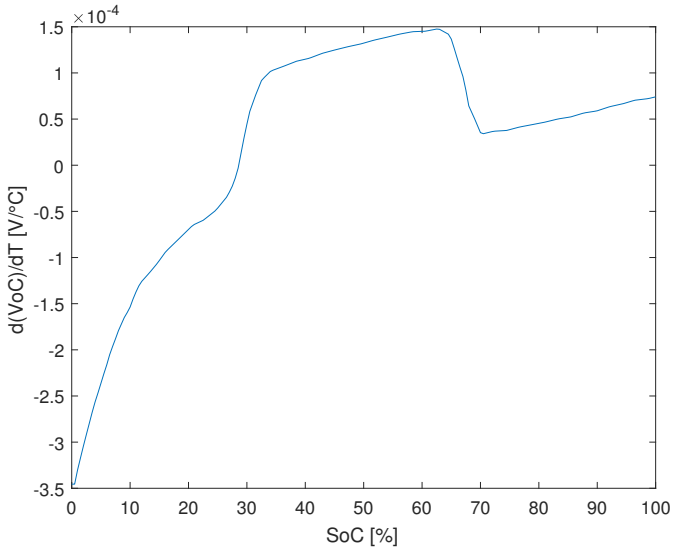

Figure 3.3: Temperature effect on VoC as a function of SoC.

3.2.5. Battery Temperature

Battery degradation is strongly dependent on the cell temperature. In the case of this model, only cell temperatures during periods of time at which the battery was active (dis/charging) are considered, this assumption can be made as the effect of battery calender aging can be considered minimal compared to the degradation due to cycling. To estimate the battery temperature during activity periods the cell temperature is said to be homogeneous with cooling occurring due to natural free convection. It is necessary to define the heat generation of the battery (q_{battery}) and heat dissipation via free convection ($q_{\text{convection}}$) which are described by the following expressions:

$$q_{\text{battery}} = I(V - V_{\text{OC}} + T\frac{\partial V_{OC}}{\partial T}) \tag{3.9}$$

$$q_{\text{convection}} = U(T - T_a) \tag{3.10}$$

where I is the charging or discharging current, V is the voltage, T_a is the ambient temperature, U is the heat transfer coefficient and T is the battery temperature. The battery open circuit voltage (V_{OC}), voltage curve (V) and the entropy coefficient ($\frac{\partial V_{OC}}{\partial T}$) are obtained from the manufacturer [6] and presented in Figures 3.2 & 3.3. The heat balance of the system is derived to be:

$$q_{\text{battery}} - q_{\text{convection}} = 0 \tag{3.11}$$

The temperature of the battery is determined for each time step to include the effect of the charging and discharging processes on the battery's heat production to predict its degradation. The battery temperature can then be expressed as:

$$T = \frac{U.T_a + I(V - V_{OC})}{U - I.\frac{\partial V_{OC}}{\partial T}} \tag{3.12}$$

The change in battery temperature throughout 24 hours is presented in Figure 3.4. Visible in the figure is the manner in which the battery temperature fluctuates depending on whether it is charged or discharged. For lithium-ion batteries the chemical reaction associated with charging is endothermic. However, in the figure the battery is assumed to remain at ambient temperature throughout charging. The discharge process on the other hand is exothermic as seen by increasing temperatures for a decreasing SoC.

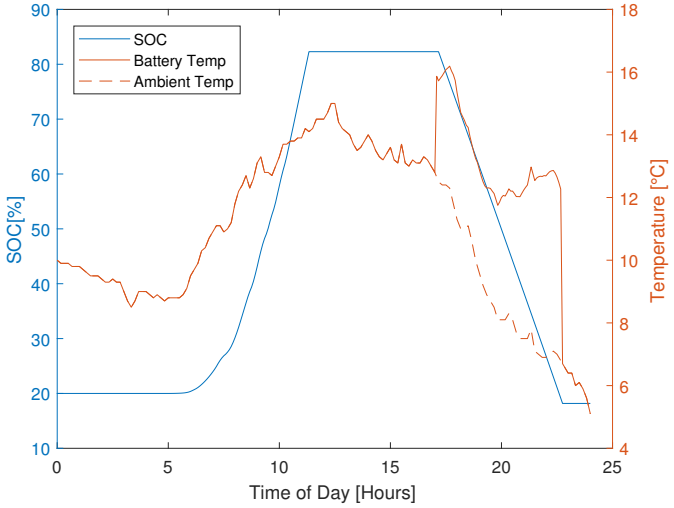

Figure 3.4: Simulated relation between battery temperature, SoC and ambient temperature

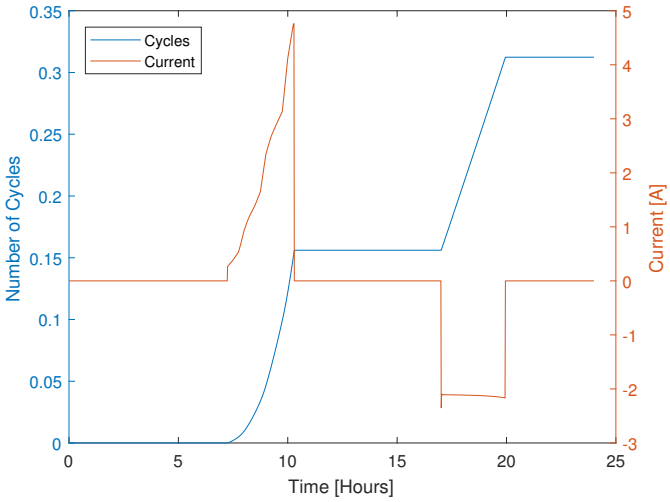

Figure 3.5: Simulation results of battery cycling.

3.2.6. Temperature Effects

Like the PV module, temperature significantly influences battery performance. Having mathematically described the battery temperature, the extent to which temperature affects the battery is explored.

- **Influence on capacity**
  The cell resistance fluctuates depending on the temperature. At low temperatures the cell's internal resistance increases, thus reducing the deliverable capacity of the battery. At high temperatures the battery is able to provide more power over a longer period of time, Figure 3.6.

- **Influence on lifetime**
  The deliverable capacity of the battery increases for higher temperatures. However, this also has the effect of accelerating the chemical degradation of the battery, as previously outlined. This effect is observable in Figure 3.7 where cycling at higher temperatures reduces the expected cycle life of the battery.

3.2.7. Cycling

In combination with temperature, the battery degradation depends on the cycling of the battery (Table 3.1). A cycle is defined as the process of complete charging and discharging [44]. Given the variability of the load and PV generation the number of cycles the battery undergoes per time-step will fluctuate. The specifications provided by battery manufacturers predict the aging of the battery for continuous and uniform cycling. The typical charging profile of batteries used for PV system applications depends on the power output of the PV module. Due to the high variability of available solar energy the battery charging current will unlikely remain constant throughout the charging cycle. This will influence the aging characteristics of the battery, therefore, the manufacturer aging specifications are inapplicable in this circumstance.

In this circumstance, the continuous charging and discharging is irregular. In this AC topology (Figure 2.6) the battery is charged according to the PV generation. Therefore the C-rate at which the battery is charged varies over the course of the charging cycle. To dynamically incorporate battery degradation, the concept of microcyling is introduced. A single microcycle is defined as the fraction of cycle the battery has undergone per activity period. As seen in Figure 3.5, during the period of time when the battery current is non-zero the cycle count is updated per simulation time step. By integrating the battery power exchange per micro-cycle the elapsed cycle number is determined. The battery current returns to zero, signalling the end of an activity period, whereby the total battery elapsed cycle number remains unchanged until the subsequent activity period begins. In this manner the battery cycling is dynamical

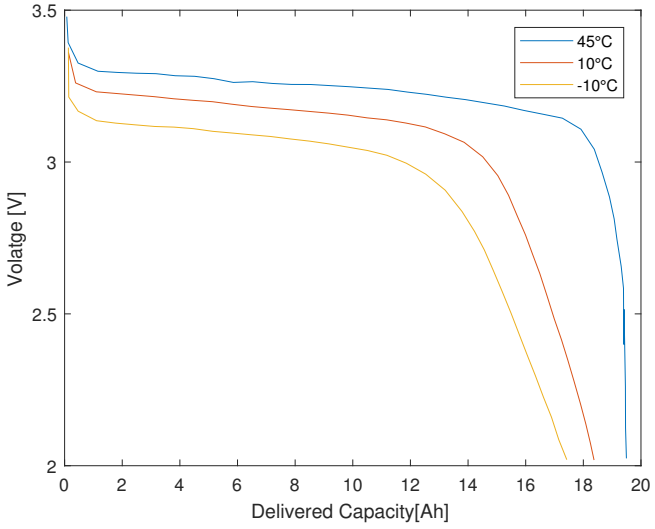

Figure 3.6: Voltage and deliverable capacity at various temperatures [6].

incorporated into the PBIM model. The dynamic, non-uniform cycling of the battery (N_{Cycles}) is incorporated into the model for each time step using the following expression:

$$N_{\text{Cycles}} = \frac{E_{\text{batt}}}{2.C_{\text{batt}}} \tag{3.13}$$

where E_{batt} is the absolute value of either the charging or discharging energy of the battery for the elapsed cycle and C_{batt} is the battery capacity.

3.2.8. AGING

The model evaluates the battery temperature and the fraction of a cycle for each time step. Combining these two battery characteristics for each time-step across the entire simulation, results in the quantification of the capacity loss. The calculated battery temperature is categorized into temperature ranges of 1°C and the aging coefficient (C_{aging}) (interpreted as the gradient of the appropriate curve) is derived from the manufacturer specifications (see Figure 3.7) for each time step. For higher temperatures the battery degrades at a much faster rate, this effect is thus included in the model.

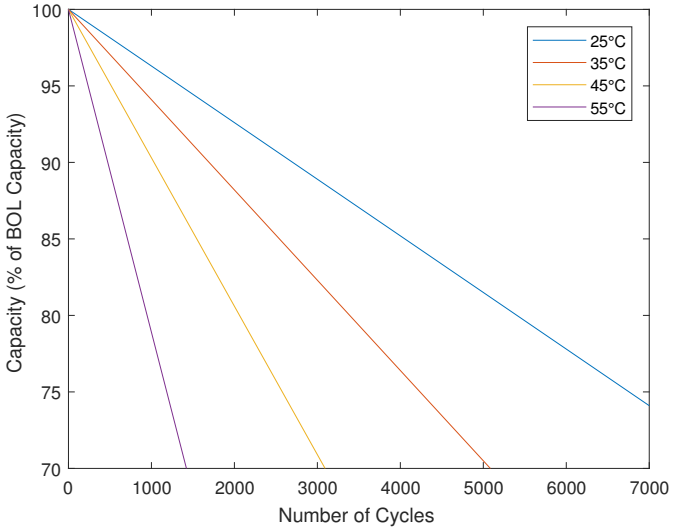

Figure 3.7: Cells Cycle Life (1C Dis/Charge rates, adapted from [6]

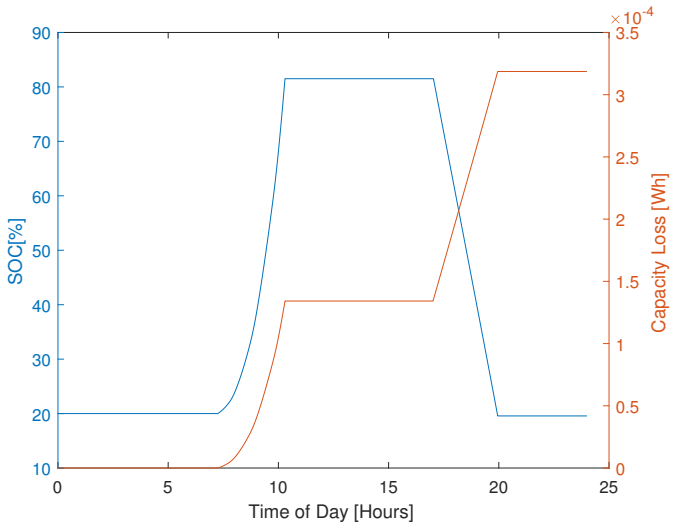

Figure 3.8: Simulation results of battery aging

The capacity loss C_{loss} per micro-cycle is then calculated:

$$C_{\text{loss}} = -\frac{C_{\text{aging}}.N_{\text{Cycles}}}{100}.E_{\text{BOL}} \tag{3.14}$$

The identified capacity loss is then used to update the nominal battery capacity in the subsequent time-step to continuously account for battery degradation. Figure 3.9 presents a flowchart which captures the manner in which the battery capacity loss is determined for each activity period. Considering the battery with no charging or discharging current its is assumed to be at ambient temperature in a state whereby there is no capacity loss.

Dynamically modelling the battery capacity loss

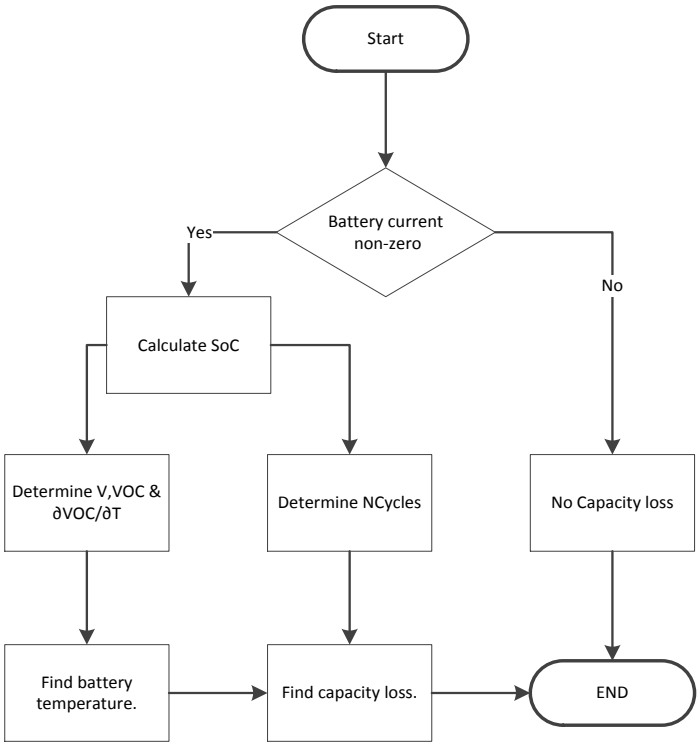

Figure 3.9: The algorithm used to model the battery capacity loss.

3.3. Power Electronics

The inverter efficiency is dependent on the input DC voltage and power. Therefore will vary depending on the load demand and PV generation [5]. The fluctuating nature of the inverter efficiency is captured in the model by obtaining the operating efficiency of the devices as a function of input power, from the manufacturer. Figures 3.10 & 3.11 present the efficiency as a function of power for the PV and battery inverter respectively. For PBIM applications each PV module is equipped with its unique inverter, which is sized according to the PV module power generation capabilities. As previously seen in Figure 3.1 the efficiency of the PV module drops below the rated STC efficiency as ambient temperatures rise throughout the day. The maximum power output of the PV module, therefore will be less than the STC power rating. The PV inverter is therefore sized based on the most probable range PV power generation so that the highest inverter operating efficiencies occur within this power range between 100W and 200W. The battery inverter on the other hand, is required to accommodate higher input powers in the event that the load dictates the discharge rate, as would be the case in off-grid applications.

3.3.1. Limitations

The theory presented in this section attempts to approximate a realistic situation as much as possible. However, the assumptions and limitations of the proposed modeling theory have been identified and are listed below.

- The battery and PV module are taken to be a single homogeneous masses with even temperature distribution, affecting the quality of the their thermal assessments.
- The battery temperature is modelled only during active periods of time. When the battery is neither being charged/discharged the degradation effects that may arise then are assumed to be negligible. (The effects of calender aging is omitted).
- Battery degradation estimates made for temperatures not provided by the manufacturer are obtained by interpolating the available data.
- The battery temperature during charging is assumed to equate to ambient temperature.

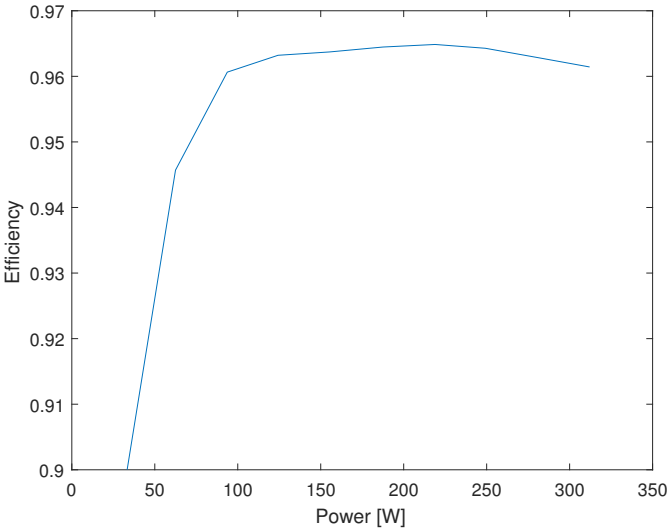

Figure 3.10: Efficiency of the PV inverter as a function of input power [9].

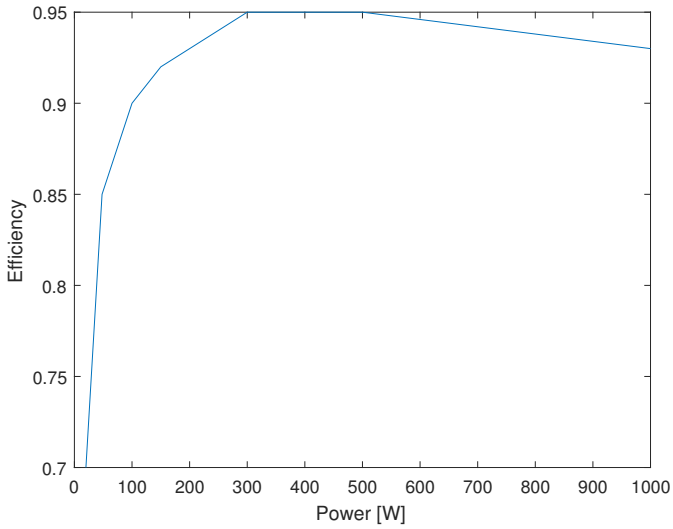

Figure 3.11: Efficiency of the battery inverter as a function of input power [9].

- The effect of temperature on the battery charging and discharging characteristics is not considered.
- The battery internal resistance is assumed to remain constant.
- The self discharge of the battery is not considered.

3.4. Conclusions

Combining the meteorological data inputs, the appropriate load profile and the modelling techniques of the individual components outlined in this section, the dynamic characteristics of the PBIM as complete system is obtained. The modelling of the individual components is based on existing hardware, whereby the simulation results of the individual components is validated using the data provided by the respective manufacturer.

4

GRID CONNECTED PEAK SHAVING CONCEPT

In Chapter 3, an outline of the PBIM component modelling is provided. However, depending on the PBIM application the energy control strategy will vary. In this chapter, the application of the PBIM in a grid connected environment for peak shaving applications is assessed for two locations: Costa Rica and the Netherlands. The dynamic behaviour of this system is presented which then extends to the implementation of energy storage sizing methodologies to determine the most appropriate battery capacity. Throughout the chapter, comparisons are made between the PBIM behaviour for the two locations.

4.1. METHODOLOGY

In order to asses the system functionality a set of objectives the system is designed to meet, and an approach applied to identify the optimally sized PBIM system are required.

4.1.1. OBJECTIVES

Given that the target PBIM users are primarily residential electricity consumers, the application of the PBIM for grid-connected scenarios can be assumed to be motivated by the potential cost savings on the energy bill. For such users, PV generation occurs 'behind the meter', enabling the self-generated energy to be either directly consumed by the household loads, stored or exported to the grid. Either option results in the decrease in demand of energy from the grid. The PBIM system for peak shaving applications can minimize the costs associated with the purchasing of electricity from the grid. This is amplified by storing energy from the PV array during time periods of low energy costs and using the energy during periods of time where the energy costs are high. In the case of a single PBIM this can be achieved by increasing the storage capacity, however this results in higher initial capital costs. The cost of a single PBIM is assumed to increase linearly with respect to its energy storage capabilities. The system objectives can therefore be summarized:

1. **Maximize peak load shaving.**
2. **Minimize the installed battery capacity.**

The identified system objectives are conflicting and thus a compromise is necessary to maximize the benefit of the PBIM to the user.

4.1.2. APPROACH

A numerical approach is adopted to identify the appropriate battery capacity to install per integrated module. The system performance indexes used are selected based on the insight they provide on the identified system objectives. Therefore the energy drawn from the grid with respect to the time-of-use pricing and the battery degradation have been selected as the performance indexes for the grid-connected energy scenarios.

A peak-shaving scenario is constructed for two locations, whereby the meteorological data, energy demands and time-of use pricing reflect a realistic situation. Simulations are carried out to determine the system's power balance per simulation time step, to gain an insight on the impact of the ambient climates and energy storage capacity on the systems ability to fulfill the identified criterion.

This project demonstrates the existence of the critical battery capacity (C_{Crit}) above which the decreasing rate of the peak load drawn from the grid worsens. In other words increasing the battery capacity above (C_{Crit}) will have less of a positive influence on the peak load drawn from the grid as compared to increasing the battery capacity by the same amount for a total battery capacity below (C_{Crit}). Identifying this battery capacity signals the point, above which the battery could be considered over-sized (method adapted from [37]). Intuitively if the battery is much greater than C_{Crit} the peak load drawn from the grid could be the same as for a scenario with a battery capacity equal to C_{Crit}. The critical battery capacity identifies the smallest possible battery capacity to ultimately maximize the benefit of PBIM usage.

4.2. System Modelling

The models of the various components are complied to create a single coherent model of the entire PBIM system, Figure 4.1. The model thus describes the energy flow and the respective efficiencies starting from its generation via the PV module and resulting in the determination of the system characteristics.

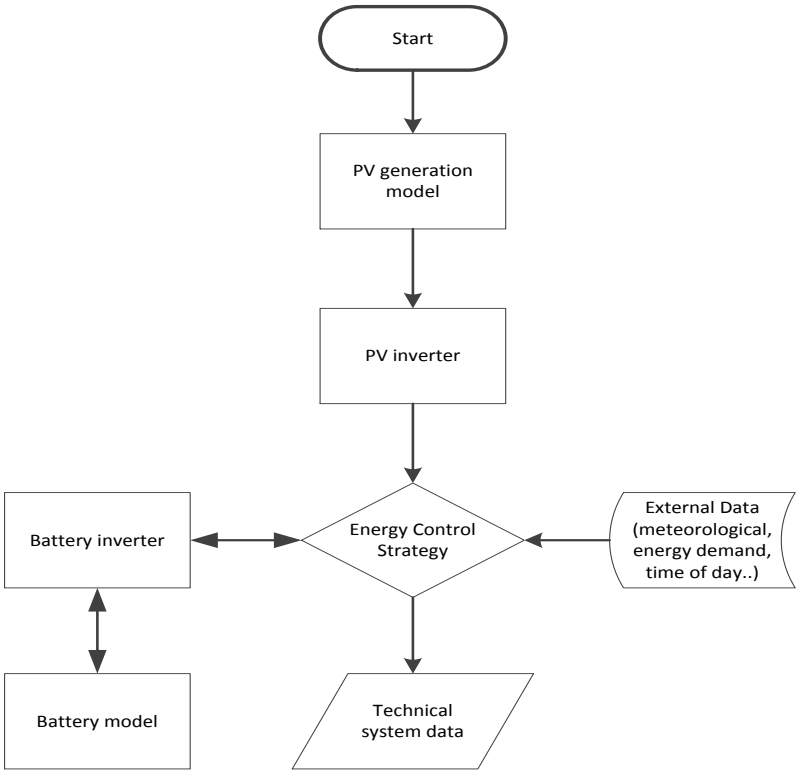

Figure 4.1: An overview of the PBIM model.

4.2.1. Energy Control Strategy

The peak shaving energy storage control strategy includes specific battery charging and discharging times based on the presence of peak hours, the underlying logic on which the energy control strategy is based on is presented in Figure 5.1. Therefore, the charging and discharging times of the battery depend on the length and frequency of peak hours throughout the day. Figure 5.1 displays the manner in which the power is control within the system, efficiency losses do occur however, they are not represented in the figure.

4.2.2. Governing Equations

The governing equations which capture the interactions between the different system components are outlined. Furthermore the essence of the energy balance occurring between the system and the utility grid is presented. The symbols used in this section are defined in Table 4.1.

PV Generation

Based on the peak shaving algorithm presented in Figure 5.1 if the battery is fully charged, the excess power generated by the PV array is used to power the load ($P_{\text{PV-Load}}$) subject to the following constraint.

$$\frac{1}{\eta_{\text{MPPT}_t}.\eta_{\text{inv}_t}}.P_{\text{PV-Batt}_t} + \frac{1}{\eta_{\text{MPPT}_t}}.P_{\text{PV-load}_t} + \frac{1}{\eta_{\text{MPPT}_t}}.P_{\text{PV-grid}_t} \leq P_{\text{PV}_t}^{\max} \quad \forall t. \tag{4.1}$$

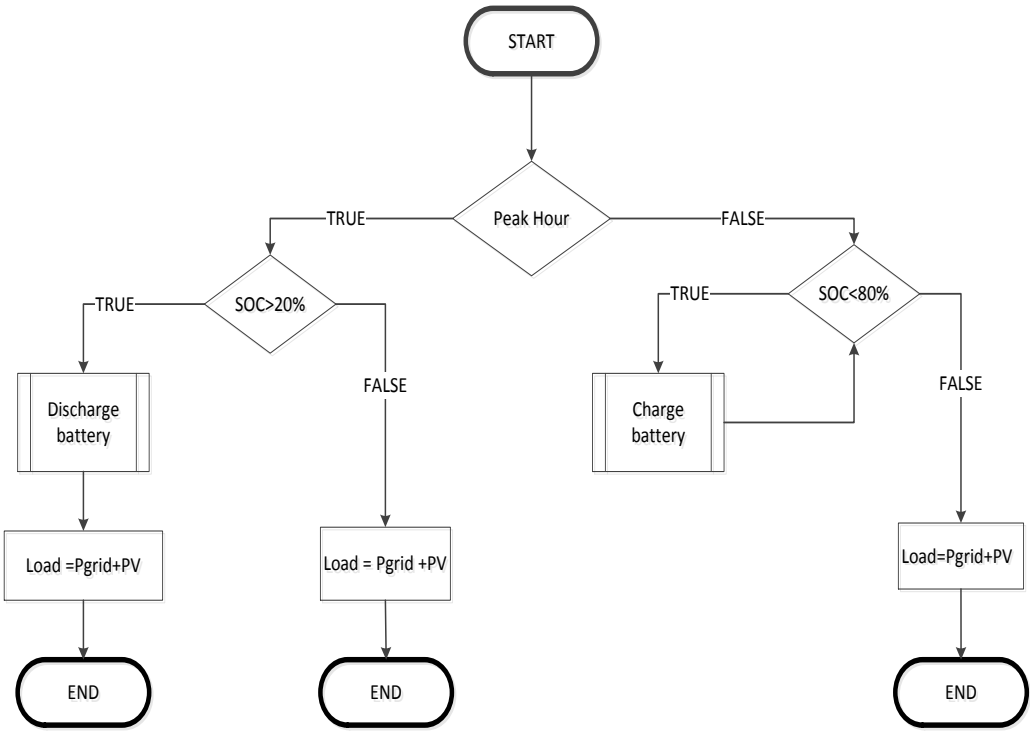

Figure 4.2: The controller logic for peak shaving

Battery

For optimal usage the battery is protected from the detrimental effects of deep discharging and overcharging as follows:

$$0.2E_t^{\max} \leq E_t \leq 0.8E_t^{\max} \quad \forall t. \tag{4.2}$$

The power delivered to the battery is described by:

$$P_{\text{Batt}_t} = \eta_{\text{ch}}.P_{\text{Batt}_t}^{\text{in}} - \frac{1}{\eta_{\text{dis}}}.P_{\text{Batt}_t}^{\text{out}} \quad \forall t. \tag{4.3}$$

The initial battery SoC is 20% .Hence the energy content of the battery is determined as follows:

$$E_t = \begin{cases} 0.2E_{\text{BOL}}, & \text{if } t \leq t_0 \\ E_{t-1} + P_{\text{Batt}_t}.\Delta t, & \text{if } t_0 \leq t \leq t_{\text{end}}. \end{cases} \tag{4.4}$$

The battery aging effects outlined in section 3.2 are incorporated such that

$$C_{\text{loss}_t} = -\frac{C_{\text{aging}}(T) * N_{\text{Cycles}_t}}{100}.E_t^{\max} \quad \forall t. \tag{4.5}$$

Electric Grid

Energy is exchanged with the grid either in an effort to satisfy the load demand or to sell excess energy such that the overall energy balance is;

$$P_{\text{load}_t} = P_{\text{PV}_t} + P_{\text{grid}_t} + P_{\text{Batt}_t}^{\text{in}} - P_{\text{Batt}_t}^{\text{out}} \quad \forall t \tag{4.6}$$

whereby

- $P_{\text{grid}_t} > 0$ if electric power is imported from the grid.
- $P_{\text{grid}_t} < 0$ if electric power is exported to the grid.

4.3. Case Studies

The performance of the PBIM in real life applications is assessed based on the dynamic technical characteristics obtained from the model. To approximate real life applications the PBIM is assessed for different case studies whereby the input data describing the scenario is implemented.

Definition	Symbol
Efficiency MPPT during time period t	η_{MPPT_t}
Efficiency Inverter during time period t	η_{inv_t}
Power transfer from PV array to battery during time period t	$P_{\text{PV-Batt}_t}$
Power transfer from PV array to load during time period t	$P_{\text{PV-load}_t}$
Power transfer from PV array to grid during time period t	$P_{\text{PV-load}_t}$
Maximum PV power during time period t	$P^{max}_{\text{PV}_t}$
Maximum Energy content of the battery during time period t	E^{max}_t
Battery capacity loss during time period t	C_{loss_t}
Power exchanged with the grid during time period t	P_{grid_t}
Power to charge the battery during time period t	$P^{\text{in}}_{\text{Batt}_t}$
Power discharged from battery during time period t	$P^{\text{out}}_{\text{Batt}_t}$

Table 4.1: List of Symbols

4.3.1. Location Analysis

Costa Rica and the Netherlands are the chosen sites at which to simulate the PBIM for peak shaving and off-grid applications. Costa Rica experiences a year-round tropical climate with minimal seasonal variations. Ambient temperatures and incident solar irradiance remain fairly consistent throughout the year. On the other hand, the climate in the Netherlands is remarkably dissimilar, with significant changes in available solar energy and ambient temperatures throughout the year. Figures 4.3 & 4.4 portray the differences in the power generation of the $265W_p$ Jinko PV module for Costa Rica and the Netherlands respectively and imply an uneven distribution of available solar energy throughout the year. These two locations are selected based on the vast differences between their climates. In this manner, the impact of ambient meteorological conditions on the PBIM can quantified and to determine whether the PBIM is a viable solution for both locations. Furthermore, to approach a realistic scenario the load profile data input is representative of the average household load profile of the respective region. The energy consumption of an average Costa Rican household differs, in terms of amount and time of usage, compared to their Dutch counterparts. Therefore these test sites were selected based on the significant dissimilarities between the two nations in an attempt to quantify the effect of these factors on the identification of the optimal PBIM battery capacity. An overview comparing the characteristics of the case studies for each location is presented in Table 4.3.1.

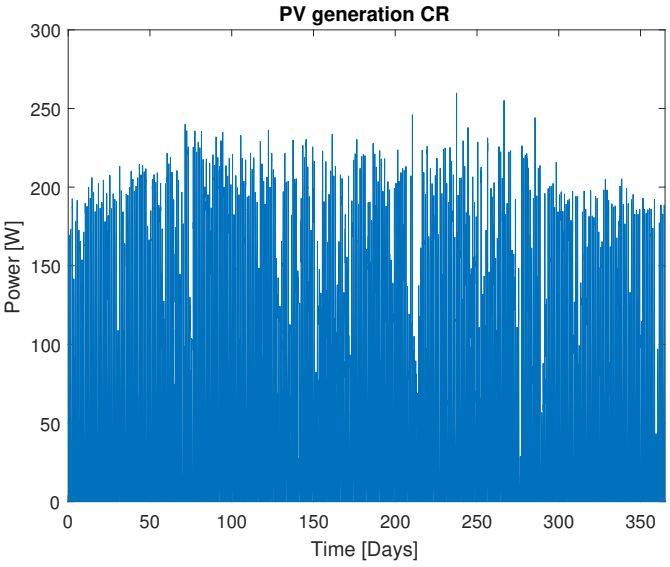

Figure 4.3: Annual PV production Costa Rica

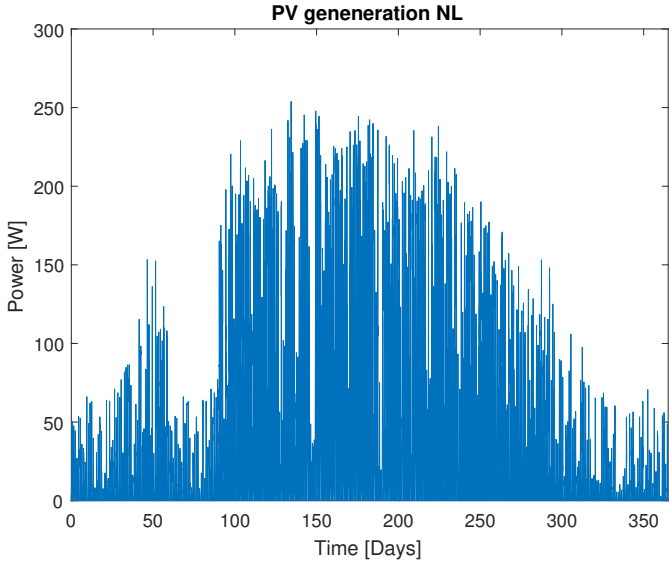

Figure 4.4: Annual PV production Netherlands

Location	Equivalent Sun hours (ESH) [hours]	Average Energy per PV module [Wh/day]	Load [kWh/day]
Costa Rica	4.8	1163	16.1
Netherlands	2.7	594	9.7

4.3.2. Scope of Data

The integrity of the simulations results depends on the assumptions and the input data. The meteorological and load profile data plays a significant role in the overall system sizing task at hand, the scope of the implemented data is

discussed.

Meteorological Data

The meteorological data has been obtained from Meteonorm database software at a 10 minute resolution, for the time span of a year. The high temporal resolution allows for accurate prediction of PV generation to account for the intermittent nature of solar energy.

Load Data

Realistic load profiles are essential in ensuring the creation of the case studies. In order to capture the high variability of residential loads, load data of a high temporal resolution is needed. Moreover, the distribution of residential energy demands differ between the Netherlands and Costa Rica on both a daily and annual basis. These variations arise due a number of differences including standard of living, climate and culture. Therefore including this difference in addition to the meteorological data into the case studies increases the robustness of this analysis.

- **Costa Rica**
  The load profile implemented into this case study to represent the energy use of an average Costa Rican household is obtained from [45] in which stochastic load profiles are created based on the statistical characterization of electricity demand in Costa Rica, Figure 4.6.

- **Netherlands**
  An approximation of the energy usage of an average Dutch household is obtained from [46], also at a resolution of 10 minutes. Based on seasonal averages the average daily energy demand varies with respect to the season. As a result the load profile is split into a winter and summer load profile, whereby the average energy demand per day is higher in the winter than in the summer, Figure 4.5.

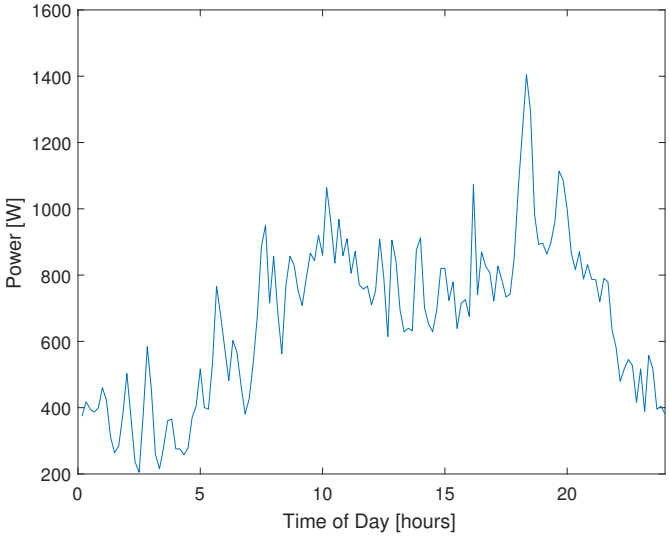

Figure 4.5: Daily load variation,Costa Rica

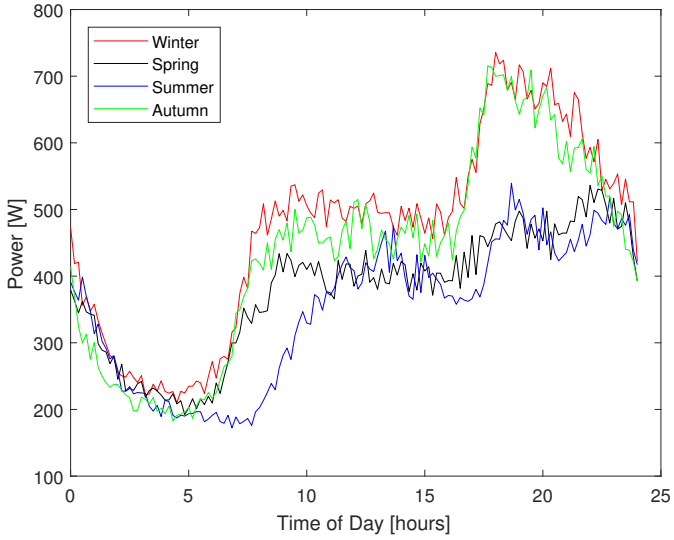

Figure 4.6: Daily load variation, Netherlands

4.3.3. Costa Rica

The load profile and ambient conditions are incorporated to approach a realistic assumption of the PBIM system for peak shaving in San Jose, Costa Rica. Figure 4.7 depicts the peak shave scenario, for two peak periods per day, this remains true throughout the course of the year. The load profile and the available solar energy are also represented, showing the need to store energy for its use during the second peak period which occurs during the night. The battery dis/charging schedule is programmed according to the controller strategy presented in Figure 4.2, which aims to reduce the energy drawn from the grid during peak hours. The presence of two peak periods per day result in the battery being charged and discharged twice in 24 hours and is represented in the battery SoC variation in Figure 4.8(a).

In this case study the peak periods are defined by the Costa Rican electricity provider 'Instituto Costarricense de Electricidad' who set electricity prices depending on the time of day, Table 4.2 . These prices reflect the national variation of the demand of energy, and the selected load profile. As a result the price experiences a dramatic increase of 144% during peak hours which acts in favour of using the PBIM for peak shaving.

To gain an insight on the technical characteristics of the system the case study is created with the aim of assessing the battery charging and discharging cycles as well as the system interaction with the grid. In this section the system dynamics on both a daily and a yearly basis are discussed.

Tariff Scheme	Symbol	Price [€/kWh]
Off-Peak electricity	λ_{OP}^{G}	0.09
Peak hours electricity (from 10.00-12.30 and 17.30-20.00)	λ_{P}	0.22

Table 4.2: Pricing Scheme Costa Rica, [12].

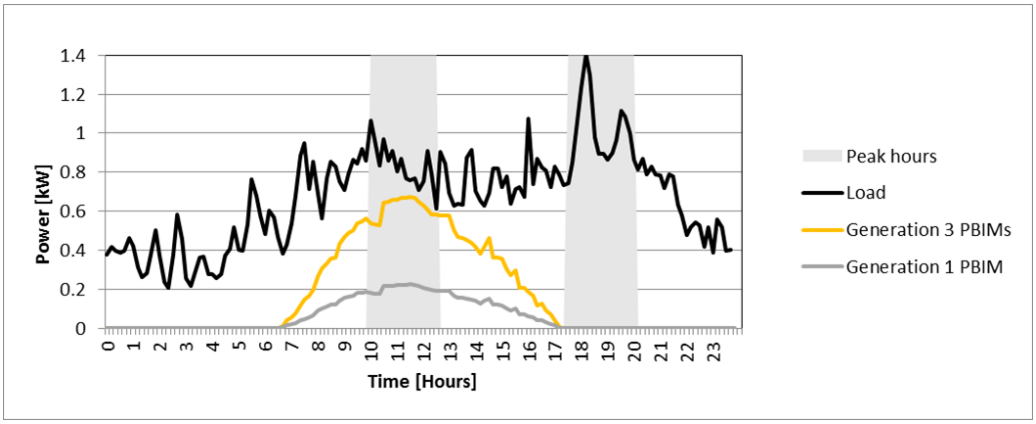

Figure 4.7: The peak shave scenario, Costa Rica.

Daily System Dynamics

Significant changes in the PBIM's characteristics and performance are predicted with respect to the size of the installed battery. To gain an insight on the nature and significance of these changes simulations for a single PBIM system were performed to determine the relation between battery capacity and desirable PBIM characteristics; an essential insight for energy storage sizing. In this section the system characteristics are presented to illustrate the applied energy control strategy.

- **Off-Peak**
  As dictated by the peak shave algorithm during off-peak hours the energy generated by the PV array, if any, is solely used to charge the battery. The initial battery SoC is set to 20% and is seen to increase for all battery sizes as soon as PV array begins converting solar energy, Figure 4.8(a). With the 90Wh battery being the smallest it is charged the quickest. Figure 4.8(b) presents the energy exchange of the battery, whereby the positive power values represent the charging of the battery. The nature of the charging profile reflects the PV power generation. For discharging the battery is discharged at a constant power

  Once charged, the the generated PV power once used to charge the battery is redirected to satisfy the load seen by the decrease in energy drawn from the grid, Figure 4.8(c). Since the 90Wh battery was fully charged before the off peak period terminated less energy was stored as compared to the 450Wh and 750Wh batteries. This indicates that the 450Wh and 750Wh batteries were able to satisfy a larger fraction of the load during the subsequent peak period. However, in the case of the 90Wh battery less energy was imported from the grid during the off-peak.

- **Peak Hours**
  During peak hours the PBIM battery begins to discharge and will continue to do so until either it is no longer peak hour or the battery is discharged. Each of the simulated batteries were discharged at the same nominal discharge current. It is clear that the larger 700Wh battery provided the most energy during the peak hours, indicating larger financial savings during this time period were incurred. The battery is discharged to its lower 20% limit twice in 24 hours. The longest peak period of the day is 2.5 hours, to ensure the battery is fully discharge by the end of the peak period and that nominal discharge rates are not exceeded, each considered battery capacity is set to discharge at 0.4C.

Yearly System Dynamics

Having simulated and understood the behaviour of the PBIM on a daily basis with respect to various battery capacities it is also essential to consider such characteristics over a longer period of time. For a variety of battery capacities the PBIM system was modeled for a year and the results are presented in this following section.

- **Peak Load Reduction**
  With energy from the grid costing the most during peak hours the battery capacity is to be optimized in such way so as to decrease the load during peak hours by as much as possible. As seen in the simulation results increasing the battery capacity generally results in a decrease in the peak load (Figure 4.9). Noticeable in the figure is the gradual reduction of the effect of increasing the battery capacity on the peak load. This observable saturation indicates that above 700Wh the battery is oversized. The battery capacity of 700Wh can thus be identified as

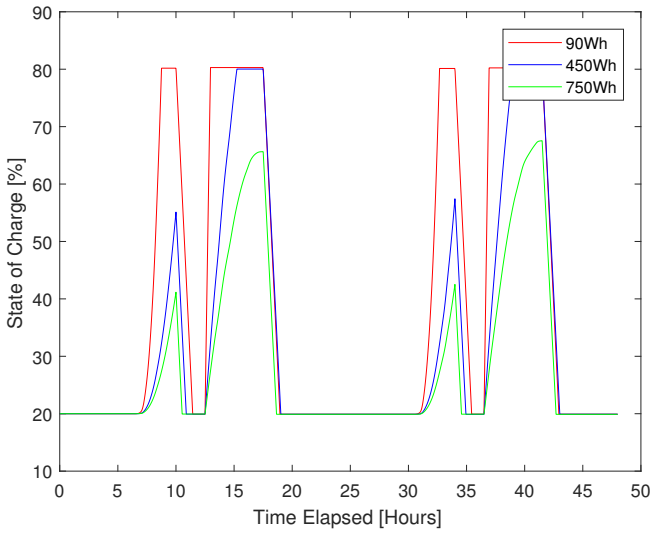

((a)) Battery State of Charge

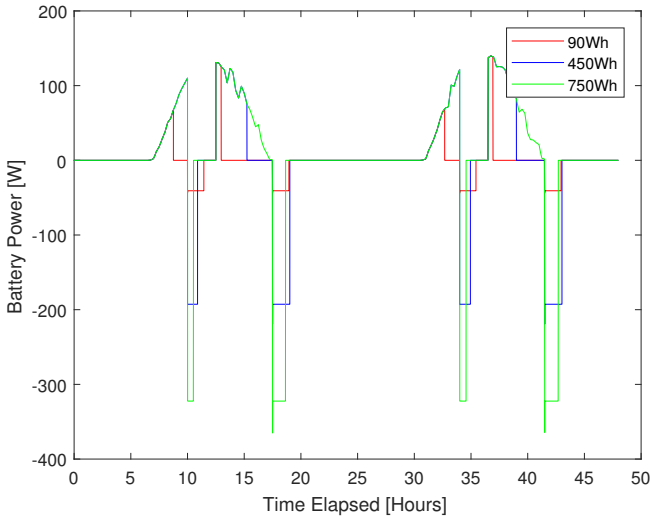

((b)) Battery Power

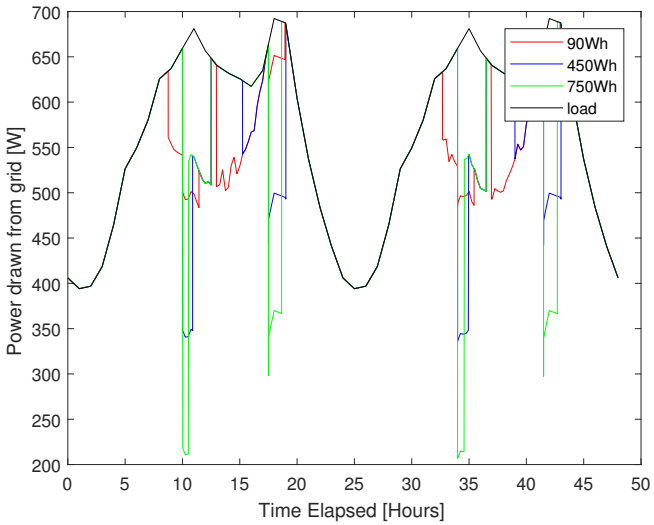

((c)) Energy Exchange with the grid(Simplified load profile used for illustration purposes)

Figure 4.8: PBIM System characteristics, simulation results for a 2 day period

C_{Crit}. The existent of the gradual decrease in peak load for batteries larger than 700Wh is due to the presence of particularly sunny days thus leading to higher than average PV production; additional energy the oversized batteries are able to store. Oversized batteries will reduce the peak load, however they will also negatively impact the financial aspects of the proposed PBIM system.

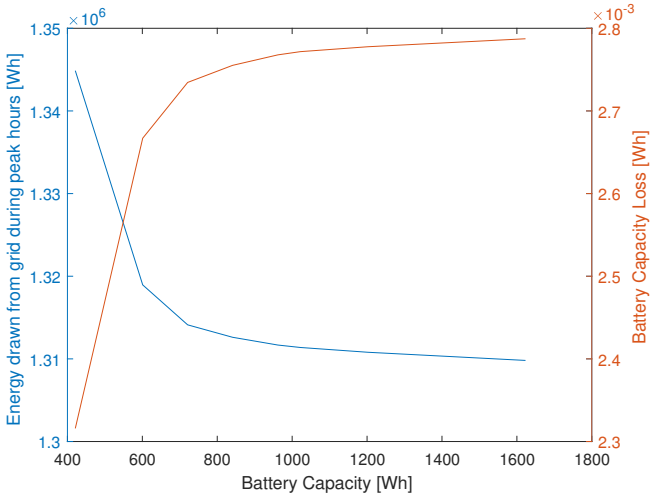

Figure 4.9: Effect of peak load drawn from the grid and battery capacity loss with respect to installed battery capacity on an annual basis.

- **Battery Degradation**
  On the other hand, with an increasing battery size, the capacity loss throughout the year increases with an increasing installed battery capacity (Figure 4.9). As is the case with the peak load reduction a saturation point is noticeable at C_{Crit}. Batteries with a capacity less than C_{Crit} experience a similar rate of degradation. This is due to the equal fraction of the usable capacity being used. In other words up to a battery with capacity C_{Crit}, the battery is charged and discharged between the 20% and 80% SoC limits an equal number of times. Batteries with a capacity larger than C_{Crit} experience a slower rate of degradation a year as the battery is considered oversized. The amount of energy available for storage purposes is insufficient to fully charge the batteries on a regular basis. These batteries are therefore less deeply cycled resulting in the plateauing of the capacity loss since the yearly energy throughput of the batteries is similar.

4.3.4. Multiple PBIMs

The effect on varying the available capacity as been assessed on both a daily and yearly basis, however most PBIM systems will consist of more than a single PBIM. It is therefore necessary to determine whether the appropriate battery capacity for a single PBIM will remain consistent for systems of different capacities. By adding a PBIM in parallel the system PV and energy storage capacity is increased. It is not the scope of this thesis to determine the optimal size of the entire system but the attention is directed to sizing the energy storage capacity of a single modular PBIM unit. In this section the PBIM's characteristics are assessed as a function of battery capacity and PV capacity. The aim of this analysis is to identify the critical battery capacity (C_{Crit}).

- **Peak hours**
  The first system design variable is the energy drawn from the grid during peak hours. Given the implemented energy control strategy, the battery is programmed to discharge the solar energy it has accumulated during daylight off-peak hours. The simulation results in Figure 4.10 show that the energy drawn from the grid during peak hours throughout the whole year is reduced as battery capacity increases, and as the number of PBIMs increase. However, note the presence of the saturation point in the curve whereby increasing the battery capacity no longer results in the reduction of the energy drawn from the grid. When a PBIM is added in parallel the PV Wp and battery capacity scale accordingly. By altering both the battery capacity and the rated PV Wp C_{Crit}, is consistent throughout the considered system sizes.

- **Off-peak hours**
  As the battery capacity increases, for a fixed PV capacity, charging times increase. During off-peak hours the power generated by the PV array is used to charge the batteries, whilst energy is drawn from the grid to meet the demand. Increasing the battery capacity for constant PV capacity will lead to longer charging times, resulting in more energy drawn from the grid before the energy generated by the PV module can be directly used (Figure 4.11). For batteries smaller than 700Wh per PBIM the energy drawn from the grid decreases for an increasing number of PBIMs connected in parallel. This is occurs since the available PV power after the battery is charged is greater. However, for battery capacities greater than 700Wh per PBIM, irrespective of the PV capacity, the

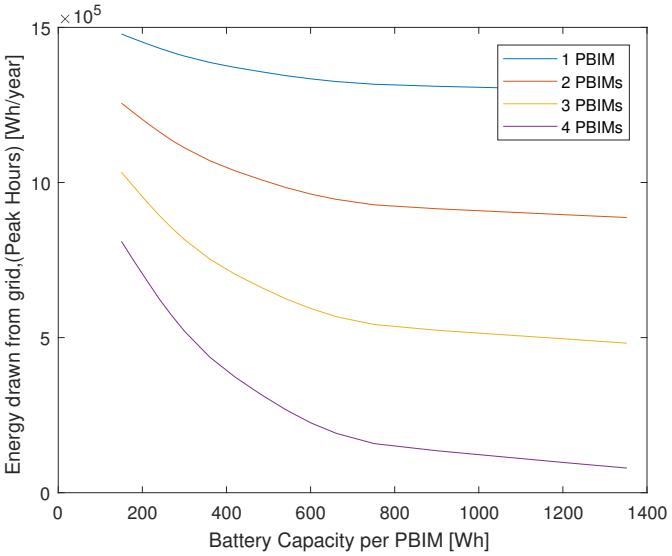

Figure 4.10: Annual energy from grid during peak hours.

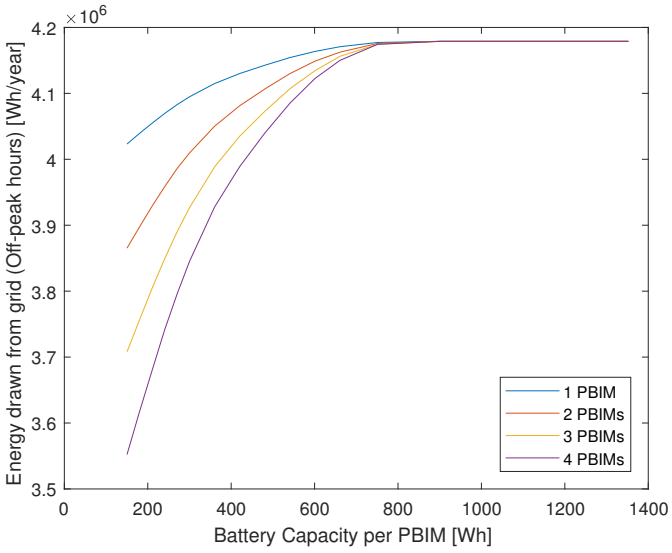

Figure 4.11: Annual energy drawn from grid during off-peak hours.

energy drawn from the grid ceases to increase for increasing battery capacity. This is due to the fact that the battery is too large to be fully charged during the allotted charging periods. This implies that the battery is now capable of storing all the energy generated by the PV module in the off-peak time period. As seen in Figure 4.3 the power output of the PV module experiences minimal variations throughout the year, since the daily energy production of a PV panel is limited by both its efficiency and the available solar irradiance. The battery capacity at which the saturation point occur will therefore remain consistent throughout the year. The critical battery capacity is again identifiable at 700Wh per PBIM at the point of convergence.

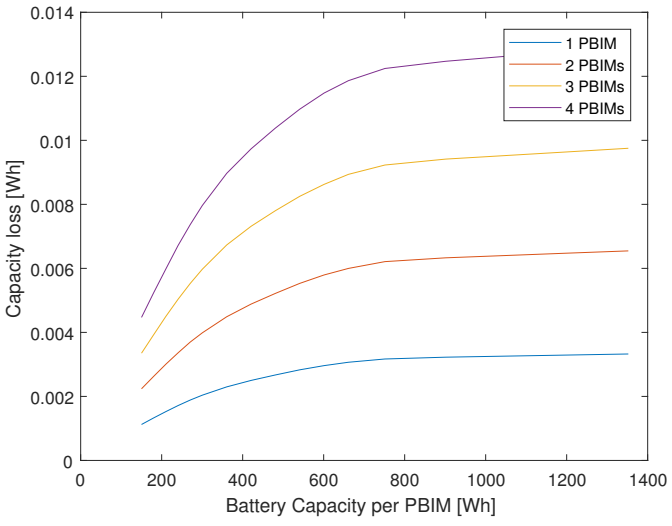

Figure 4.12: The annual battery capacity loss

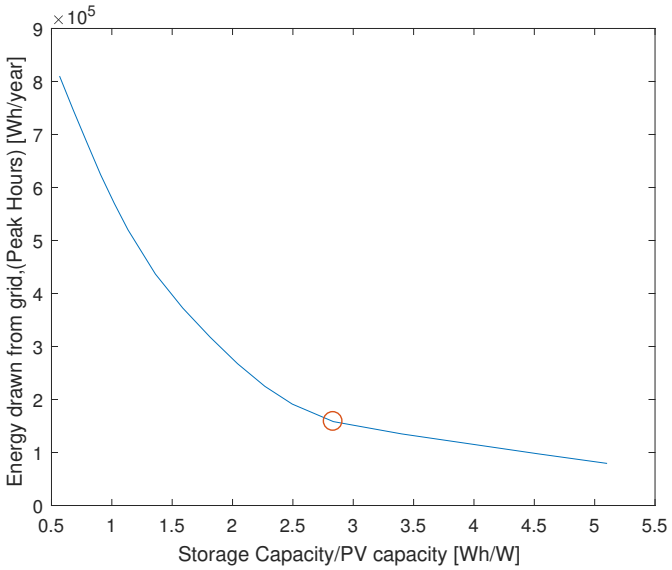

Figure 4.13: Battery sizing Costa Rica. optimal battery sized circled

- **Battery degradation**
  As the battery is repeatedly charged and discharged its capacity begins to fade, as explained in section 3.2. The rate of battery degradation is dependent on how often it is cycled and the temperatures and which this process occurs. Batteries of smaller capacities, less than (C_{Crit}), will have a larger average State of Charge than a larger battery. Since these smaller batteries are regularly fully charged and discharged they will be cycled more often resulting in a faster rate of degradation. If the battery capacity is increased a smaller fraction of the usable battery capacity is regularly used and which thus equates to fewer cycles over the same period of time. The simulation results in figures 4.12 both demonstrate the existence of a saturation point above which the total capacity loss is no longer affected by increasing the total installed storage capacity. Figure 4.12 demonstrates that in terms of battery degradation C_{Crit} remains consistent for the considered PBIM system sizes.

- **Energy storage sizing**
  Figure 4.7 illustrates the first peak period of the day coinciding with the highest irradiance levels of the day, indicating that during this time period the energy generated by the PV array is fed directly to the loads and not to charge the battery. The energy stored in the battery is also discharged. After the termination of the first peak period the power generated by the PV module is stored in the battery to be used during the second peak period Figure 4.7. Therefore, due to the adopted energy control strategy, the battery is not required to have the capacity to store all the converted solar energy throughout the day. Instead it is only required to store the PV energy generation during a single off-peak period. Although the equivalent sun hours experience a slight variation throughout the year it will remain relatively constant, leading to the conclusion that the available charging periods of the battery will also be consistent, given that the peak periods remain unchanged.

  The energy drawn from the grid during peak hours is not strictly required to be minimized. However it can be optimized for a single PBIM. Increasing the storage capabilities above a certain point will cease to have a significant effect in reducing the energy demand from the grid, i.e the critical battery capacity. Increasing the battery capacity beyond this point will be less beneficial for the PBIM user as higher capital costs are required for the additional energy storage. Figure 4.13 identifies the optimal battery/PV ratio for peak shaving applications in Costa Rica and is found to be 2.75Wh/W. This equates to an energy storage capacity capable of storing the energy generated by the PV module operating at rated efficiency for 2.75 hours. This time period is comparable to the equivalent sun hours present during the allotted charging periods of the battery. In the case of a 265Wp PV module the optimal battery capacity is found to be 729Wh. Looking at Figures 4.10 through to 4.12 the battery capacity per PBIM at which the saturation point occurs for the energy drawn from the grid and the capacity fade occurs at the identified optimal capacity of 729Wh, and remains true for the considered range of PV capacities. In this case, the critical battery capacity is defined to be the most appropriate battery size to install in the PBIM.

Economic Considerations

Having taken into account the energetic system characteristics to provide an indication of the appropriate battery size, the economic characteristics related to the sizing issue are now considered. In this section the system is assumed to have a lifetime of 15 years; a conservative estimate since most commercially available PV module are expected to operate up to 25 years. However a worst-case scenario is assumed here. The profit the system generates over its lifetime is defined by the following equation:

$$\text{Lifetime Profit} = \text{Lifetime Energy savings} - \text{Lifetime capital costs} \tag{4.7}$$

where Lifetime energy savings is defined as the savings on the electricity bill by reducing the energy drawn from the grid. The lifetime capital costs refer to the capital investment costs of the PBIM system throughout its lifetime, including battery replacement costs, if necessary. A break down of the PBIM capital costs is provided in Table 6.2 and the battery costs in this case is seen as variable. Due to the rapid evolution of the technology and to highlight the influence of the battery costs on the sizing task, a range of battery costs are considered.

Component	Price [€]
PV Module	150
Micro inverter	45
Charge Controller	220
Battery	Figures 4.14 & 4.15

Table 4.3: PBIM component costs.

Figure 4.14 presents the historic trend of lithium-ion battery costs and continues to estimate the battery costs in the future. In the case a battery replacement is required, it is more than likely that the purchasing for the new battery replacement will be a fraction of its costs today. As can be derived from Figure 4.14 within the next 7 years the cost per Watt-hour is expected to decrease by 50%, this is taken into consideration when estimating the system lifetime capital costs.

Figure 4.15 presents the profits expected from a single PBIM over its lifetime for its application is Costa Rica for peak shaving applications. This analysis also takes into account battery costs, represented as €/kWh, and the installed battery size. Figure 4.16 presents the total expected battery capacity loss over the system's lifetime. As outlined in previous sections, once the BOL capacity decreases by 20% the battery is required to be replaced. As can be derived from the figure batteries with capacity smaller than 900Wh will need to one replacement throughout the system's lifetime. Therefore, batteries with a capacity lower than 900Wh a reduction in profits is observed due to the cost of the necessary battery replacement.

To conclude, the economic considerations the most profitable battery capacity to install per PBIM is 900Wh, this represents a battery over-sizing of 23% compared to the optimal battery capacity derived in Figure 4.13. Irrespective of the considered battery costs this battery capacity remains to be considered the most economically favorable. This

larger 900Wh battery will result in having a lower average DoD than smaller batteries, therefore experiencing fewer complete cycles across the system's lifetime.

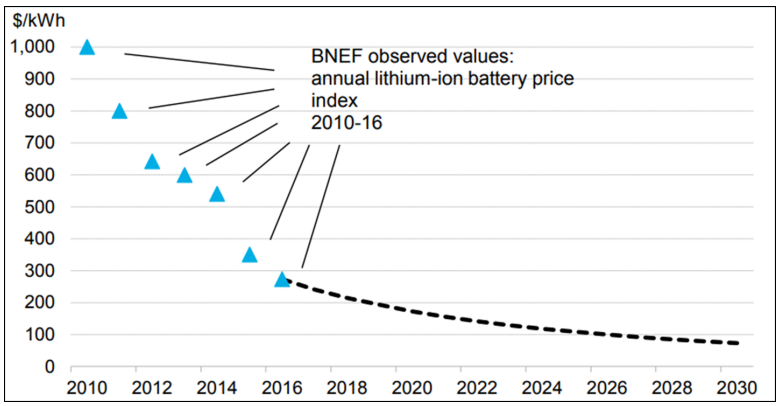

Figure 4.14: Lithium-ion battery price trend. Source [10].

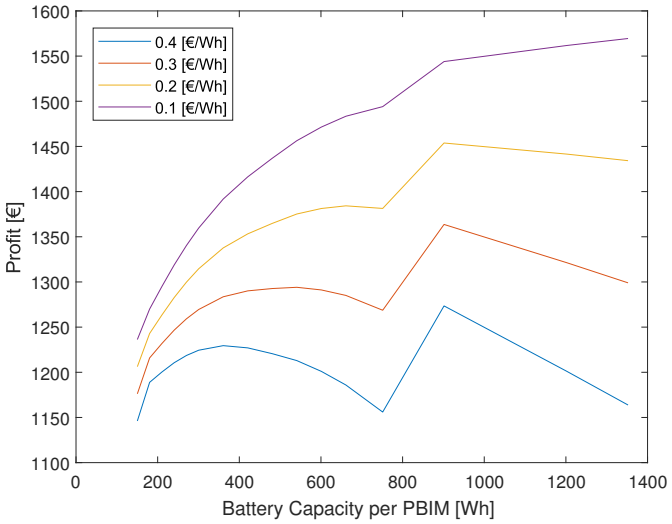

Figure 4.15: The lifetime profit of a single PBIM as a function of battery costs and installed battery capacity.

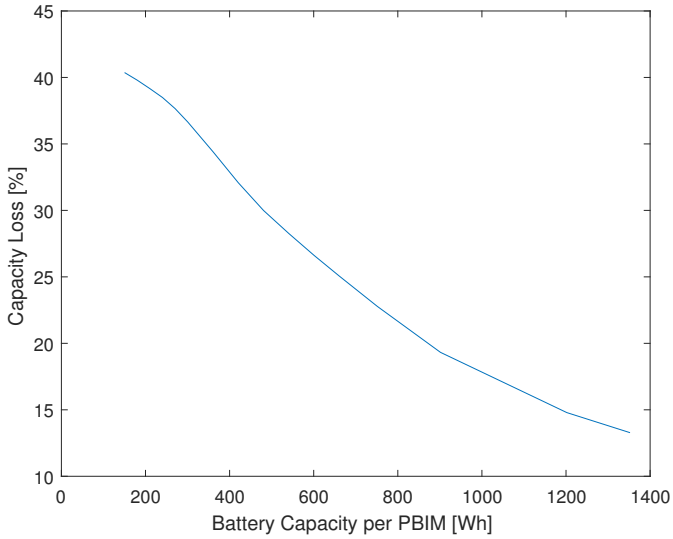

Figure 4.16: The total simulated capacity loss as a function of battery size.

4.3.5. Netherlands

In comparison to Costa Rica, the Netherlands experiences a greater variation in irradiance throughout the year which significantly impacts the performance of the PBIM. The manner in which this affects the optimal battery capacity to be installed in the PBIM for peak shaving applications is outlined in this section. The peak shaving scenario for the Netherlands is shown in Figure 4.17 which displays the available solar energy for an average spring day in March. Only a single peak period is defined for the Netherlands occurring in the early evening and coinciding with the end of the average work day. This implies that the battery is only required to be charged and discharged once every 24 hours. With the peak period occurring for a few hours in the evening this allows ample time for the battery to be charged throughout the day. The appropriate battery size to install per PBIM will therefore be dependent on the average daily power generation of a single module. The peak period is identified using the pricing scheme of e-on, a dutch energy provider, the pricing scheme is presented in Table 4.4. In this scenario the price increase during peak hours is 65% .

Tariff Scheme	Symbol	Price [€/kWh]
Off-Peak electricity	λ_{OP}^{G}	0.2
Peak hours electricity (between 17.00-21.00)	λ_{P}	0.33

Table 4.4: Pricing Scheme Netherlands, [13]

4.3.6. System Characteristics

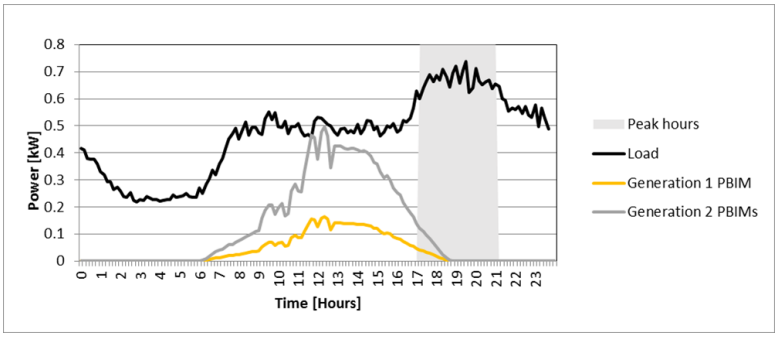

Figure 4.17: The peak shave scenario, Netherlands (March).

Daily System Dynamics

The battery SoC and power exchange are presented in Figures 4.18(a) & 4.18(b) respectively, while the system's energy exchange with the grid is presented is Figure 4.19 for a time period of 48 hours.

- **Peak hours**
  The peak period occurs for 4 hours, this is assumed to remain constant. The battery discharge rate is based on this time period to ensure that all the stored energy is discharged. A discharge rate that is to low will result in the battery storing energy that will not be used. On the other hand discharge rates that are too high will result in a heightened battery temperature during discharging and result in the acceleration of its degradation. Therefore the discharge rate is set to 0.25C.

- **Off Peak hours**
  During the off-peak hours the battery is programmed to charge, Figure 4.18(b) presents the charging and discharging of the battery, whereby the charging power experiences fluctuations due to the intermittent nature of solar energy. The charging C-rate is therefore dependent on the power generated by the PV module. As was the case in the previous case studies, larger batteries take longer to charge thus having the effect of importing more energy from the grid during off-peak hours. On the other hand larger batteries are able to store more energy resulting in a larger portion of the load during off-peak hours met using self-generated energy.

Multiple PBIMs

The effect on the energy drawn from the grid and the battery capacity loss is analyzed as a function of PV and battery capacity. The high variability of the available solar energy makes sizing the battery in this scenario considerably more complex than in the case of Costa Rica. The PBIM system is modelled and the simulation results of the energy exchange with the grid and the battery capacity loss over the course of an entire year are presented in Figures 4.19 through to 4.21. Based on these system characteristics the critical battery capacity is identified.

- **Peak hours**
  The energy drawn from the grid during peak hours is simulated for an entire year and the effect of varying the battery capacity and the number of PBIMs is presented in Figure 4.19. Since the peak period is present in the evening, the addition of a PBIM in parallel each installed with a 200Wh battery, will not have a significant effect in reducing the peak load. This is due to the lack of solar energy in this time period indicating that the majority of self-generated energy is drawn from the battery with minimal energy being drawn directly from the PV array. As battery capacity increases, more energy is able to be stored for peak period usage and thus has a greater impact in reducing the peak load. As seen by the changing slope of the curves, for an increasing battery capacity the positive impact in reducing the peak load decreases. This observable change in effectiveness arises due to the over-sizing of the battery in the winter. As the battery exceeds a certain capacity it is larger enough to store a significant fraction of a the energy generated by a single module during a typical winter day. The continuation of peak load reduction for increasing battery capacity occurs due to new found ability of the system to store more energy during the times of abundant sunshine in the summer months. Unlike in the case of the system in Costa Rica no saturation point on which to identify the critical battery capacity is noticeable. Due to the high variation of available solar irradiance throughout the year, as a result of this analysis no single optimal battery capacity is identifiable as an appropriate size for this application.

- **Off-Peak hours**
  As in the previous case study the off-peak energy demand from the grid increases as the installed battery capacity increases, Figure 4.20. This is due to the longer charging times required for the larger batteries, before the energy generated by the PV is directly used to power the load. As the PV capacity of the system increases, the off-peak energy demand decreases as there is an increase in self- generated energy. As the installed battery capacity per PBIM increases the curves representing the different system sizes begin to converge. Although not

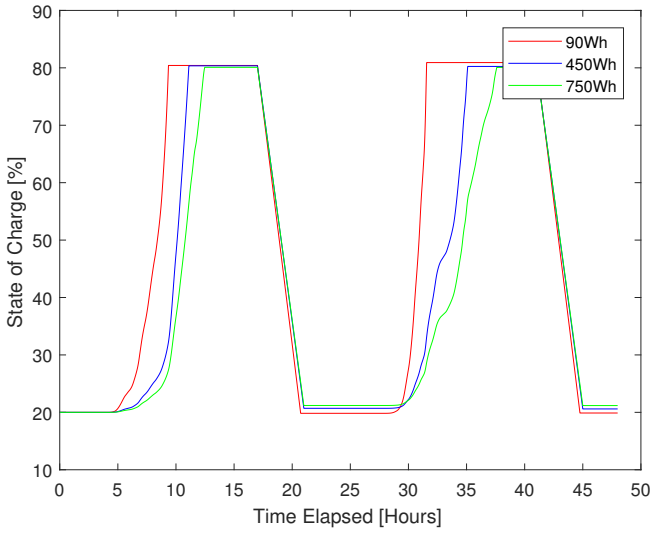

((a)) Battery State of Charge

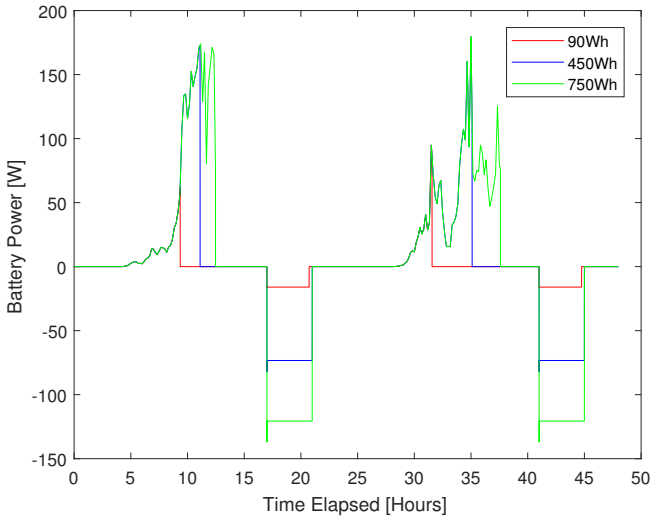

((b)) Battery Power

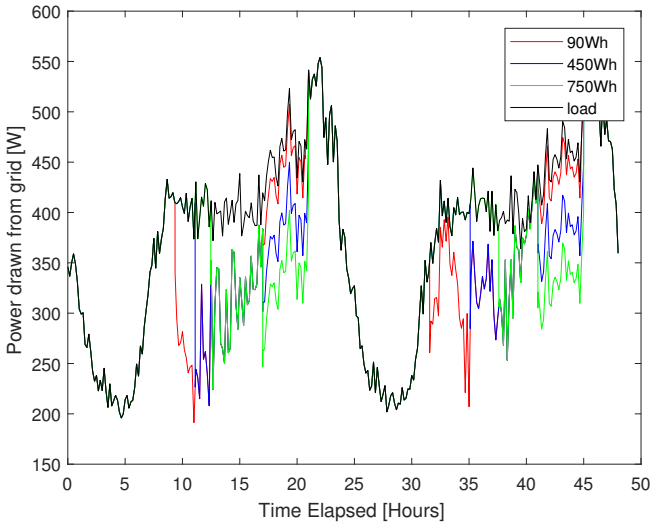

((c)) Energy Exchange with the grid.

Figure 4.18: PBIM System characteristics, simulation results for a 2 day period

seen in the figure the actual point of convergence represents the battery capacity which is able store all the energy generated by the PV array on any given day. Unlike the case study in Costa Rica this point of convergence is not identified as the saturation point or the critical battery capacity, as the battery is considered too large for PBIM applications due to limited space.

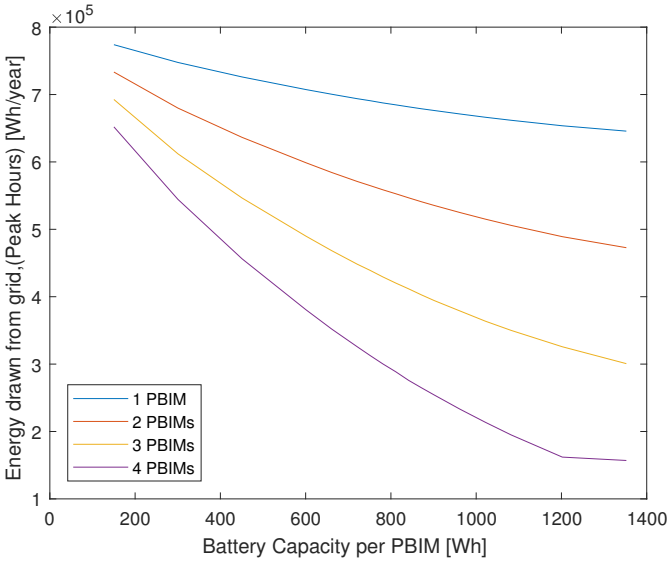

Figure 4.19: Annual energy from grid during peak hours.

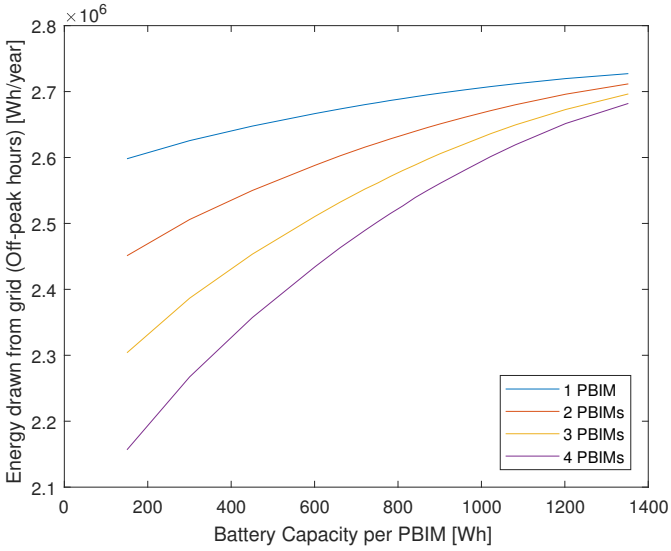

Figure 4.20: Annual energy drawn from grid during off-peak hours.

- **Battery degradation**
  The capacity fade represented in total Wh lost increases for an increasing battery capacity, however the rate at which the capacity loss increases decreases for larger batteries. As the battery capacity increases and the PV energy generation remains constant, the percentage of the battery's total capacity range which is used decreases. The battery is therefore operated at cycles less deeply resulting in a decreased rate of degradation. In this instance no observable critical capacity can be identified.

- **Energy storage sizing**

  Due to the disparity in meteorological conditions throughout the year. The most appropriate battery size to install per PBIM would equate to the PV module energy generation per day; since the peak period peak occurs at the close of the day, and as dictated by the energy control strategy this is the only time period at which the battery is required to be discharged. However the PV module generation varies throughout the year and the installed battery capacity is fixed. If the battery is optimized for the winter period the battery would be appropriately sized for this period alone. If it were to be used during the summer such a capacity would be non-optimal as additional peak load reduction would be feasible for larger battery capacities. Therefore a trade-off is required with the extremities of the acceptable battery range being either a large battery with low usage during the winter, or a small battery that severely limits the benefits for the consumer during the summer.

  Based on the analysis of the performance indexes, the relation between the system characteristics and the battery capacity is understood. However it is insufficient to propose an optimal battery capacity. A cost analysis is required to determine whether the installation of a battery makes economical sense, and which battery will maximize the economic savings. The savings incurred by reducing the peak load will compared to the cost of increasing the energy storage capabilities of the PBIM.

Economic Considerations

Adopting the same economic analysis methodology as outlined in section 4.3.4, the optimal battery size for PBIM peak shaving applications in the Netherlands is analyzed in terms of economic benefits, whereby the profits incurred by a single PBIM is assessed as a function of battery capacity and battery costs. As a consequence of the less frequent usage and significantly lower average ambient temperatures, the battery for peak shaving in the Netherlands experiences a considerably slower degradation rate as compared to the Costa Rican case. The simulation results presented in Figure 4.24 indicates that no battery replacements are necessary, throughout the considered system lifetime. Applying equation 4.7 the total lifetime profit for a single PBIM as a function of battery capacity and battery costs is presented in Figure 4.23. In this case the economically favorable battery capacity is heavily influenced by the battery prices. At the higher end of the battery costs spectrum considering 0.4 €/Wh and 0.3 €/Wh, the most economically battery capacity is 200Wh whereby savings can potentially be incurred on the energy costs. However, considering

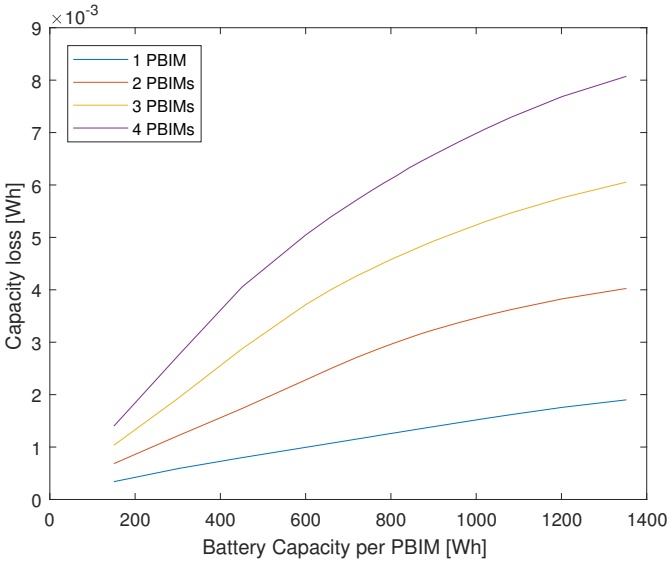

Figure 4.21: The annual battery capacity loss.

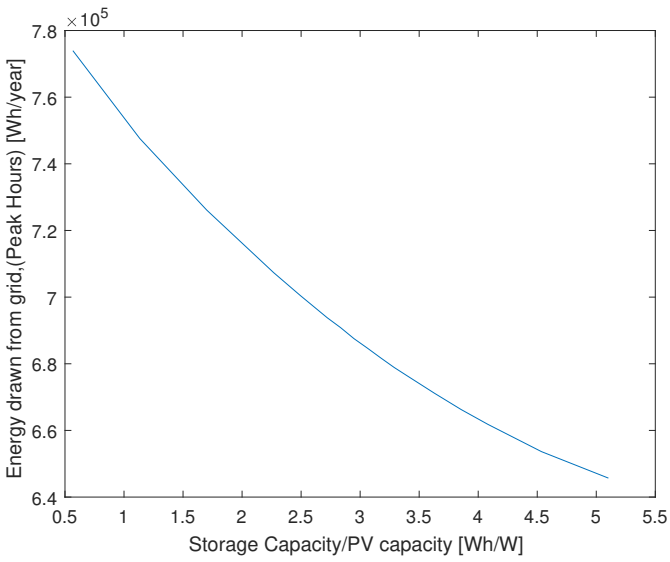

Figure 4.22: Battery sizing Netherlands.

battery costs 0.2 €/Wh the optimal battery capacity increases to 600Wh. Prices lower than 0.2 €/Wh do not reflect current battery costs, and is presented for a future scenario. In this case, the optimal battery size will only be restricted by the available physical space at the rear of the PV module for the battery installation.

To conclude the economic considerations for optimally sizing the battery; the optimal battery size is heavily influenced by battery prices, however this economic approach provides an additional insight into the considerations for energy storage sizing for peak shaving applications. The result presented in Figure 4.22 proved to be inconclusive regarding the identification of optimal Storage/ PV array capacity ratio. In [47], the average costs for Lithium-ion batteries quoted to be 0.17 €/Wh. Therefore, using a conservative estimate of 0.2 €/Wh an optimal battery capacity of 600Wh is identified, equating to a Storage Capacity / PV capacity ratio of 2.26Wh/W.

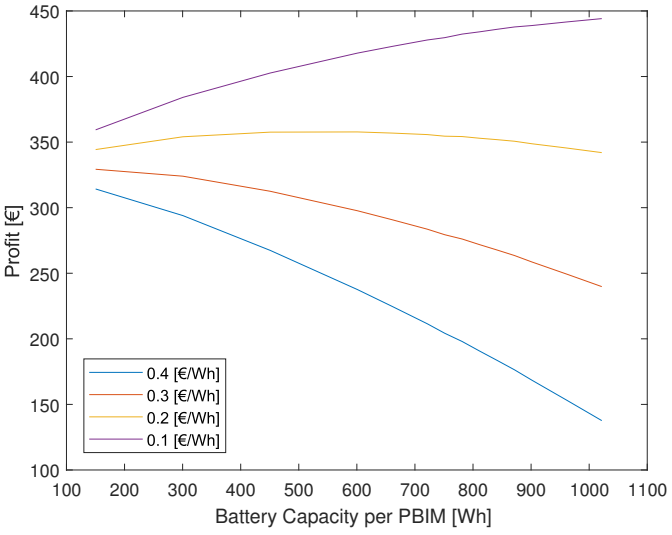

Figure 4.23: The lifetime profit of a single PBIM as a function of battery costs and installed battery capacity.

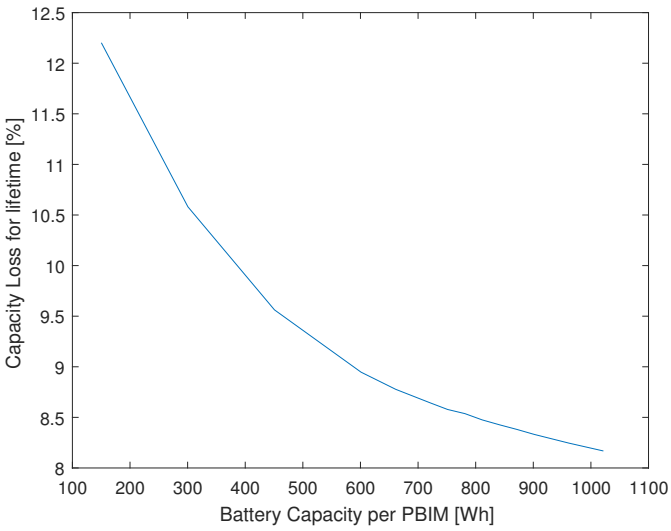

Figure 4.24: Total battery capacity loss over system lifetime.

4.3.7. Optimal system characteristics

The characteristics of the optimally sized PBIM for peak shaving applications in Costa Rica and the Netherlands is expected to significantly differ. The extent of these differences are analyzed in this section, to quantify the impact of the meteorological conditions and the peak shaving scenario on the appropriate battery size. For the PBIM system in the Netherlands a battery capacity of 600Wh was considered whilst for the system in Costa Rica a PBIM with battery capacity of 729Wh was used. In both locations the effectiveness of a single PBIM is assessed.

AUTARKY

The implemented energy management system is programmed to reduce the load demand during peak hours by discharging the battery. To asses the effectiveness at which this occurs the concept of autarky is introduced which provides an indication of the self-sufficiency of the system. In this particular case the system autarky is used to asses the system's independence from the grid exclusively during peak hours. Autarky is therefore defined as the percentage of energy used to satisfy the load that originates from either the battery or the PV array and in this case is only considered for peak hours. The autarky is defined to be:

$$\text{AUTARKY} = \frac{\text{Delivered self generated energy (Peak hours)}}{\text{Peak load demand}} * 100 \tag{4.8}$$

where: Delivered self-generated energy= Energy drawn from battery + Energy from PV array.

Therefore an autarky of 100% indicates that the entire load demand was met using exclusively self generated energy and the system is entirely independent from the grid, however in this case this would require the additional PBIMs to be connected in parallel. In this analysis the performance of only a single PBIM is analyzed. It is assumed that system characteristics will scale relative to the number of PBIMs in the system as seen in Sections 4.3.4 and 4.3.6.

Figures 4.25 & 4.26 display the monthly autarky for Costa Rica and the Netherlands respectively. The variation of autarky levels are seen to match the corresponding irradiance profiles, with consistent autarky levels seen throughout the year in Costa Rica. The autarky levels for the system in the Netherlands experiences significant variations. Due to low PV generation during the winter a larger fraction of the peak load is met by drawing energy from the grid, whereas in the summer average autarky levels of 14% is recorded for a single PBIM system. Even during the summer, when the available solar energy is plentiful the PBIM installed in the Netherlands achieve lower autarky levels than compared to Costa Rica due to the higher load demand during the peak hour period.

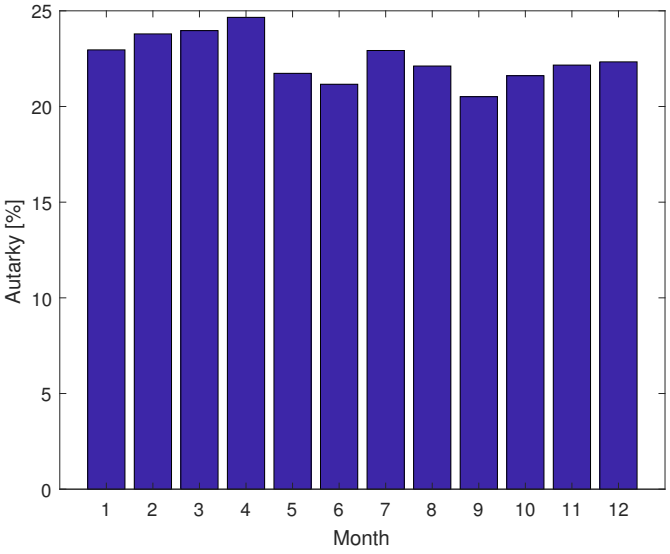

Figure 4.25: Monthly peak load autarky, Costa Rica

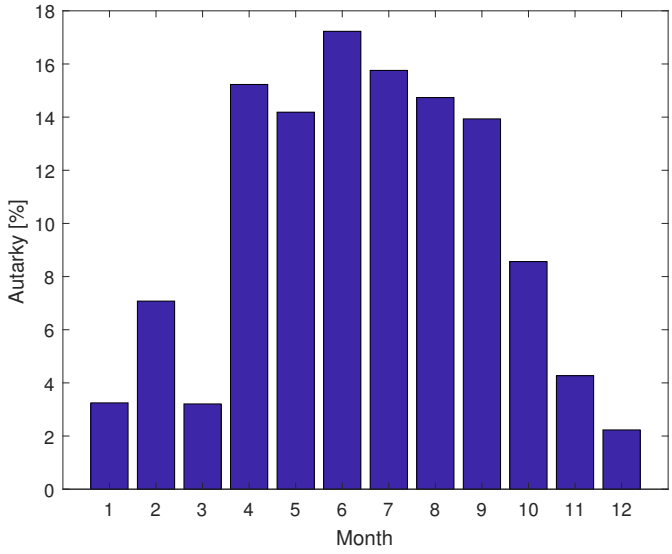

Figure 4.26: Monthly peak load autarky, Netherlands

STATE OF CHARGE

The variation in battery usage throughout the year is presented in Figures 4.27 & 4.28 with the battery SoC in Costa Rica reaching the set upper and lower usage limits of 80% and 20% throughout the year. The battery in the Netherlands on the other hand is never fully charged during the winter and can be regarded as over sized for this time period. However during the summer the battery is regularly fully charged due to the abundant sunshine. Since the installed battery capacity is fixed, a trade-off is observed in the case of the Netherlands.

BATTERY DEGRADATION

Due to consistently warmer temperatures, a higher depth of discharge and performing twice the number of cycles a day the battery in Costa Rica experiences a much greater degradation rate than the battery used in the Netherlands. Figure 4.29 provides a comparison between the battery capacity loss in the PBIM system for both locations. The degradation rate for Costa Rica appears relatively uniform for each month since the battery usage remains largely unchanged as the year progresses. The capacity loss for the Netherlands on the other hand differs greatly, with a larger capacity loss observed during the summer months. This heightened degradation rate is due to higher ambient temperatures and the deeper cycling of the battery as compared to its usage during the winter months. The PBIM battery for peak shaving applications in Costa Rica experiences a capacity loss of 1.56% per year whereas the battery in the

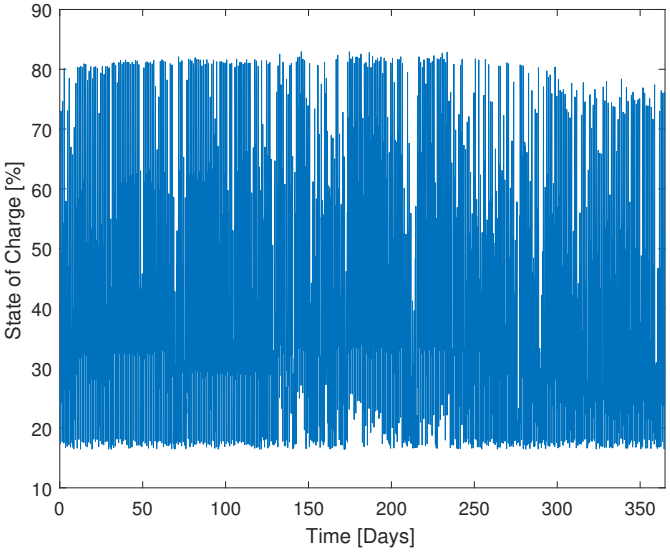

Figure 4.27: Annual SoC variation, Costa Rica

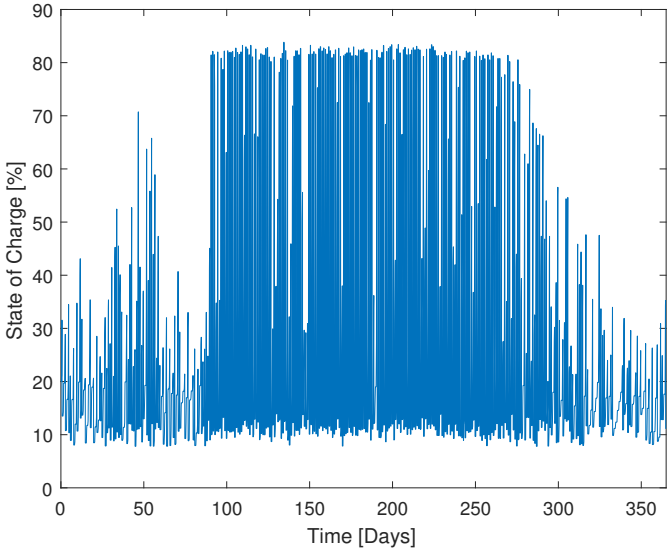

Figure 4.28: Annual SoC variation, Netherlands

Netherlands degrades by 0.8% per year.

Based on the degradation estimates the battery for peak shaving applications in Costa Rica has a lifetime of 12.8 years before its capacity reduces to 20% of BOL. On the other hand, in the Netherlands the battery lifetime is expected to last up to 25 years, matching the predicted lifetime of the PV module.

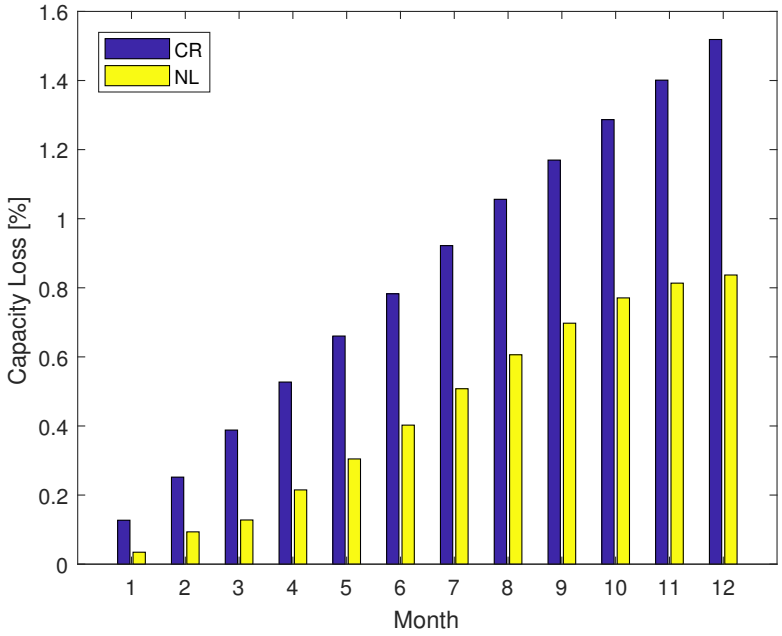

Figure 4.29: Monthly battery degradation, Costa Rica

4.4. CONCLUSIONS

- **Energy storage sizing**
  The appropriate energy storage size for peak shaving applications in Costa Rica and the Netherlands has been identified and the performance of the optimally sized systems are compared. The scenarios have been created to be as realistic as possible through the application of meteorological data, load profiles and the identification of peak periods all of which impact the optimal battery capacity.

  1. **Peak Shave Scenario** The time and frequency of the peak periods affect the required battery size. In the case of Costa Rica, peak periods occur twice a day affecting the number of hours where the battery is programmed to charge (during periods of PV module energy generation and off-peak times.) The optimal battery size is therefore based on the energy generated by the PV module during the allocated battery

charging times. In the Netherlands, the peak period occurs in the evening, therefore the battery is charged uninterrupted throughout the day, limited only by the available solar energy.

2. **Meteorological effects** The system characteristics of the grid-connected PBIM in Costa Rica is seen to remain relatively constant throughout the year and is able to meet, on average, 21% of the peak load with self generated energy. The system autarky in the Netherlands is seen to vary from 2% on the worst month to 17% during the summer, for a single PBIM.

- **Reliability**
  Despite the varying levels of autarky the system is always 100% reliable due to presence of a grid connection. However considering a single PBIM, the system based in Costa Rica is able to meet a greater fraction of the peak load with self-generated energy, than the system based in the Netherlands.

5

OFF-GRID PBIM SYSTEM

In this chapter the usage of the PBIM concept for off-grid applications is assessed. The energy control strategy and the energy balance of such a system is presented. This extends further to include two case studies whereby the off-grid system is applied in two locations. The appropriate battery capacity for these two systems is then identified.

5.1. METHODOLOGY

To assimilate the dynamic characteristics of the off-grid system an energy management control is implemented. The performance of the system is assessed based on the fulfillment of the system objectives.

5.1.1. OBJECTIVES

The system objectives for stand-alone applications differ from those presented in the grid-connected case study. The standalone system relies exclusively on the energy generated by the PV to meet the load requirements. The optimal system from a residential user's point of view would be minimize the frequency of power interruptions. This relates to the reliability of the system and its ability to store energy during daylight hours and satisfy the load demand throughout the night or during periods of time with unfavorable meteorological conditions. However the reliability increases with respect to the energy storage capabilities of the system. Therefore as the system becomes increasingly reliable the capital costs associated with it will also rise. Again in this instance the capital costs of the PBIM are assumed to increase linearly with respect to increasing the installed battery capacity. The system objectives can thus be summarized:

1. **Maximize system reliability**

2. **Minimize the installed battery capacity.**

5.1.2. APPROACH

Similar to the sizing methodology in the grid connected case the appropriate battery size is selected based upon the concept of a saturation point of desirable system characteristics as a function of battery capacity. In the case of the grid connected system in the Netherlands economic factors had to be taken into consideration. The capacity at which this occurs, the critical capacity, indicates the lowest possible installed capacity at which the desirable system characteristics are improved minimally if this capacity is increased. In essence, this point highlights the lowest battery capacity at which the identified system performance indexes are optimized.

Unlike the grid-connected scenario there is no source of revenue or potential savings in the case of an off-grid system. However by modelling the dynamics between system reliability and battery capacity a saturation point at which C_{Crit} occurs can be determined. The system reliability is found to be the governing decision variable. Reliability is reflected in the Loss of Load Probability (LLP) [5] which is described by;

$$\text{LLP} = \frac{E_{\text{fail}}}{\int_{\text{year}} P(t)_{\text{load}}\, dt} \tag{5.1}$$

where E_{fail} is the total energy required by the load that cannot be delivered by the PBIM.

To take into account the manner in which the battery is used, battery degradation is also considered as a performance index. The battery aging process is accelerated if the battery is regularly deeply cycled. Having a larger battery will reduce the aging process, however the additional investment cost of over-sizing the battery should be considered. The battery sizing is based on the LLP of the system. Once identified the characteristics of the optimally sized systems are analyzed.

5.2. System Modelling

The concepts implemented to model the off-grid PBIM system are presented in this section.

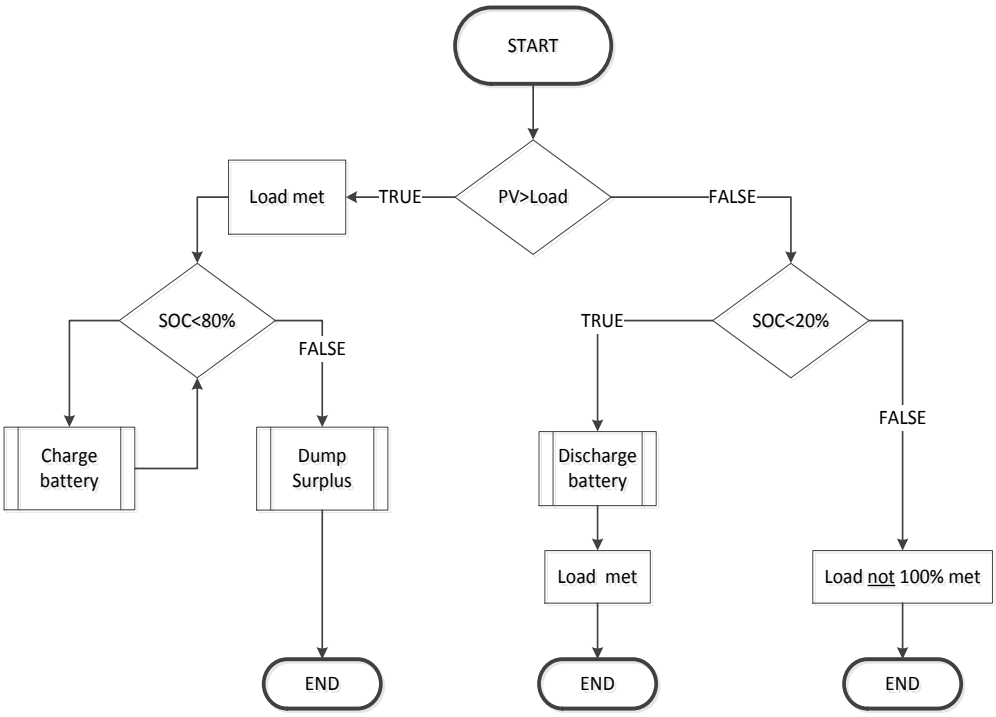

Figure 5.1: The controller logic for peak shaving

5.2.1. Energy control strategy

The logic used to model the system dynamics and energy flow in an off-grid system is presented in Figure 5.1. In the instance that neither the PV energy generation nor the battery is able to meet the load demand a loss of load is considered. If the opposite holds true whereby the battery is fully charged and the PV array generates more energy than is required by the load, there is excess energy which needs to be dumped.

5.2.2. Governing equations

The governing equations represent the energy balance in the off-grid system and the dynamic relation between the supply, storage and consumption of energy at any given time. The symbol definitions are presented in Table 4.1.

PV Generation

Without the presence of the grid additional parameters P_{fail} and P_{excess} are the power required that cannot be delivered and the excess power generated that is not used or stored respectively.

$$\frac{1}{\eta_{\text{MPPT}_t}.\eta_{\text{inv}_t}}.P_{\text{PV-Batt}_t} + \frac{1}{\eta_{\text{MPPT}_t}}.P_{\text{PV-load}_t} + P_{\text{fail}} + P_{\text{excess}} \leq P_{\text{PV}_t}^{\text{max}} \quad \forall t. \tag{5.2}$$

Battery

The battery constraints are identical to those outlined in section 4.2.2.

Energy Balance

The equality constraint of the off-grid system is described by;

$$P_{\text{load}_t} = P_{\text{PV}_t} + P_{\text{fail}_t} - P_{\text{excess}_t} + P_{\text{Batt}_t}^{\text{in}} - P_{\text{Batt}_t}^{\text{out}} \quad \forall t \tag{5.3}$$

5.3. Case Studies

Two case studies are created to test the performance of the PBIM for off-grid applications. Costa Rica and the Netherlands are again used as locations in which to simulate the dynamic behaviour of the PBIM. Based on the system dynamics the appropriate battery size for each case study is identified.

5.3.1. SCOPE OF DATA

The scope of the input data used throughout the off-grid case studies is touched upon in this section.

METEOROLOGICAL DATA

The required meteorological data inputs remains unchanged and is described in section 4.3.2.

LOAD DATA

The average daily energy consumption is assumed to be less for an off-grid household as compared to a grid connected household. In addition off-grid energy users are assumed to be more willing to shift their energy usage with respect to the energy supply, and therefore resulting in lower night time energy usage as compared to grid connected households. The profile used to represent the energy consumption is the same for each off-grid case study, and is considered for a resolution of 10 minutes, Figure 5.2. The average daily energy demand is 6.3KWh.

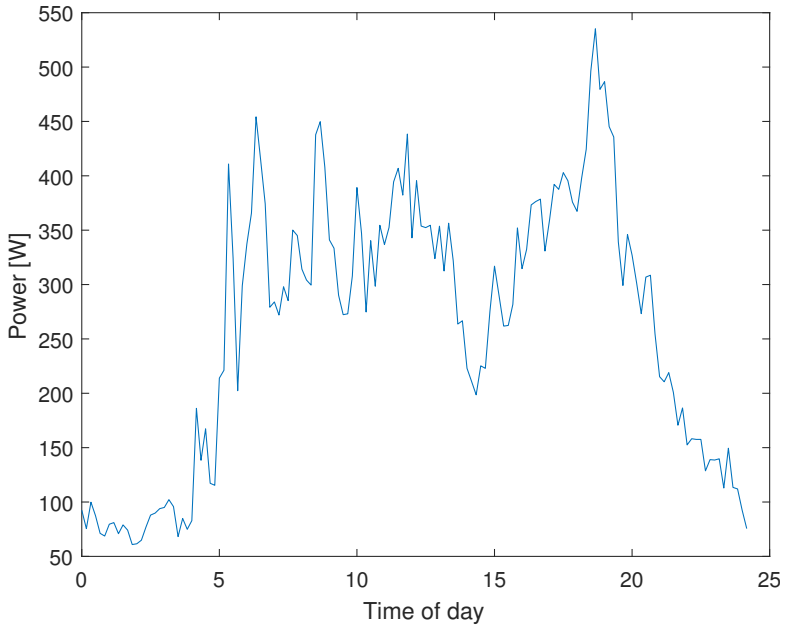

Figure 5.2: Applied load profile for off-grid case studies

5.3.2. PV ARRAY SIZING

To enable the creation of a realistic off-grid scenario it is necessary to derive an estimation of the required PV array capacity. In the off-grid case study analyzing the effectiveness of a single PBIM for a given load profile and meteorological conditions is unrealistic unlike in the grid connected case study. The reasoning for this alteration in the methodology is summed up in two reasons. Firstly, as dictated by the energy control strategy, once the conditions have been met to commence the discharging of the battery, the discharge C-rate is governed by the energy demand and the PV generation at that instant in time. Given a scenario whereby the PV array does not generate any energy, the battery is required to discharge at a rate such that the load demand is met until either the PV array resumes generating energy or the battery is fully discharged. Considering a single PBIM, the discharge requirements of the battery will not be within its nominal operating range, a scenario which is unlikely to occur in real-life applications. This heightened discharge C-rate required from the small battery capacity implies that the degradation that will occur will be unrealistically high and therefore analyzing this effect will not provide any valuable insight on the system characteristics.

The second reason to estimate the PV array size is to ensure that a realistic range of the battery-PV ratio is ascertained. In the case an unrealistic ratio is assumed, the energy generated by the PV array will be directly used to meet the energy demands the instant it is generated, this will remain true throughout the entire time period of PV energy generation throughout the day. However, for a more realistic scenario the PV array is sized such that it produces sufficient energy during the day to meet the energy demand at that instant in time and to charge the battery to store energy for future use.

An estimation of the PV array sizes is derived using the following expression obtained from [5].

$$N_{\text{modules}} = \frac{E_Y^L . SF}{A_M . \int_{\text{year}} . G_M(t) . \eta(t) dt} \tag{5.4}$$

where the number of modules, N_{modules}, is a function on the yearly energy demand, E_Y^L, the yearly energy generation per PV module ($A_M . \int_{\text{year}} . G_M(t) . \eta(t) dt$). A sizing factor, SF, is introduced to prevent the under-sizing the system

and equates to 1.1. The required number of modules for each location is presented in Table 5.1.

Location	Load [kWh/day]	$N_{modules}$
Costa Rica	6.3	6
Netherlands	6.3	11

Table 5.1: PV Array sizing for the considered locations

5.3.3. Costa Rica

In this section the PBIM characteristics for its off-grid application in Costa Rica are analyzed. A 6 PBIM system is taken into consideration as presented in Table 5.1.

Loss of load probability

The probability of the load demand not being met as a function of installed battery capacity per PBIM and PV capacity is pictured in Figure 5.3. Intuitively larger battery capacities enable the system to operate in a more reliable manner, the same applies for increasing the PV capacity of the system. The critical battery capacity describes the capacity at which a saturation point is observed, whereby increasing the battery capacity will not result in a more reliable system. In terms of available solar energy the identifiable saturation point indicates a battery size that is able to accommodate the energy generated by the PV module that is not required by the load during the day. Since the energy generated by a single PV module is limited, installing a larger battery would not result in more energy being stored; thus the LLP is not significantly improved for batteries larger than the critical capacity. Particularly noticeable in the 6 PBIM system, is the continued decrease in LLP beyond the identified saturation point,this is due to the presence of outlier days whereby the daily PV module energy production is considerably higher than average. Larger batteries will be able to store this additional energy, however this will only be beneficial on days where PV generation is extraordinarily high, which has a low probability of occurring.

Battery degradation

The battery degradation losses are presented Figure 5.4. Again, a saturation point is observable and is consistent throughout the different system sizes and occurs at a capacity of 800Wh per PBIM. For batteries larger than 900Wh per PBIM the increase in degradation due to cycling is minimal. This feature is due to the over-sizing of the battery with respect the energy generation of the PV module and the energy demands during the day. The energy storage capacity is greater than the energy available to be stored. Therefore the energy throughput of the battery no longer increases as the battery capacity increases; degradation remains constant.

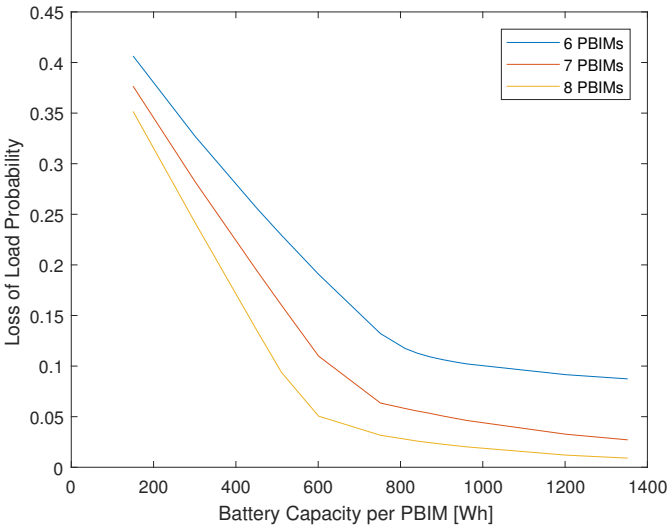

Figure 5.3: Loss of Load probability, as a function of system size, Costa Rica

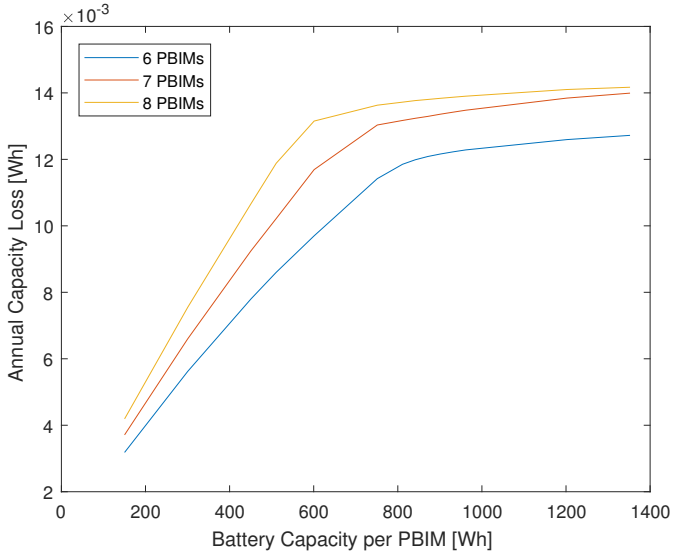

Figure 5.4: Battery capacit losses as a function of system size, Costa Rica.

Energy storage sizing

The sizing of the energy storage capacity is presented in Figure 5.5 as a function of energy storage and PV capacity for 6 PBIMs connected in parallel. The optimal battery capacity to PV capacity ratio is found to be an energy storage size capable of storing the energy generated by the Jinko PV module operating at rated capacity for 3 hours. By increasing the battery to PV capacity ratio from 1 Wh/W to 3 Wh/W a decrease in the LLP of 0.3 is observed. However increasing the battery to PV capacity ratio from 3Wh/W to 5Wh/W a significantly smaller decrease in LLP of 0.045 is observable. The saturation point equating to battery capacity of 800Wh, marks the capacity above which there is no significant improvement in the system reliability.

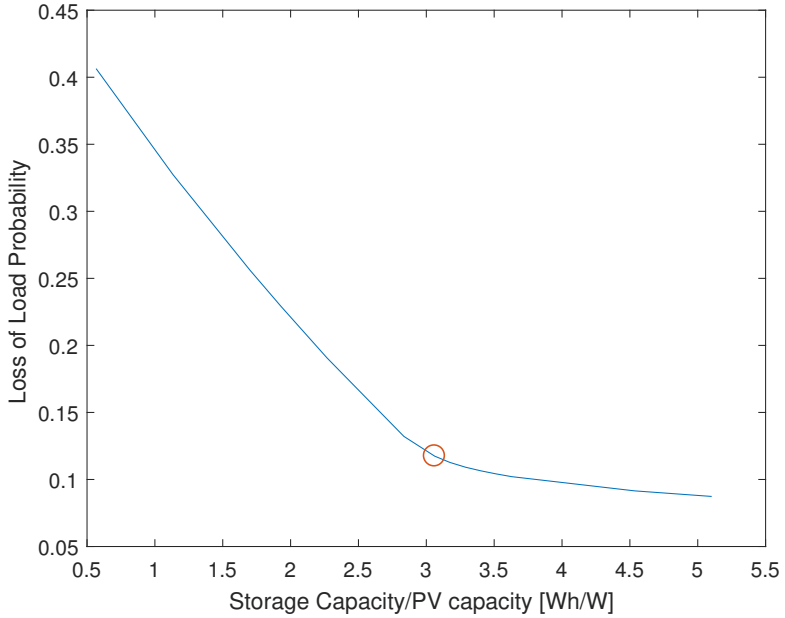

Figure 5.5: Identification of the critical battery capacity, Costa Rica.

5.3.4. NETHERLANDS

The off-grid application of the PBIM in the Netherlands is analyzed in this section, resulting in the proposal of an appropriately sized battery capacity to install per PBIM. In order to satisfy the energy demand during the winter energy is required to be available during periods of time of minimal available solar energy. Therefore the required number of modules for the Netherlands case study is considerably larger than the array required in Costa Rica.

LOSS OF LOAD PROBABILITY

The loss of load probability is presented in Figure 5.6. With double the number of PV modules to power the same load profile as in the Costa Rican case, the PBIM system in the Netherlands still suffers from low reliability, which is primarily due to the uneven distribution of solar energy throughout the year. The rate of system reliability improvement due to the increase of available battery capacity reduces for as battery capacities increase above 400Wh. However unlike in the Costa Rican case study, slight improvements in the system reliability can be made by increasing the available energy storage above the critical capacity of 400Wh.

BATTERY DEGRADATION

The battery degradation for each system capacity is presented in Figure 5.7, above a capacity of 400Wh per PBIM the rate of increase of the battery capacity loss slows. This is due to the over-sizing of the battery above this capacity resulting in a lower percentage of the available capacity being used to store energy.

ENERGY STORAGE SIZING

The system reliability as a function of the PV-battery ratio for PBIM off-grid applications in the Netherlands is presented in Figure 5.8. The optimal battery-PV ratio is found to be 2Wh/W. A lower optimal capacity is found for the Netherlands as compared to Costa Rica since on a yearly basis there is less available energy. With Costa Rica experiencing on average 5 equivalent sun hours a day the energy generated by the 6 module PV array is sufficient to meet both the day and night-time loads at a low LLP. In the Netherlands however, the energy generated by a single PV module, as a daily average, is considerably less and experiences 3 equivalent sun hours a day. To generate sufficient energy an increased number of PV modules is required. The optimal battery capacity/ PV capacity of the PBIM in the Netherlands is therefore less than required in Costa Rica due to the distributed nature of the energy storage.

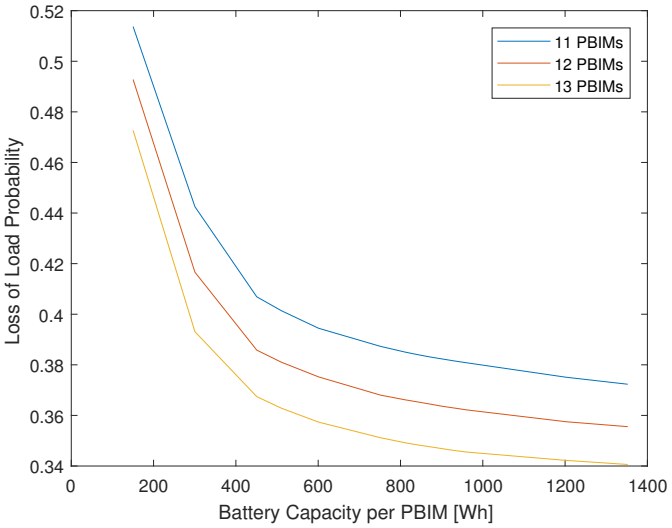

Figure 5.6: LLP as a function of installed battery capacity, Netherlands

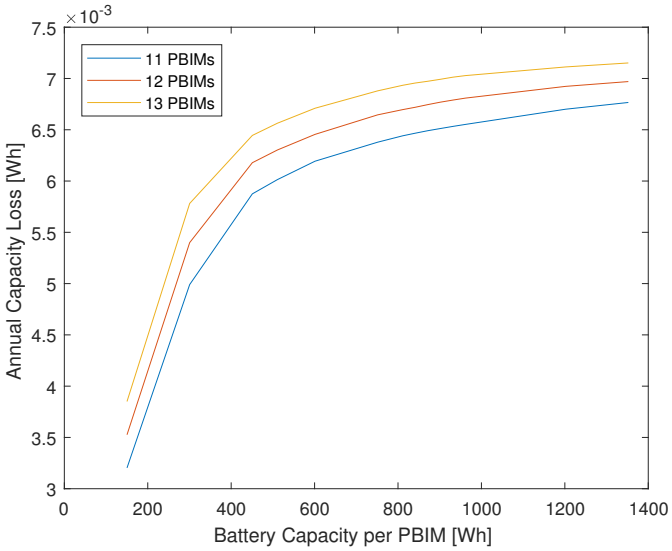

Figure 5.7: Annual capacity loss, Netherlands.

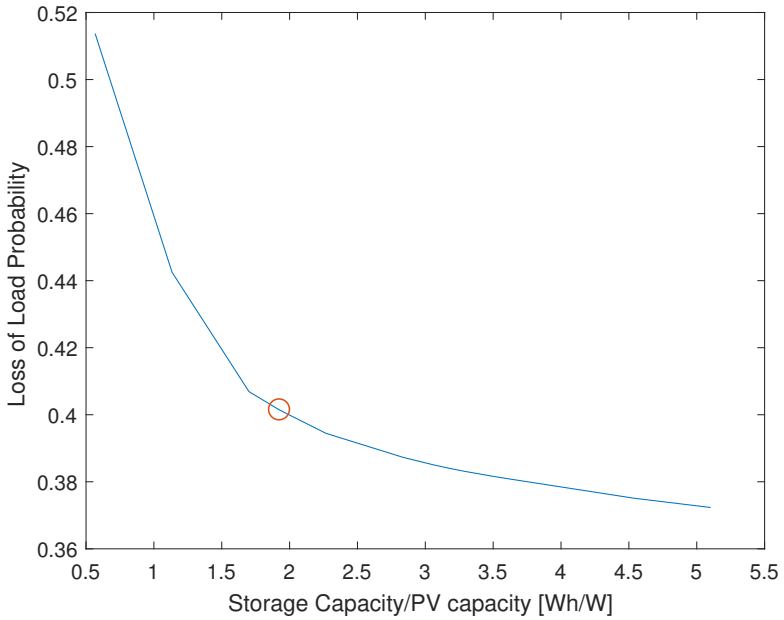

Figure 5.8: Identification of the critical battery capacity, Netherlands

5.3.5. Optimal system characteristics

The performance and the system characteristics differ greatly when comparing between the PBIM's off-grid application in Costa Rica and the Netherlands. In this case with the entire supply of energy being self generated, the ability of the system to meet the load requirements is dependent on the ratio between the energy storage and battery capacity, which have been identified in the previous section. For each location the optimal system is defined by the PV array sizes presented in Table 5.1 and the optimal battery-PV ratios presented in Figures 5.5 & 5.8 for Costa Rica and the Netherlands respectively.

Autarky

Compromising of 6 PBIMs, within each a 800Wh battery installed, the system in Costa Rica is able to maintain monthly autarky levels of above 80%, Figure 5.9. On the other hand the autarky levels for the PBIM system in the Netherlands varies between monthly autarky levels as low as 10% in December and rising above 70% in June despite consisting of an 11 module PV array.

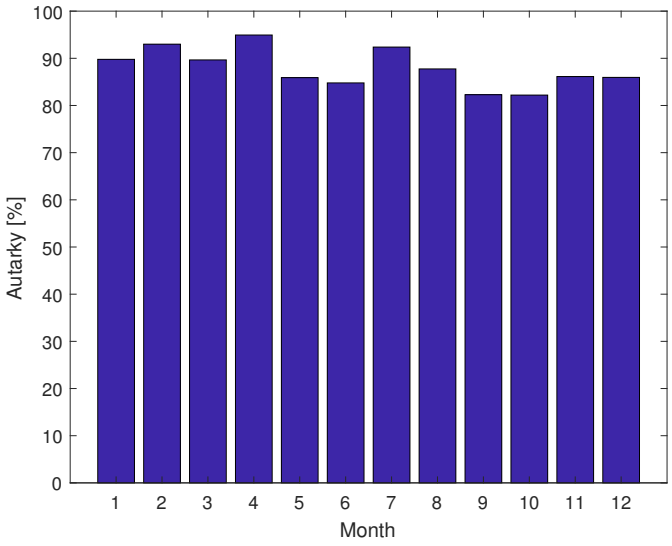

Figure 5.9: Monthly system autarky, Costa Rica.

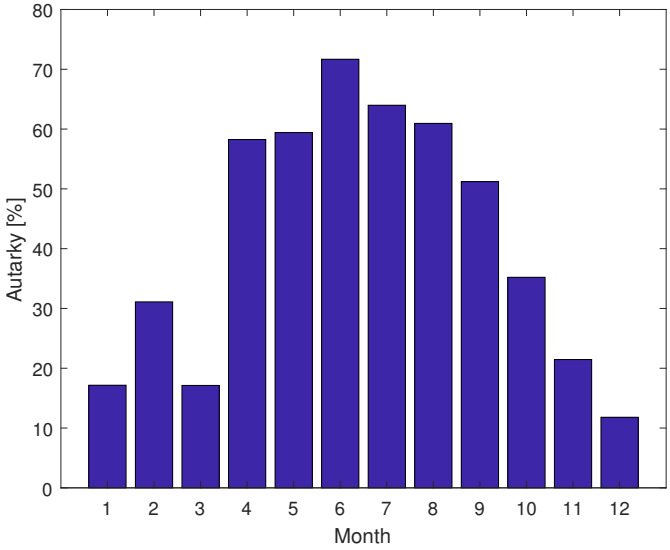

Figure 5.10: Monthly system autarky, Netherlands.

State of Charge

The SoC variations over the entire year are presented in Figures 5.11 & 5.12 for Costa Rica and the Netherlands respectively. In the Costa Rican case the battery is uniformly used throughout the year, with the battery being fully charged and discharged between restricting SoC limits on a regular basis. For scenario in the Netherlands throughout the winter the months, the battery usage is minimal with the battery SoC rarely rising above 50%. However, during the summer, the battery SoC variations is comparable to that in Figure 5.11, whereby the entire available energy storage capacity is used.

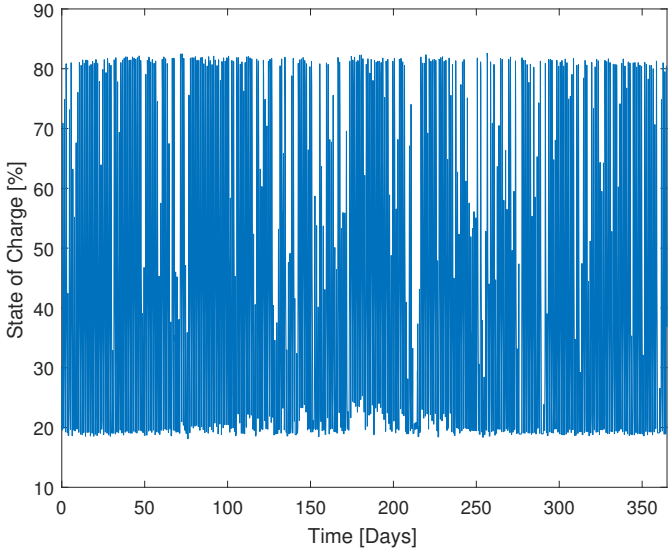

Figure 5.11: SoC variations, Costa Rica

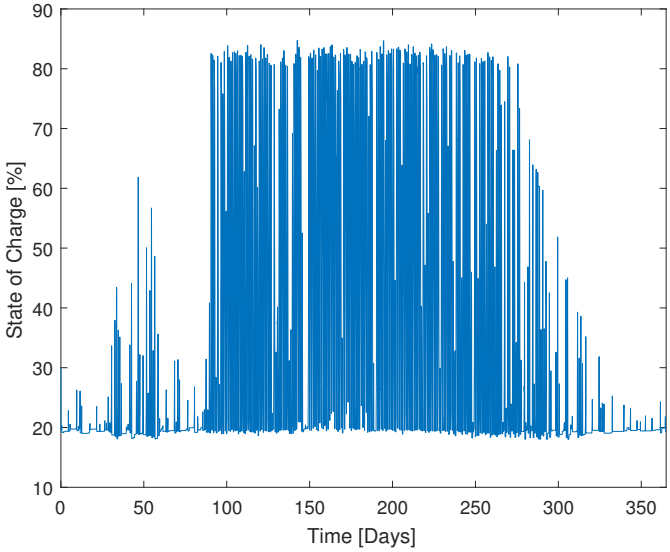

Figure 5.12: SoC variations, Netherlands

Energy Dump

The energy dump refers to the available excess energy that occurs once the load energy demand is met and the battery is fully charged. During this time the PV array continues to generate energy which needs to be dumped. The excess energy generated by the systems in Costa Rica and the Netherlands are presented in Figures 5.13 & 5.14 respectively. The excess energy in the Costa Rican system varies on a monthly basis and with the total energy dumped per month seemingly high. As a result of the high reliability of the system it is designed to perform during periods of time with unfavorable conditions. Therefore in the presence of consistently favorable conditions an excess of energy is generated. When the batteries are fully charged the energy from the PV array is directly used to meet the energy demands at that instant in time. During such a scenario should the energy generation of the PV array exceed the instantaneous energy demand, this generated energy is dumped. Combining the high variability of both the available solar energy and the energy demands (Figure 5.2) a mismatch between the two is expected. The system in Costa Rica boasts an LLP of 0.12 it is therefore able to meet the energy demands throughout most of the unfavorable conditions,

a draw-back of such a system is the consistent presence of excess energy.

The energy dump in the Netherlands is remarkably low during the winter, indicating that throughout these months the battery is able to store a significant amount of energy not used directly for the load. However, during the summer the energy being dumped is quite large. Due to the autonomous nature of the system the only manner in which to use the high levels of excess energy during the summer is through the implementation of seasonal storage. This option will however lead to higher system costs.

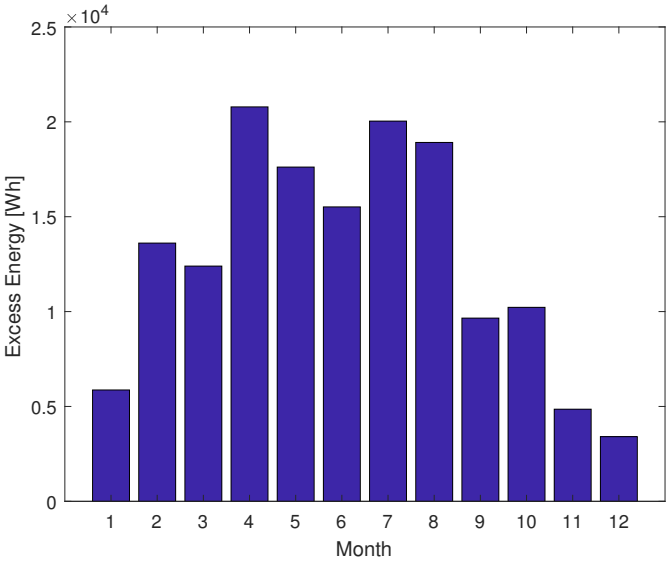

Figure 5.13: Monthly energy dump, Costa Rica.

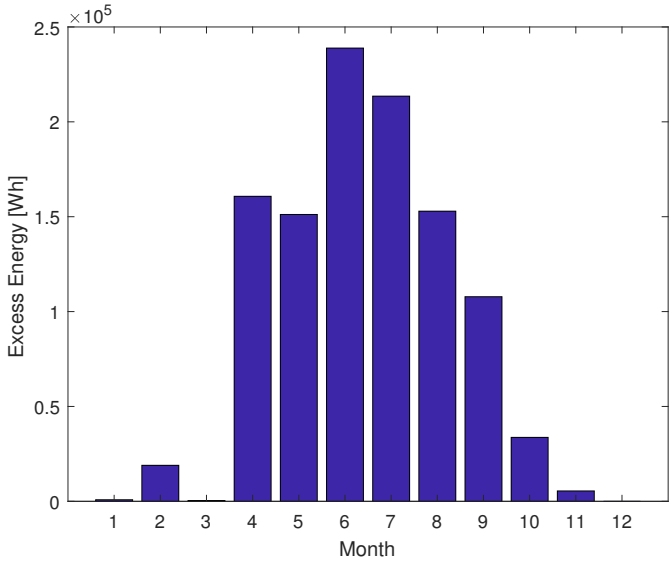

Figure 5.14: Monthly energy dump Netherlands.

Battery Degradation

The percentage of battery capacity loss for the system in both locations is presented in Figure 5.15. The total capacity loss per year for the battery in Costa Rica is 1.62% whereas in the Netherlands it is only 0.9%. The battery in Costa Rica experiences a high degradation rate due to its more frequent deep cycling and the consistent high ambient temperatures at which this occurs. This degradation rate remains consistent throughout the year whereas for the battery in the Netherlands the degradation rate increases during the summer when the battery undergoes more frequent cycling than during the winter.

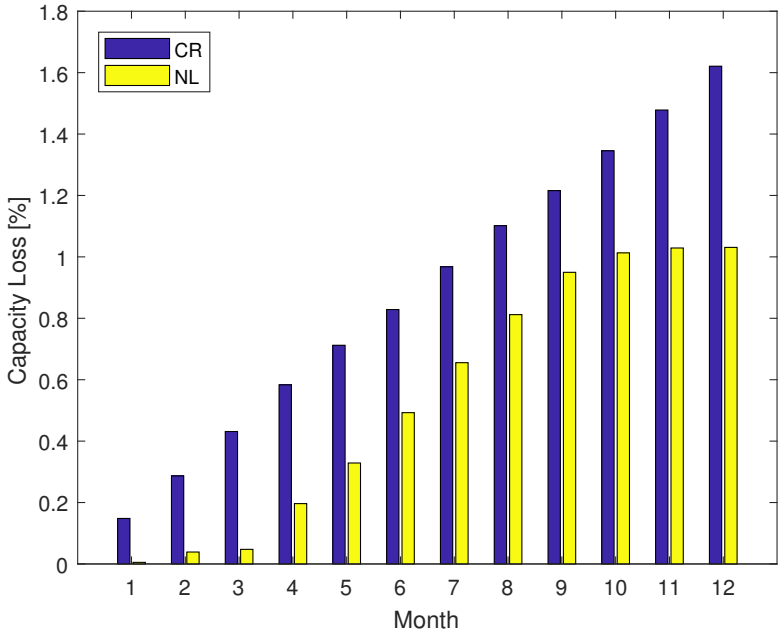

Figure 5.15: Comparison of the monthly battery degradation between Costa Rica (CR) and the Netherlands (NL).

5.3.6. CONCLUSIONS

- **Storage** Observable in the LLP figures, for a fixed PV capacity is an optimal battery capacity. Increase the available capacity above a certain limit no longer proves to have a positive impact on the system reliability, this is observable for both locations. The off-grid system in the Netherlands is found to require a lower battery/PV capacity compared to an off-grid system in Costa Rica, however the total system size in the Netherlands is required to be much larger than in Costa Rica in order to overcome the negative effects of poor solar irradiance during the winter.

- **Energy Dump** The distribution and quantity of energy dumped a year varies between the two locations. However the energy dumped for both locations is considered to be high and let unavoidable. In order to minimize the dumping of excess energy, alternative energy storage technologies could be considered for the longer term seasonal storage.

- **Degradation** Higher ambient temperatures and more frequent deep cycling of the battery result in a greater capacity loss for the system in Costa Rica. As a result the battery can be expected to be replaced sooner than that installed in the system in the Netherlands.

6

PV-Battery Integrated Module Feasibility

In this section, the PV-Battery integrated Module is compared to a conventional solar system in terms of both their technical and economical aspects. The PBIM design aims to reduce the initial capital costs of residential solar systems. However this will only become the case if its performance characteristics remain comparable to that of conventional solar home systems. The characteristics of the PBIM and conventional system are modelled and the results are analyzed. The technical and economic comparisons are performed between a conventional and PBIM system in the Netherlands.

6.1. Scenario Design

The modelling of the PBIM has been explained in detail in Chapter 3. In this performance comparison between a convention solar home system and the PBIM the effect of temperature is considered. The operating temperature of the PV module and the battery are considered to be the aspects which heavily influence the PBIM performance. A comparison is provided to determine the extent to which this affects the system performance; the conventional system is first defined. Both systems are modelled for the same application: grid connected peak shaving in the Netherlands. To preserve the integrity of the comparison the storage and PV capacity of both systems are identical. In this section the scenario in which the two systems are compared is defined.

6.1.1. Energy Storage

As is common practice the batteries for conventional residential system are placed away from the PV modules and stored indoors. The ambient temperatures in a Dutch household do not reflect outdoor ambient temperatures. The battery of a convectional system is exposed to, is therefore assumed to remain constant throughout the year. The indoor ambient temperatures remain well within the nominal temperature range, (Table 2.2. On the other hand the battery in the PBIM is exposed to a much wider range of ambient temperatures throughout the year.

6.1.2. PV Module

The efficiency of the PV module varies as a function of the module temperature. For conventional solar systems the convective cooling of the module is dependent on the applied mounting structure whereby rack mounts, installed approximately 1 meter above the ground allow for a larger heat transfer between the module and the environment as compared to a stand-off mount which typically leaves the module placed 20cm above the ground. As a result of high wind speeds the cooling of the module is accelerated due the turbulent nature of the airflow around the PV module.

Regarding the PBIM concept the BoS components are encased at the rear of the PV module resulting in a lower module surface area that is directly in contact with the surrounding environment. As a result of this encasing the heat dissipation from the module to the ambient air is reduced. The PV module of the PBIM will therefore experience higher operating temperatures than a solar module in conventional systems. The extent to which the elevated module temperatures affect the system performance as a whole is discussed.

6.2. Technical Feasibility

To asses the deliverable performance of the PBIM, the manner in which the PV and battery are affected by temperature is studied.

6.2.1. PV Module temperature

Simulations were performed to asses the system characteristics of the PBIM as compared to a conventional system and to quantify the effect of elevated temperatures on the system. The methodology on which the modelling on the PV module temperature is based is derived from [18]. To illustrate the effect of the poorer heat dissipation of the PBIM

PV module the simulation result presented in Figure 6.1 presents the temperature variation of the module applied in a conventional and the PBIM system for an average spring day.

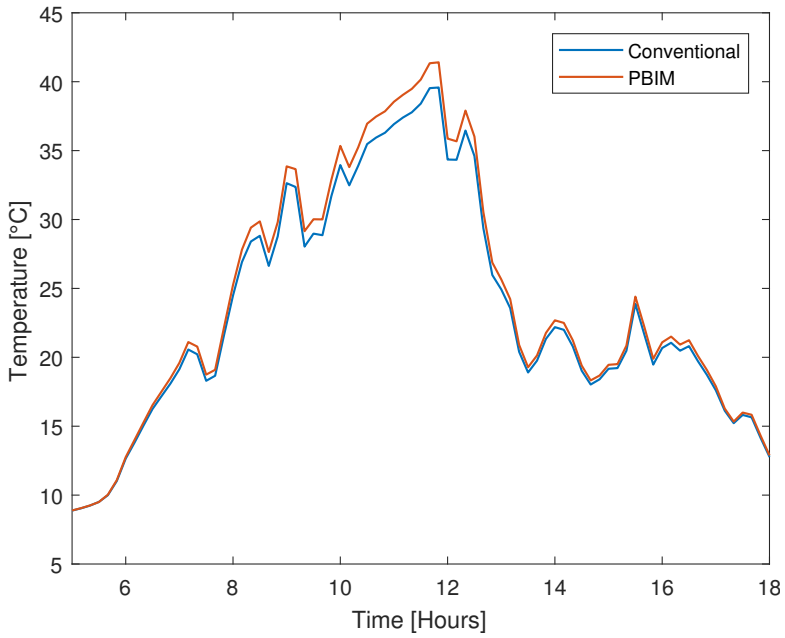

Figure 6.1: PV temperature in conventional and PBIM systems for day 100 of the year.

During the middle of the day, where the highest ambient temperatures are present the difference in the temperature between the two modules reaches a maximum of 1.5 °C, for the 100th day of the year. The difference is expected to become more pronounced during the warmer periods of the year. This elevated temperature will affect the PV module performance, resulting in its operation at lower efficiencies.

6.2.2. PV Energy Yield

With both modules exposed to same ambient irradiance and temperature conditions in the Netherlands, the dynamic operating efficiency of each test module is determined and resulting in an estimation of the the annual energy generation of each module, Table 6.1. The PV module in the conventional system is predicted to generated 0.4 % more energy compared to the module used in the PBIM system. This decreased PV energy production can be considered to be insignificant. To provide additional perspective the energy yield results for the different system in Costa Rica have also been provided. In this case the difference in energy production is considerably more, with the PV module in the conventional system generating 10.5% more energy per year than the module in the PBIM system. This justified by effect of the ambient meteorological conditions for each location.

System	**Energy generation [kWh/year]**	
	NL	CR
PBIM	255.14	384.25
Conventional	256.16	424.45

Table 6.1: Energy generated by the 265Wp Jinko PV module in PBIM and conventional applications, for the different locations

6.2.3. Battery Degradation

Included in this comparison is the extent to which the elevated ambient temperatures affects the degradation of the battery installed at the rear of the PV module according to the PBIM design. According to [18] when placed at an optimal distance from the PV module to battery in the PBIM experiences a temperature equal to the ambient temperature, such that the heat dissipation of the PV module does not influence the ambient temperature of the battery. On the other hand the battery in the conventional system, located in the household, is assumed to experience a constant ambient temperature of 21 °C throughout the year [48]. The extent to which these conditions influence the battery degradation for each system is presented in Figure 6.2.

These results indicate the battery in the PBIM experiences a greater loss in capacity throughout a year of usage, as compared to the battery used in conventional systems. This is due to the elevated temperatures of the outdoor PBIM battery. The total degradation of the PBIM battery is found to be 0.11% higher per year than in the conventional system, for the applied peak shaving algorithm. This is considered to be a negligible difference.

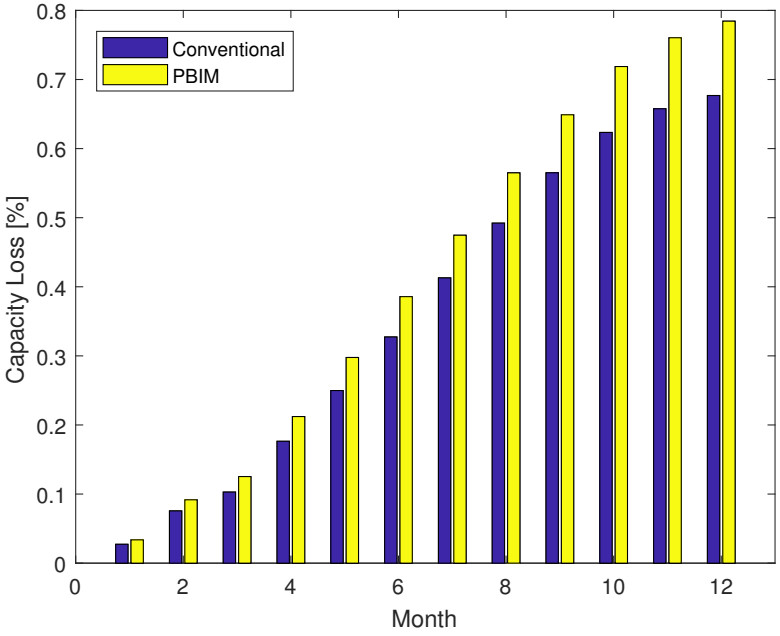

Figure 6.2: Battery capacity loss for the conventional and PBIM solar systems.

6.2.4. Energy Drawn From The Grid

The objective of the grid-connected system is to reduce the energy costs by reducing the peak load demand. The effectiveness of the conventional and the PBIM systems at realizing this goal is assessed. Figure 6.3 compares the annual peak load energy costs for the different systems. For comparison the energy consumption exclusively during peak hours is presented for a the normal household with no PV or storage capacity (NO PV), for a system with only PV and no storage capabilities (PV) and for the PBIM and conventional systems. These comparisons are performed for a 6 module array with the optimal battery capacity equating to a Battery-PV ratio of 2.3 Wh/Wp. The energy consumption is normalized for the peak hour requirements of the load. Having solely a PV array with no storage capabilities has a minimal effect in reducing the energy consumption. This is due to the presence of the peak hours in the evening whereby the available solar energy is minimal. The ability of the PBIM and conventional system to meet the system requirements have what can be considered to a negligible difference in peak load reduction by taking into account solely temperature effects.

For the same system, the impact on the total energy drawn from the grid is presented in Figure 6.4. With No-PV indicating the total household energy demand. Noticeable in this figure is the reduced energy demand for a PV array as compared to both the conventional and PBIM systems. This is due to the higher losses associated to the battery usage and therefore, more energy is drawn from the year on an annual basis for the systems incorporated with energy storage capabilities.

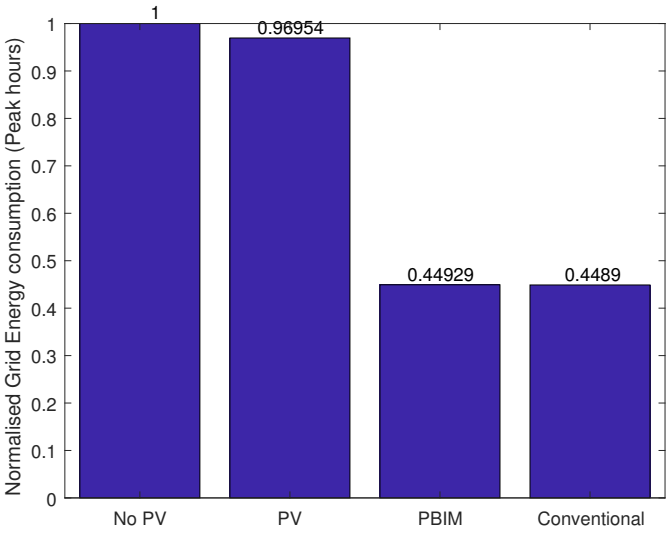

Figure 6.3: Annual Energy drawn from grid during peak hours

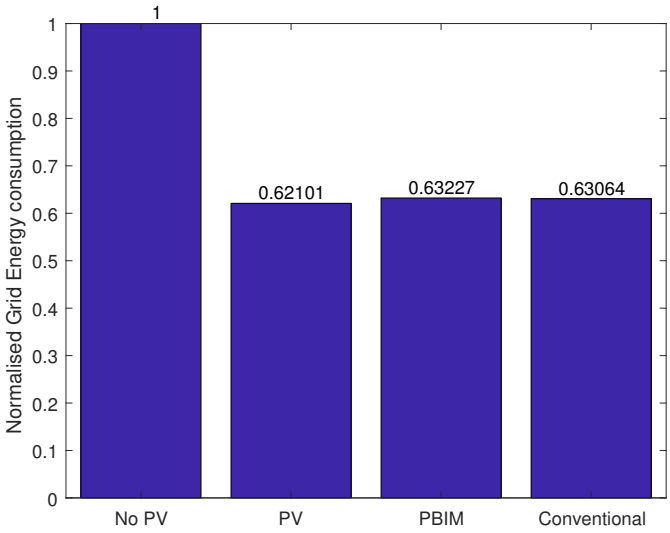

Figure 6.4: Total annual energy drawn from grid

Component	Price [€]
PV module	150
Charge Controller (MPPT)	220
Micro inverter	45
Battery (10 Ah,33 V)	250

Table 6.2: PBIM component cost.

Component	Price [€]
PV module	150
Charge Controller (MPPT)	440
Inverter	340
Battery (10 Ah,33 V)	185

Table 6.3: Conventional system component costs.

6.3. Economic Feasibility

In addition to the technical aspects of the PBIM, a cost analysis is also performed to provide an indication of the potential economic benefits for the end-user. In this case such benefits are in the form of savings made on the energy bill.

6.3.1. Energy Bill Reduction

Through the implementation of the peak shaving energy savings on the residential electricity bill are incurred by the energy user. With the algorithm dictating that the self-generated is used exclusively during peak periods unless the battery is fully charged. Figure 6.5 presents the energy costs with respect to the different systems. The annual costs for the system without nay batteries (PV) is 23% higher than the PBIM and convectional systems in which batteries are present. This demonstrates that the addition of batteries to store self-generated energy for use during periods of time with high energy prices has a significant effect on reducing energy costs. Capital costs need to be taken into consideration to asses the financial viability of introducing the batteries into the renewable energy system.

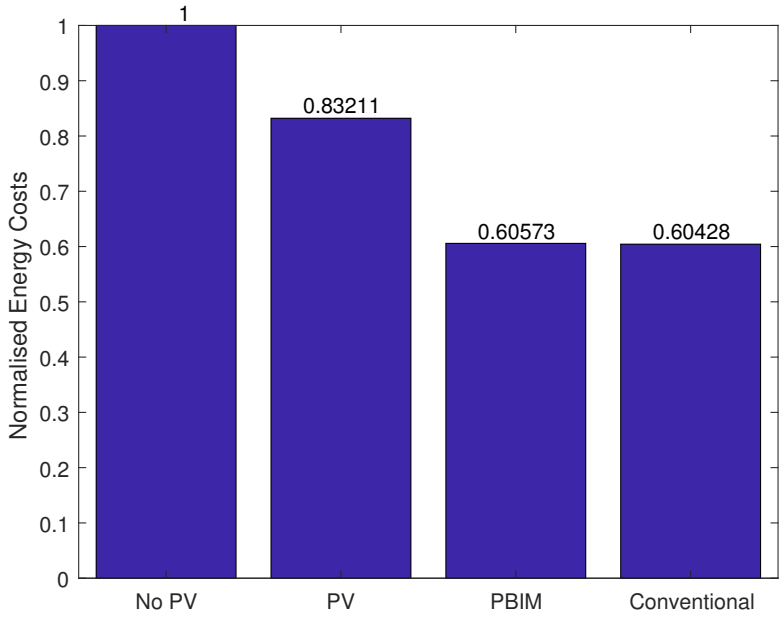

Figure 6.5: Normalized annual energy costs.

6.3.2. Initial Capital Costs

The component costs for a single PBIM are presented in Table 6.2. For the 6 module PBIM system considered in Figures 6.3 through to 6.5 the total capital cost of such a system amounts to a total of 6618 €. It has to be noted that the PBIM concept is still in the early stages in development and therefore high capital costs are associated with the necessary components.

6.3.3. Payback Time

The payback time is widely used financial metric used across the industry to asses the financial viability of upcoming projects. It is defined as the time, in years, that it takes for the system to generate enough savings such that it covers the initial investment costs. The payback time is calculated as follows:

$$\text{Payback time} = \frac{\text{Initial Investment}}{\text{Annual return}} \tag{6.1}$$

The energy costs of the energy demand per year, whereby the 100% of the energy used is drawn from the grid the household electricity bill stands at 915 €. Figure 6.2 demonstrates that the application of the 6 module PBIM system reduces the energy bill by 40%. The PBIM system therefore has a payback time of 11.8 years, which is remarkably high

for a residential PV system. Furthermore, for its application in the Netherlands, the system remains relatively unused during the winter, due to the low levels of available irradiance, which is unlike the case for the its application in Costa Rica. On the other hand, a conventional solar home system of the same capacity the payback time is estimated to be 7.6 years.

The PBIM is still in the early stages of development and requires the implementation of state-of-the-art batteries and micro-inverter. These high cost components negatively influence the financial attractiveness of the PBIM system, over a conventional system. However as these technologies develop and economies of scale is introduced instead of the single component purchasing, which the prices in Table 6.2 and 6.3 are based upon, the cost of a PBIM can be expected to significantly decrease.

6.4. Conclusions

In this section the financial and technical feasibility of the PBIM has been assessed and compared to that of a conventional solar system. In terms of technical capabilities the PBIM performs slightly worse than a conventional system, in terms of lower PV generation and a faster battery degradation. However, the differences between the two systems can be considered insignificant as concluded by this comparisons for the grid connected system in the Netherlands. In terms of financial feasibility the PBIM currently does not fare well as compared to a conventional system despite the promise of reduced installation and labour costs. This is primarily due to the high costs of the components. The costs of the PBIM components are based on the costs of a PBIM prototype, with the components origination from various suppliers and regions leading to a remarkably high cost. With further development the PBIM has potential to compete with conventional solar systems in the future.

7

CONCLUSIONS & RECOMMENDATIONS

Throughout this thesis the PBIM concept was tested under different energy storage scenarios and locations. Case studies were created to asses the PBIM performance in off-grid and grid-connected applications for the Netherlands and Costa Rica. Based on the system objectives and characteristics the optimal battery capacity for each case study is proposed. The project extends further to asses the performance of the PBIM system with the optimal energy storage capacity for each of the case studies. Furthermore, the technical and economic feasibility of the PBIM is compared to a conventional system for peak shaving applications in the Netherlands.

7.1. CONCLUSIONS

To set the scope of the project research questions were formulated. In this section, the identified questions are answered based on the analysis performed throughout the project.

1. **What is the impact of local weather conditions and energy storage motivations on the PV-Battery Integrated Module?**

    - **In which applications is the PBIM an effective solution?** The full benefits of the PBIM are taken advantage of in residential applications, by offering a standardized and optimized solar system. The PBIM is found to be an effective solution for grid connected applications by reducing the peak load of a household and benefiting the consumer by reducing the energy costs. The PBIM is also an effective solution for off-grid applications particularly in remote rural areas, offering a user-friendly, modular energy system.

    An analysis on the impact of ambient conditions on the performance indicators was implemented, concluding that the ambient conditions significantly impact the operation of the PBIM. In Costa Rica the PBIM is seen as a more effective solution as its energy generation is consistently high throughout the year. The Jinko 265Wp PV module generates on average, 424kWh yr^{-1} *in Costa Rica, whilst in the Netherlands for the same PV module, an energy yield of 217kWh* yr^{-1} *is estimated. The ambient temperatures of the different locations were also concluded to have a significant impact on the PBIM battery. The higher ambient temperatures in Costa Rica were found to accelerate the battery aging mechanisms resulting in a shorter lifetime than its operation in the cooler ambient temperatures of the Netherlands.*

    The analyzed energy storage motivations dictated the manner in which the internal power flow was controlled. For peak shaving applications in Costa Rica the battery was required to undergo more frequent cycling than in the Netherlands, due to the year-round abundance of solar energy. The energy pricing scheme in Costa Rica dictated the presence of two peak periods. To meet the peak shaving requirements the battery was programmed to discharge twice a day, whilst in the Netherlands a single peak period was defined on a daily basis, therefore requiring the battery to discharge once. The combined effect of higher temperatures and more frequent cycling resulted in an annual battery capacity loss of 1.5% in Costa Rica. On the other hand the annual capacity loss in the Netherlands was significantly lower 0.8%. Regarding the application of the PBIM for off-grid applications the battery capacity loss was found to be 1.6% in Costa Rica per year and in the Netherlands an annual capacity loss of 1% is expected.

    The application and location of the PBIM significantly impacts the system characteristics of the PBIM. The effects in terms of battery degradation, autarky, reliability have been defined and quantified based on the analysis of 4 different case studies. The case studies were designed to include locations with significantly different climates.

2. **What is the most appropriate battery size to install in a single PV-Battery Integrated Module for each energy storage scenario?**

    - **What are the system requirements for each energy storage scenario?** The objectives of the considered system applications were determined to be conflicting. Regarding the gird-connected topology for peak

shaving, the system requirements were defined to be maximizing the shaving of the peak load and minimize the capacity of the installed battery bank. Off-grid applications were also considered and were required to posses a higher level of autonomy. The system objectives for the off-grid system were defined to be: maximize the reliability and minimize the installed battery capacity.

- **How can the appropriate battery size be identified?** The defined set of performance indicators are battery degradation, autarky and for the off-grid scenario, energy dump. This project demonstrated the existence of a saturation point whereby increasing the battery capacity for a fixed PV array did not result in an increase of the beneficial system characteristics. This was found to be true for all the considered cases except the grid connected PBIM system in the Netherlands which required economic factors to be taken into account.

For peak shaving applications the appropriate battery capacity per PBIM with respect to the Jinko 265Wp PV module for grid connected applications in Costa Rica is found to be 729Wh. For the same application in the Netherlands the optimal capacity is found to be 600Wh (taking economic considerations into account). Regarding off grid applications, the optimal battery capacity to PV capacity ratio has been found to be 3Wh/Wp and 2Wh/Wp for Costa Rica and the Netherlands respectively.

3. **How effective is an optimally sized PBIM for the identified scenarios?**

   - **Grid Connected** For grid connected peak shaving applications a single PBIM system with an optimal battery capacity of 729Wh is able to reduce the peak load by 26% which equates to the system generating 101 € in savings per year. Regarding the PBIM system in the Netherlands which, on an annual basis, reduced the peak load by 28% generating annual savings of 76 €.
   - **Off-grid.** For the off-grid case study the the PV array size and the energy storage was optimized for each case study. In Costa Rica a 1.5kWp PV array with each PBIM installed with a 800Wh the system is found to have a LLP of 0.1. Whereas the 2.9kWp PV array necessary in the Netherlands, with each PBIM installed with a 530Wh battery is only able to achieve an LLP of 0.4.

4. **How does an appropriately sized PV-Battery Integrated Module compare to a conventional solar system?**

   - **How does the performance of the PV-Battery Integrated Module compare to a conventional system?** Foe the assessed case in the Netherlands the PV module of the PBIM was estimated to generate 0.4% less in the Netherlands and 10.5% less in Costa Rica. The rate of battery degradation is 0.11% higher per year for grid connected PBIM applications in the Netherlands as compared to a conventional system.
   - **Is the PV-Battery Integrated Module a financially viable solution?** At the time of writing the PBIM is not considered a financially viable solar solution. The PBIM for grid-connected applications in the Netherlands was found to have a payback time of 11.8 years, whereas for a conventional system the payback time is found to be significantly less standing at 7.6 years.

In conclusion the PBIM is has been proven to be slightly less efficient as compared to a conventional system however, it is found to be technically feasible. With the potential to deliver multiple advantages over conventional PV systems, with further development the PBIM concept is poised to become a promising a concept within the solar industry, whereby the advantages it provides justifies the reduced working efficiencies it possesses.

7.2. Recommendations

With this thesis providing an overview on the impact of energy storage motivations and locations on the appropriate battery size and system performance a continuation and improvements can always be made.

7.2.1. System Modelling

In hindsight, additional features to take into consideration regarding the PBIM modelling are identified.

- **Temperature Effects** In this project, the effect of the elevated PBIM temperatures on component lifetime was only considered for the battery. To provide a more comprehensive overview the effect of such temperatures on the lifetime of the other components; namely the PV module and the power electronics can be taken into consideration. In this manner the deterioration of the PV module's power output and the impact of the power electronics' operating efficiencies.

- **Performance indexes** In addition to the performance indexes implemented in this project, the number of performance indexes can be increased to include parameters such as maximum allowable battery Depth of Discharge of the battery. This will provide the added benefit of identifying the optimal battery operation scheme.

- **Dynamic time-of-use pricing** Regarding the analysis of the PBIM for peak shaving applications, the scope of this project considered fixed peak hours throughout the assessed time-span. However, based on the market clearing price energy pricing may fluctuate on an hourly basis, affecting the time and length of peak periods.

Furthermore, with the rapid integration of distributed energy sources electricity prices can be expected to experience significant fluctuations based on the supply of energy (especially from intermittent sources such as wind or solar) as well as the energy demand. For future considerations a more realistic peak shave scenario may be considered such that a dynamic pricing scheme is included thus influencing the manner and frequency at which the battery is operated.

7.2.2. Model Validation

Throughout this project the PBIM model has been applied in a dynamic manner and producing consistent results for each of the case studies. However a more robust validation approach can be adopted, by using data from either experimental or real-life systems to asses how well the model simulates a realistic scenario. Via such validation methods the consequences of physically integrating the battery and the BoS components to the rear of the PV module can be fully understood and quantified.

7.2.3. PBIM Battery Sizing

In the light of the PBIM becoming a standardized solar system, the ideal system design is required to be sized to suit all applications and locations. This standardized sizing would require a compromise in the system's performance in every application therefore it would be interesting to determine an energy storage capacity whereby the negative impact on the fulfillment of the system's objectives would be minimized. In this manner the battery sizing methodology outlined in this project would be expanded to include multiple locations in a single sizing analysis.

A

Appendix

A.1. Data Sheets

A.1.1. PV module Data Sheet

A.1.2. Battery Data Sheets

www.jinkosolar.com

Solar JinKO
Building Your Trust in Solar

JKM265P-60
245-265 Watt
POLY CRYSTALLINE MODULE

Positive power tolerance of 0/+3%

ISO9001:2008·ISO14001:2004·OHSAS18001 certified factory.
IEC61215·IEC61730 certified products.

KEY FEATURES

High Efficiency:
High module conversion efficiency (up to 16.19%), through innovative manufacturing technology.

Low-light Performance:
Advanced glass and solar cell surface texturing allow for excellent performance in low-light environments.

Severe Weather Resilience:
Certified to withstand: wind load (2400 Pascal) and snow load (5400 Pascal).

Durability against extreme environmental conditions:
High salt mist and ammonia resistance certified by TUV NORD.

LINEAR PERFORMANCE WARRANTY

10 Year Product Warranty • 25 Year Linear Power Warranty

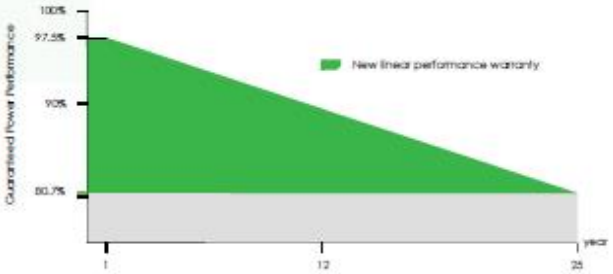

Engineering Drawings

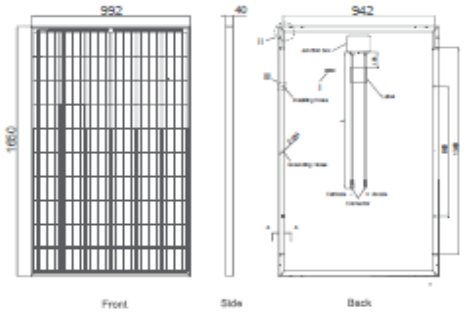

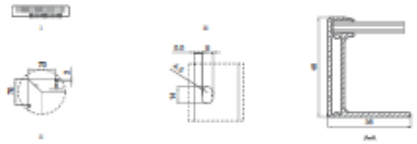

Packaging Configuration

(Two boxes=One pallet)

25pcs/ box, 50pcs/pallet, 700 pcs/40'HQ Container

Electrical Performance & Temperature Dependence

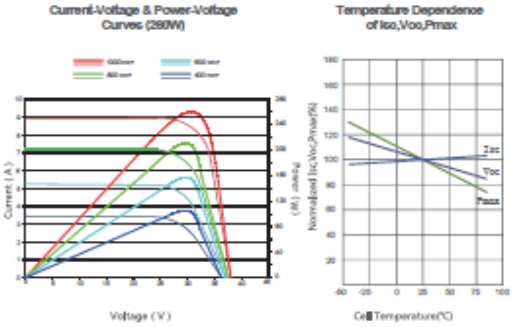

Mechanical Characteristics

Cell Type	Poly-crystalline 156×156mm (6 inch)
No.of cells	60 (6×10)
Dimensions	1650×992×40mm (65.00×39.05×1.57 inch)
Weight	19.0 kg (41.9 lbs)
Front Glass	3.2mm, High Transmission, Low Iron, Tempered Glass
Frame	Anodized Aluminium Alloy
Junction Box	IP67 Rated
Output Cables	TÜV 1×4.0mm², Length:900mm

SPECIFICATIONS

Module Type	JKM245P		JKM250P		JKM255P		JKM260P		JKM265P	
	STC	NOCT	STC	NOCT	STC	NOCT	STC	NOCT	STC	NOCT
Maximum Power (Pmax)	245Wp	181Wp	250Wp	184Wp	255Wp	189 Wp	260Wp	193Wp	265Wp	197Wp
Maximum Power Voltage (Vmp)	30.1V	27.8V	30.5V	28.0V	30.8V	28.5V	31.1V	28.7V	31.4V	29.0V
Maximum Power Current (Imp)	8.14A	6.50A	8.20A	6.56A	8.28A	6.63A	8.37A	6.71A	8.44A	6.78A
Open-circuit Voltage (Voc)	37.5V	34.8V	37.7V	34.9V	38.0V	35.2V	38.1V	35.2V	38.6V	35.3V
Short-circuit Current (Isc)	8.76A	7.16A	8.85A	7.21A	8.92A	7.26A	8.98A	7.31A	9.03A	7.36A
Module Efficiency STC (%)	14.97%		15.27%		15.58%		15.89%		16.19%	
Operating Temperature(℃)	-40℃~+85℃									
Maximum system voltage	1000VDC (IEC)									
Maximum series fuse rating	15A									
Power tolerance	0~+3%									
Temperature coefficients of Pmax	-0.41%/℃									
Temperature coefficients of Voc	-0.31%/℃									
Temperature coefficients of Isc	0.06%/℃									
Nominal operating cell temperature (NOCT)	45±2℃									

STC: Irradiance 1000W/m² Cell Temperature 25°C AM=1.5

NOCT: Irradiance 800W/m² Ambient Temperature 20°C AM=1.5 Wind Speed 1m/s

* Power measurement tolerance: ± 3%

Power From Innovation

A123 SYSTEMS

20Ah Prismatic Pouch Cell

Nanophosphate®Lithium-Ion

A123's patented Nanophosphate technology provides this prismatic cell with outstanding cycle life and a very high power output. With a high usable energy range and industry-leading abuse tolerance, this cell delivers excellent performance even under the most rigorous testing. Packaging these light weight cells is easy because of the compact design that's ready for virtually any high power application.

Applications

- HEV Heavy Duty Commercial Vehicles
- PHEV & HEV Passenger Vehicles
- Starter Battery

Abuse Test	Result
Nail Penetration	Pass—EUCAR 4
Overcharge	Pass—EUCAR 3
Over-discharge	Pass—EUCAR 3
Thermal Stability	Pass—EUCAR 4
External Short	Pass—EUCAR 3
Crush	Pass—EUCAR 3

Product Specifications	
Cell Dimensions (mm)	7.25 x 160 x 227
Cell Weight (g)	496
Cell Capacity (minimum, Ah)	19.5
Energy Content (nominal, Wh)	65
Discharge Power (10-second, W))	1200
Voltage (nominal, V)	3.3
Specific Power (nominal, W/kg)	2400
Specific Energy (nominal, Wh/kg)	131
Energy Density (nominal, Wh/L)	247
Operating Temperature	-30°C to 55°C
Storage Temperature	-40°C to 60°C

www.a123systems.com +1.734.772.0300

Power From Innovation

A123 SYSTEMS

14Ah Prismatic Pouch Cell

Nanophosphate®Lithium-Ion

A123's patented Nanophosphate technology provides this prismatic cell with outstanding cycle life and a very high power output. With a high usable energy range and industry-leading abuse tolerance, this cell delivers excellent performance even under the most rigorous testing. Packaging these light weight cells is easy because of the compact design that's ready for virtually any application.

Applications

+ HEV Heavy Duty Commercial Vehicles
+ HEV Passenger Vehicles
+ Starter Battery

Abuse Test	Result
Nail Penetration	Pass—EUCAR 4
Overcharge	Pass—EUCAR 3
Over-discharge	Pass—EUCAR 3
Thermal Stability	Pass—EUCAR 4
External Short	Pass—EUCAR 3
Crush	Pass—EUCAR 3

Product Specifications

Cell Dimensions (mm)	7.25 x 160 x 227
Cell Weight (g)	510
Cell Capacity (minimum, Ah)	14
Max Discharge Current (10-second, A)	500
Discharge Power (10-second, W))	1400
Voltage (nominal, V)	3.3
Specific Power (nominal, W/kg)	2700
DCR (10-second, MΩ)	1.3
Cycle Life at 100A Discharge, 100% DOD	>1000
Operating Temperature	-30°C to 55°C
Storage Temperature	-40°C to 60°C

www.a123systems.com +1.734.772.0300

BIBLIOGRAPHY

[1] IRENA, *Renewable energy technologies: Cost analysis series; solar photovolatics,* IRENA Working Paper **1** (2015).

[2] V. Vega-Garita, *Pv-battery integration design, construction, and evaluation,* .

[3] J. Reynaud, C. Alonso, P. Aloisi, C. Cabal, B. Estibals, G. Rigobert, G. Sarre, H. Rouault, D. Mourzagh, F. Mattera, and S. Genies, *Multifunctional module lithium-ionstorage and photovoltalc conversion of solar energy,* Photovoltaic Specialists Conference (2008).

[4] V. Vega-Garita, A. Harsarapama, L. Ramirez-Elizondo, and P. Bauer, *Physical integration of pv-battery system: Advantages, challenges, and thermal model,* 2016 IEEE International Energy Conference (ENERGYCON) (2016).

[5] A. Smets, K. Jäger, O. Isabella, R. van Swaaij, and M. Zeman, *Solar energy; the physics and engineering of photovoltaic conversion, technologies and systems,* UIT Cambridge (2016).

[6] A123, Energy, and Solutions, *Battery pack design, validation and assembly guide using a123 systems amp20hd-a nanophophate cells,* Design Guide (2014).

[7] V. Sulaeman, I andVega-Garita, G. Chandra Mouli, N. Narayan, L. Ramirez-Elizondo, and P. Bauer, *Comparison of pv-battery architectures for residential applications,* 2016 IEEE International Energy Conference (ENERGYCON) (2016).

[8] G. Karmiris, , and T. Tengnér, *Peak shaving control method for energy storage,* ABB AB, Corporate Research Center (2015).

[9] ABB, *Abb micro inverter system,* Product Datasheet (2017).

[10] C. Curry, *Lithium-ion battery costs and market,* BLoombergy New Energy Finance (2017).

[11] J. Vetter, P. Novák, M. Wagner, and C. Veit, *Ageing mechanisms in lithium-ion batteries,* Journal of Power Sources **147**, 269 (2005).

[12] I. C. de Electricidad, *Tipos de tarifa residencial,* (2017).

[13] e on, *Huishoudelijk en kleinzakelijk,* e-on **75**, 1 (2016).

[14] World, Energy, and Council, *World energy scenarios,* (2016).

[15] UNDP and WEC, *Energy and the challenge of sustainability,* World energy statistics (2016).

[16] ISPRE, *Research and development on renewable energies: A global report on photovoltaic and wind energy,,* Progress in Photovoltaics: Research and Applications (2009).

[17] Z. Yang, L. Li, Y. Luo, R. He, L. Qiu, H. Lina, and H. Peng, *An integrated device for both photoelectric conversion and energy storage based on free-standing and aligned carbon nanotube film,* Journal of materials chemistry A **1**, 954 (2013).

[18] V. Vega-Garita, L. Ramirez-Elizondo, and P. Bauer, *Physical integration of pv-battery system: thermal analysis,* Applied Energy **208**, 446 (2017).

[19] Z. Yang, L. Li, Y. Luo, R. He, L. Qiu, H. Lina, and H. Peng, *The ac photovoltaic module concept,* Energy Conversion Engineering Conference, **1** (1997).

[20] J. Reynaud, C. Alonso, P. Aloisi, C. Cabal, B. Estibals, G. Rigobert, G. Sarre, H. Rouault, D. Mourzagh, F. Mattera, and S. Genies, *Cascaded dc-dc converter connection of photovoltaic modules,,* IEEE Transactions on Power Electronics **19**, 1130 (2004).

[21] N. Shani, *Architecture of integrated pv-battery module: modeling, simulation, and comparison,* Master Thesis (2016).

[22] V. Vega-Garita, D. De Lucia, N. Narayan, L. Ramirez-Elizondo, and P. Bauer, *Pv-battery integrated module as a solution for off-grid applications in the developing world,* ENERGYCON 2017 (2017).

[23] G. Gyimesi and R. Viswanathan, *The shift to electric vehicles,* IBM Institute for Business Value (2013).

[24] L. Chuan and A. Uki, *Modeling and validation of electrical load profiling in residential buildings in singapore,* IEEE Transactions on Power Systems **30**, 2800 (2015).

[25] L. Chuan and A. Uki, *Understanding the present and the future electricity needs: Consequences for design of future solar home systems for off-grid rural electrification,* Domestic Use of Energy Conference (2017).

[26] K. S. RT. Khatib, A. Mohamed, *A review of photovoltaic systems size optimization techniques,* Renewable and Sustainable Energy Reviews **22**, 454 (2013).

[27] T. Khatib, I. Ibrahim, and A. Mohamed, *A review on sizing methodologies of photovoltaic array and storage battery in a standalone photovoltaic system,* Energy Conversion and Management **120**, 430 (2016).

[28] E. Egid, M Lorenzo, *The sizing of stand alone pv-system: A review and a proposed new method,* Solar Energy Materials and Solar Cells **26**, 51 (1992).

[29] Y. Ru, J. Kleissl, and S. Martinez, *Storage size determination for grid-connected photovoltaic systems,* IEEE Transactions on Sustainable Energy **4**, 68 (2013).

[30] C. Cabral, D. Filho, A. Diniz, J. Martins, O. Toledo, and L. Neto, *A stochastic method for stand-alone photovoltaic system sizing,* Solar Energy **84**, 1628 (2010).

[31] M. Kolhe, *Techno-economic optimum sizing of a stand-alone solar photovoltaic system,* IEEE Transactions on Energy Conversion **24**, 511 (2009).

[32] T. Khatib, A. Mohamed, K. Sopian, and M. Mahmoud, *A new approach for optimal sizing of standalone photovoltaic systems,* International Journal of Photoenergy **2012**, 7 (2012).

[33] A. Celik, T. Muneer, and P. Clarke, *Optimal sizing and life cycle assessment of residential photovoltaic energy systems with battery storage,* Progress in Photovolatics **20**, 6 (2012).

[34] H. Kazem and K. Khatib, T Sopian, *Sizing of a standalone photovoltaic/battery system at minimum cost for remote housing electrification in sohar, oman,* Energy and Buildings **61**, 108 (2013).

[35] S. Mandelli, C. Brivio, E. Colombo, and M. Merlo, *A sizing methodology based on levelized cost of supplied and lost energy for off-grid rural electrification systems,* Renewable Energy **89**, 475 (2016).

[36] T. Khatib and W. Elmenreich, *An improved method for sizing standalone photovoltaic systems using generalized regression neural network,* International Journal of Photoenergy **2014** (2014).

[37] Y. Ru, J. Kleissl, and S. Martinez, *Storage size determination for grid-connected photovoltaic systems,* IEEE Transactions on Sustainable Energy **4**, 68 (2013).

[38] A. Oudalov, R. Cherkaoui, and A. Beguin, *Sizing and optimal operation of battery energy storage system for peak shaving application,* Power Tech IEEE Lausanne (2007).

[39] M. Shadmand and R. Balog, *Multi-objective optimization and design of photovoltaic-wind hybrid system for community smart dc microgrid,* IEEE Transactions on Smart Grid **5**, 2635 (2014).

[40] M. Fuentes, *A simplified thermal model for flat-plate photovoltaic arrays,* Tech. Rep. (Sandia National Laboratories (1987).

[41] M. Kabir and D. Demirocak, *Degradation mechanisms in li-ion batteries: a state-of-the-art review,* Int. J. Energy Res. **41** (2017).

[42] A. Mukhopadhyay and B. S. m. Sheldon, *Deformation and stress in electrode materials for li-ion batteries,* Progress in Materials Science **63**, 58 (2014).

[43] O. Tremblay and D. L.-A, *Experimental validation of a battery dynamic model for ev applications,* World Electric Vehicle Journal **3** (2009).

[44] X. Han, M. Ouyang, L. Lu, J. Li, and Z. Zheng, Y Li, *A comparative study of commercial lithium ion battery cycle life in electrical vehicle: Aging mechanism identification,* Journal of Power Sources **251**, 38 (2014).

[45] D. D. Leiva, C. Araya, G. Valverde, and J. Quiros-Tort, *Statistical representation of demand for gis-based load profile allocation in distribution networks,* 2017 IEEE Manchester PowerTech (2017).

[46] B. Asare-BediakoaW, W. Kling, and P. Ribeiroa, *Future residential load profiles: Scenario-based analysis of high penetration of heavy loads and distributed generation,* Energy and Buildings **75**, 228 (2014).

[47] M. Chediak, *The latest bull case for electric cars: the cheapest batteries ever,* BLoomberg Technology (2017).

[48] R. Kemma, *Average eu building heat load for hvac equipment,* Van Holsteijn en Kemna B.V. (2014).

B

ACKNOWLEDGMENTS

Firstly, I would like to express my sincere gratitude to everyone that offered their support, inputs, criticism and most of all their encouragement throughout the course of this project. Specifically, I would like to thank Victor Vega-Garita, who supervised me for the entire duration of the project, I am especially grateful to him for always having an open door and an armoury of valuable inputs: providing a fantastic environment in which to develop this project. I would also like to thank Dr. L. Ramirez Elizondo, Prof. dr P. Bauer and Dr. O. Isabella for their feedback and suggestions.

Having called the Netherlands home for half a decade, I would like to express my gratitude to all the incredible personalities that have made it a truly remarkable experience that I will always cherish. Finally, I would like to thank my parents who never cease to believe in my abilities and without whom I would never be where I am today.